ABSTRACT

Title of Thesis:	GEOMORPHIC AND HYDROLOGIC CONTROLS ON TIDAL PRISM AND INLET CROSS SECTIONAL AREA FOR CHESAPEAKE BAY LAGOONS
	Brittany Anna Jenner, Master of Science, 2011
Directed By:	Associate Professor Karen L. Prestegaard Department of Geology

Previous studies have defined a power function between tidal prism and inlet cross sectional area for many lagoon systems. The goals of this study are to first, determine underlying processes that generate the area-prism relationship and then, examine whether the area-prism relationship extends to the small lagoons of Chesapeake Bay. Geomorphic data were measured, compiled and compared for Chesapeake Bay lagoons, Chesapeake Bay regional tidal marshes, and New South Wales, Australia lagoons and creeks. These data generated two inter-regional emergent relationships: 1) An area-prism relationship that included Chesapeake Bay data and 2) A relationship between lagoon surface area and drainage basin area. Examination of Chesapeake Bay data suggests that lagoon water surface area, tidal prism, and inlet geometry are primarily determined by streamflow. Results also indicate that Chesapeake Bay lagoon inlet geometry is modified over time by wave processes, which generates two alternate states for inlet characteristics.

GEOMORPHIC AND HYDROLOGIC CONTROLS ON TIDAL PRISM AND INLET CROSS SECTIONAL AREA FOR CHESAPEAKE BAY LAGOONS

by

Brittany Anna Jenner

Thesis submitted to the Faculty of the Graduate School of the
University of Maryland, College Park, in partial fulfillment
of the requirements for the degree of
Master of Science
2011

Advisory Committee:

Associate Professor Karen L. Prestegaard, Chair
Assistant Professor Sujay Kaushal
Associate Professor Wenlu Zhu

Acknowledgements

First, I would like to thank my advisor Dr. Karen Prestegaard, and my committee, Dr. Sujay Kaushal and Dr. Wenlu Zhu for their support and interest in my research project. I would like to specifically thank Dr. Prestegaard for her insight, encouragement and motivation throughout this entire process. Dr. Prestegaard has been an exceptional mentor and I am very thankful for her guidance and enthusiasm about my research. I would also like to thank Emily Seldomridge for her assistance with field work, in addition to her support as a colleague and friend.

I would also like to extend my gratitude to Brian Connolly for his assistance with field work and grain size analyses. Brian has also been unwavering in his support and encouragement. He has been a source of inspiration and sometimes distraction, but only when I needed to take a break from working. I am truly grateful for his patience, love and reassurance.

Finally, I would like to thank my family for their unconditional love and encouragement. They have taught me to dream big and reach for the stars, and I have learned throughout this process that if I work hard enough I can accomplish any goal I set out to achieve. I would like to specially thank my parents for being the over-involved parents that they are, because without their support I would not be where I am today. My two nephews, Mason and Drew, hold a very special place in my heart as they inspire me every day to enjoy the simple things, learn as much as I can and be a better person.

Table of Contents

List of Tables

List of Figures

List of Symbols

a	hydraulic geometry coefficient for width
A	drainage basin in square miles for Dillow (1996) equations
A_B	drainage basin area
$\underline{A_B}$	cumulative number of drainage basin areas
A_C	inlet cross sectional area
A_i	cross sectional area of rectangle i
A_S	water surface area
$\underline{A_S}$	cumulative number of water surface areas
b	hydraulic geometry exponent for width
BR	basin elevation for Dillow (1996) equations
c	hydraulic geometry coefficient for depth
C	empirical coefficient in area-prism relationship
d_{16}	16^{th} percentile grain size
d_{50}	median (50^{th} percentile) grain size
d_{85}	85^{th} percentile grain size
d_{MEAN}	mean grain size
D	mean inlet depth
D_i	depth of rectangle i
D^*	dimensionless depth
f	hydraulic geometry exponent for depth
F	percent forest cover for Dillow (1996) equations
g	acceleration due to gravity
h_R	tidal range
k	hydraulic geometry coefficient for velocity
L	inlet channel length
m	hydraulic geometry exponent for velocity
n	empirical exponent in area-prism relationship
N	total number within a population
Q_2	two-year recurrence interval peak discharge
Q_B	basin discharge
Q_M	maximum inlet discharge

Q^*	dimensionless discharge
RCN	run-off curve number for Dillow (1996) equations
ST	percent storage for Dillow (1996) equations
S_S	sediment specific gravity
t	time
T	tidal period
U_M	maximum inlet cross sectional velocity
U_B	basin velocity
W_i	width of rectangle *i*
W	inlet width
$\underline{W}$	cumulative number of inlet widths
W^*	dimensionless width
x	empirically derived coefficient for discharge-cross section relationship
z	empirically derived exponent for discharge-cross section relationship
α	empirically derived coefficient in power-law relationships
β	empirically derived exponent in power-law relationships
η	tidal stage
ρ_S	density of the sediment
ρ_W	density of the water
ϕ	phi size; equivalent to $-\log_2 d$
Ω	tidal prism

Chapter 1: Introduction

1.1 Motivation

Coastal lagoons are ecosystems that are formed by interactions among terrestrial stream discharge, tides, and waves to create a dynamic system that is particularly responsive to changes in climate, land-use, or coastal engineering (Haines and Thom, 2007; Roy et al., 2001). The 86 lagoons of the Chesapeake Bay (CB) are nested within coastal watersheds and are responding to changes in climate such as sea level rise, increased variability in streamflow, and changes in storminess and thus wave climate (Kaushal et al., 2008; Najjar et al., 2000; Schmith et al., 1998). Analysis of regional geomorphic data for lagoons in New South Wales, Australia, has demonstrated the usefulness of these data in predicting lagoon vulnerability to these climate change variables (Haines et al., 2006). Previous research has been conducted on some inlet-basins in CB (Byrne et al., 1980); however the geomorphic features of this ecosystem as a whole have not been well characterized, which limits reliable predictions of environmental change.

1.2 The lagoon as an evolving and dynamic physical system

Lagoons have formed in the mouths of coastal streams behind sediment barriers as sea level rose during the Holocene (Kjerfe and Magill, 1989). Tidal, streamflow and wave processes interact to build and maintain lagoon and inlet morphology (Figure 1.1). Lagoons are connected to the sea or larger estuary through an inlet that cuts through a sand barrier. The geometry of inlet channels is both shaped by and governs tidal and stream discharge between the lagoon and the CB. Although tides and streams provide discharge through the inlet, local grain size characteristics are determined by sediment transported landward by waves. The coastal grain size is determined by local sediment sources and the wave heights and wave periods that influence their transport (Kraus, 2007; Elwany et al., 1998; Hume and Herdendorf, 1992; Bruun et al., 1978; O'Brien, 1976, Bruun and Gerritsen, 1960). Therefore, coastal sediment transport provides an additional influence on inlet channel geometry and is the main driver for inlet closure (Kraus, 1998; Bruun et al., 1978; Bruun, 1967; Bruun and Gerritsen, 1960).

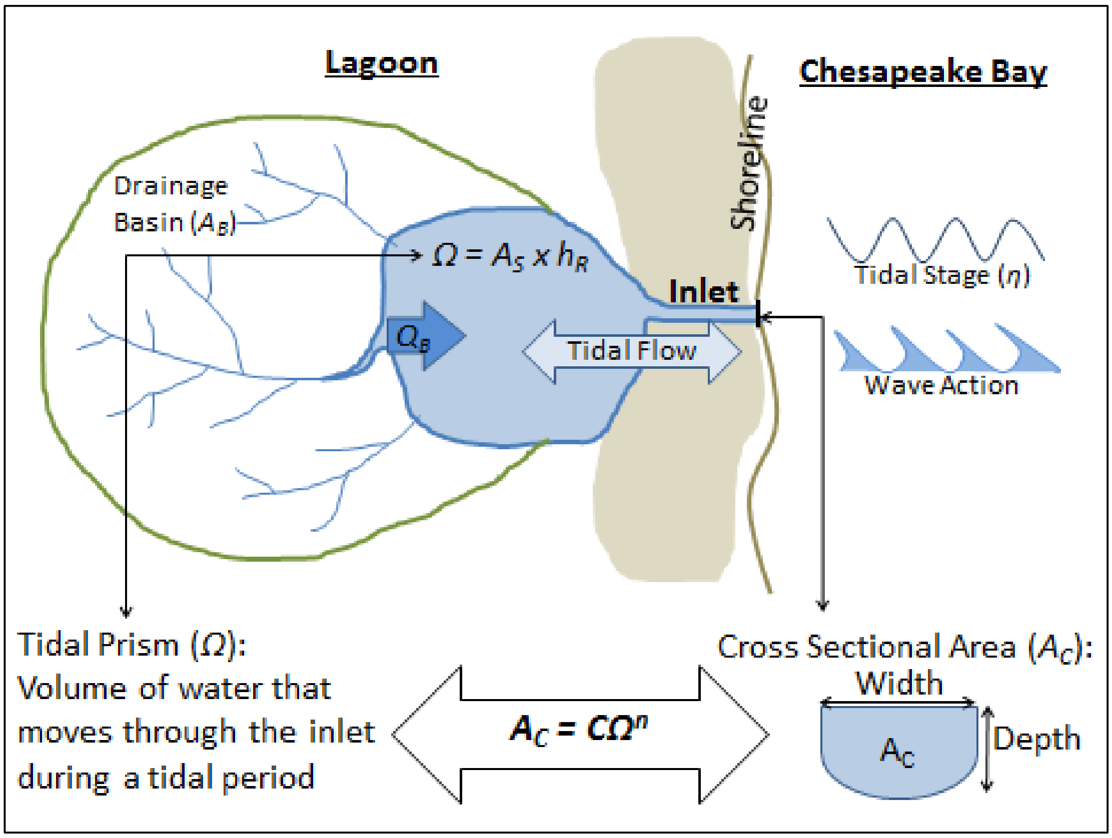

Figure 1.1: Definition sketch of a CB lagoon. Wave action transports sediment and creates a sediment barrier across a lagoon. Flux of water from tides and streamflow form a channel through this material. The tidal prism can be estimated as the water surface area (A_S) multiplied by the tidal range (h_R).

By conservation of mass, the discharge through the inlet must be equivalent to fluctuations in the level of the lagoon (Gao and Collins, 1994; Bruun et al., 1978), thus a continuity equation for the inlet can be written as:

$$A_C U_M = A_S\left(\frac{d\eta}{dt}\right) + Q_B \tag{1.1}$$

where A_C is cross sectional area, U_M is mean inlet velocity, A_S is water surface area, η is tidal stage, and Q_B is basin discharge. Note that all of these variables change with time, therefore static variables can only be defined for specified conditions. When basin discharge is assumed to be zero, this relationship reduces to the area-prism relationship defined as:

$$A_C = C\Omega^n \tag{1.2}$$

where tidal prism (Ω) is defined as $\Omega = h_R A_S$, h_R is tidal range, A_S is water surface area and C and n are empirically derived and have units that are dependent on the units used for analysis (Haines et al., 2006; Townend, 2005; Spaulding, 1994; Jarrett, 1976; Johnson, 1973).

Previous research on tidal inlets has focused on defining this area-prism relationship for various lagoon-inlet systems (Townend, 2005; Seabergh et al., 2001; Hume and Herdendorf, 1993; Byrne et al. 1980; Jarrett, 1976; O'Brien, 1976). This relationship is often used to assess the stability of an inlet, even though it does not take into account all of the variables that control lagoon morphology. The area-prism relationship is a power function that describes many independent lagoon systems. It does not account for drainage basin area or the streamflow that it may contribute, therefore the area-prism relationship must be an emergent property and I can therefore examine populations of data, test hypotheses and determine the underlying controls on inlet cross sectional area and tidal prism by using a data-driven downward modeling approach.

1.3 Previous research

Tidal inlets govern flow rates and volumes of water exchanged between two water bodies. For coastal lagoons, this exchange can include water derived from terrestrial watersheds. Geometric and stability analyses of tidal inlets were initially conducted to facilitate commercial navigation; therefore many of these studies were conducted in large inlets (through which boats would pass) to determine natural stable inlet cross sections (Machemehl et al., 1991; Jarrett, 1976; Escoffier, 1940).

Tidal inlets, however, come in a range of sizes and they serve many functions in coastal environments. They are a permeable boundary between two distinct ecosystems, and inlet channels are sites for exchanges of water, organic matter, sediment, organisms and nutrients. Inlet connections also make it possible for lagoons and bays to provide nursery or temporary habitats for many species that need shelter from oceanic waves, currents, and large predatory species (Roy et al., 2001; Machemehl et al., 1991). The exchange of water through the tidal inlet controls lagoon water quality, which affects physical and biological aspects of the coastal embayment (Battalio et al., 2006; Roy et al., 2001; Smith and Atkinson, 1994). In tidal marshes, the inlet channel regulates hydrologic fluxes and thus the amount of nitrate that can be processed by marsh surfaces (Seldomridge, 2009). Therefore, inlet stability is not only important for navigational purposes, but also for ecosystem functioning and services.

Tidal inlets are found along coastlines around the world and they range in size from very small ($A_C < 1$ m^2) to orders of magnitude larger ($A_C > 10^4$ m^2) (Hughes, 2002;

Byrne et al., 1980; Jarrett, 1976). Large inlets have been well characterized due to commercial navigation needs, but small inlets have not received much attention until recently (Hughes, 2002; Byrne et al., 1980). The most widely used stability model is the empirical area-prism relationship, first established by O'Brien (1931) after initial work done by LeConte (1905). Jarrett (1976) used data from 108 tidal inlets spanning all three United States coastlines to determine an area-prism relationship of:

$$A_C = 1.576 \times 10^{-4} \Omega^{0.95} \quad (1.3)$$

where A_C and Ω are measured in SI units and therefore the coefficient and exponent also have SI units (Hughes, 2002). While various studies around the world support Jarrett's relationship (e.g. Townend, 2005; van de Kreeke, 2004; Hume and Herdendorf, 1993; 1992), the CB inlets measured by Byrne et al. (1980) are not consistent with the empirical trend established by Jarrett (1976). Additionally, small-scale inlets in experimental (model and laboratory) studies (Seabergh et al., 2001; Mayor-Mora, 1977) do not follow the defined trend of the area-prism relationship indicated by Jarrett's (1976) compilation. The purpose of Byrne et al.'s (1980) study was to examine mid-range sized inlets in an effort to improve navigation into inlet-basin systems that are found along the many shorelines of CB. The observations from their study demonstrated that small to mid-ranged tidal inlets tend to have larger channel areas than expected from the trends derived from large inlets. CB itself is a drowned river valley estuary with its own inlet that shelters the bay from oceanic tide and wave action. Therefore, tidal inlets in CB experience different distributions of waves and tidal forcing than oceanic tidal inlets. Many authors, however, have questioned whether this provides a sufficient explanation for the behavior of CB inlets (Townend, 2005; Hughes, 2002), particularly since laboratory experiments also found different characteristics for small inlets. A third population of small tidal inlets is found at the entrance to tidal marshes (Seldomridge, 2009; Jenner, 2010; Rinaldo et al., 1999a; 1999b), but there have been no comparative studies of the geomorphic characteristics of these two types of tidal inlets. Therefore, comparison of tidal inlet geometry and stability for small CB lagoon inlets and Patuxent River (PR) tidal marsh inlets might provide new information about inlet morphology.

1.4 Research approach

Previous tidal inlet stability studies have taken two main approaches: 1) *Case Studies*: the study of one or a few tidal inlets in a specific region with detailed field measurements (e.g. Battalio et al., 2006; van de Kreeke, 2004; Gao and Collins, 1994; Hume and Herdendorf, 1992; Gammisch et al., 1988; van de Kreeke, 1985; Byrne et al., 1980) or 2) *Regional or Inter-regional Comparison Studies*: in this approach, previously acquired and/or new geomorphic and other data from multiple sites is pooled together and further analyzed by new methods and technology (e.g. Townend, 2005; Hughes, 2002; Hume and Herdendorf, 1993; Machemehl et al., 1991; Jarrett, 1976). In this study, I will conduct a modification of the second approach. The main difference in this study is that entire populations of geomorphic data will be used in the regional and inter-regional comparative analysis. This portion of the study will be used to define inter-regional relationships, which are emergent properties of lagoon-inlet systems. Once these relationships are defined, a data-driven “downward modeling” approach will be used to identify controlling processes for both inlet cross sectional area and tidal prism. Although this analysis will be conducted on multiple data sets, the focus is CB lagoons.

Lagoon-inlet systems are often referred to as "tidal inlets" even though they may not be built or formed by exclusively tidal processes. Therefore, in this study, I will compare CB inlet-lagoons with data from CB tidal inlets that *are* formed by tidal processes alone. Geomorphic features (e.g. inlet width, water surface area, marsh area) are measured for all PR tidal marshes in the freshwater and oligohaline portions of the Patuxent Estuary. Comparison of these two populations may help elucidate the relative roles of tidal and streamflow processes in determining tidal prism for CB lagoons. Tidal marshes are self-formed basins; during tidal inundation, channels are filled and the upper marsh is flooded. Previous studies suggest that headward erosion and migration of channels occurs during outgoing (ebb) tides, when water drains from the marsh basin (French and Stoddart, 1992). Furthermore, feedbacks between vertical marsh accretion and the tidal prism redistribute tidal energy, which maintains the characteristics of these tidal marshes (French and Stoddart, 1992; Pethick, 1981). Thus, water surface area and basin area for tidal marshes is controlled by tidal processes.

In addition to tidal processes and waves, streamflow from terrestrial watersheds also influences lagoon-inlet morphology and behavior (Haines et al., 2006; Elwany et al., 1998). Therefore, CB lagoon systems are compared with data from other lagoon-inlet systems that have different tidal and wave conditions. Geomorphic features such as water surface area and basin area were compiled for New South Wales (NSW) lagoons and creeks by the NSW Office of the Environment and Heritage (http://www.environment.nsw.gov.au/estuaries/index.htm). The NSW lagoons are along an oceanic coast that has larger wave heights and wave periods than the CB. The NSW lagoons and creeks provide a great comparison to CB data, as these inlet-basins along the southeastern coast of Australia experience a spring tidal range similar to CB lagoons, but are subject to higher and longer period oceanic waves (Haines et al., 2006). A more limited geomorphic data set (lagoon water surface areas and inlet area only) were compiled for United Kingdom (UK) estuaries from the study by Davidson and Buck (1997). Estuaries along the UK coastline experience micro- (< 3 m) to supra-tidal (> 9 m) ranges, therefore providing a comparison to inlet-basin systems with large tidal ranges.

Many geomorphic features exhibit self-similarity over many orders of magnitude (Rodriguez-Iturbe and Rinaldo, 1997; Plotnick and Prestegaard, 1993; Mandelbrot, 1983). Therefore, the size distributions of geomorphic features commonly exhibit power-law scaling behavior within geomorphic constraints. If size distributions exhibit power-law behavior, then they do not vary randomly around a mean and there is no "representative" average size (Plotnick and Prestegaard, 1995). Therefore, selecting random sites for field measurements may not provide information that is sufficient to determine controls on inlet size. This research uses an alternative design: 1) Measure entire regional populations of inlet dimensions; 2) Determine upper and lower bounds on inlet size, and 3) Compare populations of inlet sizes that experience significantly different physical processes to elucidate controlling variables.

In this thesis, I use the inter-regional data sets to search for power law relationships among geomorphic and hydraulic variables. Using these emergent relationships as a guide, I then use a data-driven "downward modeling" approach to search for underlying processes that give rise to these emergent relationships, and can cause differences among these regions. The term "downward modeling" was first introduced by Klemes (1983) and later re-introduced into hydrologic studies by Sivapalan et al. (2003) to describe this top-down approach to understanding behavior in dynamic systems. "Downward modeling" is an alternative approach to reductionistic approaches that are used to forward-model complex systems. If sufficient data are available, these forward and down-ward modeling approaches can merge to provide enhanced understanding of the system. Downward modeling encourages large data sets to be obtained, such that multiple hypotheses can be derived and tested in a stepwise manner. This enables controlling processes to be identified and tested through a hierarchal procedure (Sivapalan et al., 2003). For example, if CB lagoons and PR tidal marshes exhibit similar probability distributions of all geomorphic parameters, then the controlling factors (e.g. tidal controls on inlet width) must be present in both environments. If different geomorphic probability distributions are found, then the environmental condition(s) present in one ecosystem but not the other, might explain differences in geomorphic distributions.

This report is organized in the following manner. Emergent relationships and the underlying controls on tidal prism are presented in Chapter 2. The area-prism relationship and underlying controls on inlet cross sectional area are presented in Chapter 3. The final chapter focuses on CB lagoons and integrates results from Chapters 2 and 3 to present methods for assessing equilibrium among lagoon-watershed system components.

Chapter 2: Geomorphic Controls on Tidal Prism for Coastal Lagoons and Tidal Marshes

2.1 Statement of the problem

Coastal inlets govern exchanges of water, nutrients, and sediment between a coastal basin (e.g. lagoon, tidal marsh, or coastal lakes) and adjacent ocean or major estuary. These fluxes help maintain the morphology and biological productivity of these coastal ecosystems (Gale et al., 2007; Roy et al., 2001). Lagoons and coastal saline lakes are considered to be particularly sensitive to anthropogenic impacts due to the complex dynamics that affect lagoon morphology (Haines and Thom, 2007; Roy et al, 2001). Inlet closure due to wave-induced sedimentation in the inlet channel can cause environmental changes that may be either favorable or detrimental to coastal ecological communities (Gale et al., 2007; Roy et al., 2001). Rapid sedimentation and closure often results from landward transport of sediment by waves or storm surges that is not offset by stream and tidal outflows that scour sediment (Battalio et al., 2006; Elwany et al., 1998). Storm frequency and magnitude, sea level rise, and sediment transport characteristics are all subject to climate change and will have a significant effect on tidal inlet morphology and stability (Haines and Thom, 2007). Haines et al., (2006) used geomorphic indices to evaluate the sensitivity of coastal ecosystems to anthropogenic forcing. Small lagoons in Chesapeake Bay (CB) may also be vulnerable to climate or anthropogenic change, yet they have not been as extensively studied as the lagoons, coastal lakes and estuaries of New South Wales (NSW), Australia, the United Kingdom (UK) and New Zealand (NZ). Previous research indicates that the small lagoons in CB exhibit different geomorphic characteristics (e.g area-prism relationship, width to depth ratios) than oceanic inlet-basins systems (Byrne et al., 1980). Furthermore, previous researchers (e.g. Townend, 2005; Hume and Herdendorf, 1993) found that different estuary types exhibit different area-prism relationships. Thus an assessment of geomorphic features of CB lagoons and associated drainage basins may provide tools to predict responses to changes in climate or anthropogenic forcing.

2.2 The area-prism relationship

Empirical relationships between inlet cross sectional area (A_C) and tidal prism (Ω) have been used to assess inlet stability (Hughes, 2002; Jarrett, 1976; O'Brien 1976). Tidal prism is often defined as the tidal range (h_R) multiplied by the lagoon surface area (A_S) (Haines et al., 2006; Spaulding, 1994; O'Brien, 1976; Johnson, 1973). The form of the area-prism relationship suggests that tidal inlets are maintained by tidal flows only, but most studies of inlet stability indicate that tidal fluxes alone are sufficient to maintain inlets for tidal marsh channels, but not for coastal lagoon inlets (de Swart and Zimmerman, 2009; Roy et al., 2001; Elwany et al., 1998; Pethick, 1980). As indicated in Figure 2.1, tidal marsh inlets along the Patuxent River (PR) Estuary form a communication node between marsh basin processes and estuarine processes. Lagoon inlets form at the node between lagoonal processes and coastal processes (Figure 2.1). Coastal sediments are transported landward by waves, often creating a sand barrier in which the inlet is formed and maintained by tidal flow and streamflow.

Therefore, lagoon inlet characteristics are maintained by fluxes from both stream and tidal sources that generate sufficient shear, through the velocity distribution, to move sediment that has been deposited in the inlet by wave action (Hughes, 2002; Gao and Collins, 1994). Mean inlet velocity (U_M) can be expressed as a continuity equation:

$$U_M = \left(\frac{A_S}{A_C}\right)\left(\frac{d\eta}{dt}\right) + \left(\frac{Q_B}{A_C}\right) \tag{2.1}$$

(Gao and Collins, 1994; Bruun et al., 1978), where η is tidal stage; the water elevation difference between the lagoon and sea, Q_B is freshwater inflow from a watershed into the lagoon, and A_S is lagoon surface area. Note that total inlet discharge is defined as: $Q_M = U_M A_C$. This equation suggests a continuum between tidal and streamflow sources for inlet maintenance, and it describes a physical system with four main variables: Q_M, A_S, η, and Q_B, all of which vary with time. Figure 2.1 shows a diagram of how these four main variables interact.

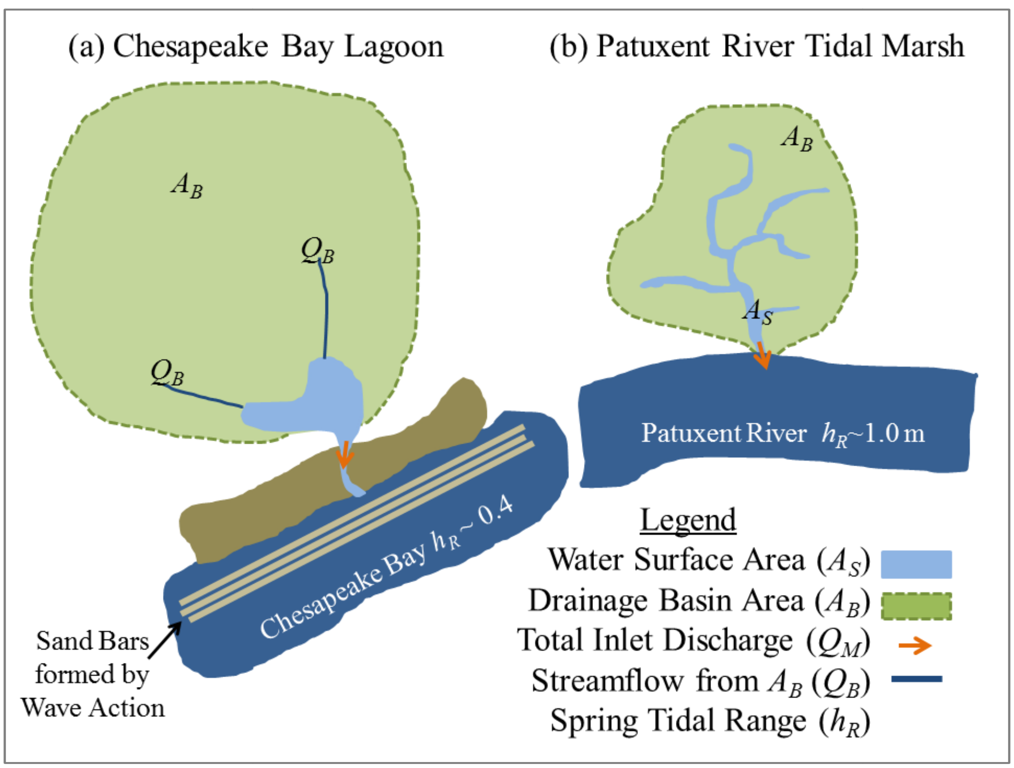

Figure 2.1: Definition sketch for tidal marsh and lagoon inlets and their associated drainage basins (A_B) and water surface areas (A_S). Tidal range (h_R) is the difference in tidal stage (η) over a given tidal period (T). (a) CB lagoons are nested within small Coastal Plain drainage basins; watershed boundaries are often truncated by

roads. (b) PR tidal marshes form their own drainage basins and inlets during tidal flows.

If the area-prism relationship is an emergent property of lagoon-inlet systems, then I should be able to search for the underlying processes that control both tidal prism and channel cross sectional area. In this chapter, I will evaluate processes that control the tidal prism.

Most studies of the area-prism relationship have focused on tidal inlet characteristics and few have examined drivers of the tidal prism. In previous studies, the role of freshwater inflow on forming or maintaining the tidal prism is often overlooked and Q_B is assumed to be zero. This assumption might be reasonable for conditions where streamflow has no role in either forming the tidal prism or the inlet channel (e.g. possibly the NZ inlet-basin systems from Hume and Herdendorf (1992)). Streamflow, however, has been shown to be important for inlet maintenance in many studies (Kraus, 2007; Haines et al., 2006; Elwany et al., 1998). For example, Elwany et al. (1998) found that periodic river flooding was the dominant long-term mechanism for maintaining an equilibrium inlet cross section and thus tidal flow through Southern California lagoon inlets. This suggests that streamflow may play a significant role in the formation of tidal prism, possibly by controlling water surface area.

Tidal prism is determined by either: a) measuring the total volume of water that passes through a tidal inlet over a tidal cycle (Bruun et al., 1978) or b) estimating tidal prism by multiplying water surface area by tidal range (Spaulding, 1994; O'Brien, 1976). The second method requires simplifying assumptions, but is commonly employed in most regional studies of tidal prism for small systems. In previous studies, tidal processes are assumed to be important for maintenance of inlet-basin systems. In this study, I will test that assumption by comparing lagoon inlet-basin systems with those of tidal marshes, which have no freshwater inflow (see Figure 2.1).

For coastal lagoons that have relatively large water surface areas, tidal range is a smaller component of the tidal prism than the water surface area. CB lagoons have significantly larger water surface areas than tidal marshes, but much smaller surface areas than many oceanic inlet-basin systems (Haines et al., 2006; Hume and Herdendorf 1993; 1992). In the UK, which experiences micro- (< 3 m) to supra- (> 9 m) tides, Townend (2005) found that lagoon tidal prisms were not particularly sensitive to tidal range. This suggests that processes that control water surface area provide a significant underlying control on tidal prism. This underlying control might be stream discharge from terrestrial watersheds that contribute to lagoon basins.

Streamflow from most watersheds varies many orders of magnitude due to seasonal and inter-annual variations in hydrological processes. Most studies of individual tidal inlets suggest that high frequency flood events form or help maintain tidal inlets (Kraus, 2007; Haines et al., 2006; Elwany et al., 1998). Streamflow data are not available for all watersheds, and data are particularly meager for small coastal watersheds (Harmel et al, 2003; Menabde and Sivapalan, 2001). Recently, however, there has been significant research on scaling relationships that can be used to estimate streamflow in small basins (Peel and Blöschl, 2011; Gupta, 2004; Sivapalan, 2003).

For most humid temperate regions, drainage basin area is the major variable used to predict streamflow for ungauged watersheds (Magilligan and Nislow, 2001; Meigh et al., 1997). Streamflow for small catchments (< 10 km^2) is often heterogeneous (Gupta, 2004; Sivapalan, 2003), and is more susceptible to variations in land-use, geology, topography, soil type, etc. (Birkinshaw et al., 2011; Villarini and Smith 2010; Daviau et al., 2000; Meigh et al., 1997; Dillow, 1996). For the regions included in this analysis, basin area is the major variable for all locations. For small watersheds in both Maryland and the UK, other variables in addition to drainage basin area affect streamflow. For example, for small watersheds in the Maryland Coastal Plain, soil type, forest cover, and land-use have significant influence on flood flows (Villarini and Smith, 2010; Dillow, 1996). Therefore, in this study, drainage basin area is investigated as a proxy for streamflow. For small basins where land-use might also affect streamflow, I will examine the effects of land-use and forested area on the use of drainage basin area as a proxy for discharge.

2.3 Hypotheses

i. Due to contributions from both tidal and streamflow sources, water surface areas will be larger for CB lagoons than for PR tidal marshes.

ii. Geomorphic probability distributions for both basin area and water surface area can be expressed as power laws.

iii. For both CB lagoons and PR tidal marshes, the water surface area component of tidal prism will exhibit a direct correlation to drainage basin area.

iv. The water surface area-drainage basin area relationship for CB lagoons is similar to that for oceanic lagoon systems.

2.4 Methods

2.4.1 Determination of geomorphic characteristics from aerial photographs

CB lagoons and PR Estuary marshes are first identified as permanent features in the landscape by viewing USGS air photo images from the period (1993 to 2011) accessed via Google Earth. Geomorphic characteristics (e.g. water surface area, basin area) were measured for the April 2007 date photographs using the GIS program MD MERLIN Online (http://www.mdmerlin.net/). Basin areas for CB lagoons are determined using a variety of resources. MERLIN Online provides watershed maps which help determine watershed boundaries for larger basin areas. Smaller basin areas are often truncated by roads. Topography and changes in vegetation are also used to determine watershed boundaries. PR marsh basin areas are identified by changes in vegetation and topography.

2.4.2 Probability distributions of water surface area and drainage basin area

Two methods for expressing probability distributions are used in this study. The first uses cumulative number and the second expresses data as a cumulative probability distribution. A cumulative frequency distribution is determined for basin area (A_B) by ranking the population of basin areas from smallest to largest where the smallest basin area is assigned the largest rank (N) and the largest basin area is assigned a value of 1. This results in a cumulative frequency distribution such that the probability that an inlet-basin has a basin area ($\underline{A_B}$) greater than or equal to A_B can be write as: $P(\underline{A_B} \geq A_B)$.

Data exhibit a power law relationship if:

$$P(\underline{A_B} \geq A_B) = \alpha A_B^{-\beta} \tag{2.2}$$

where P is the probability of a drainage basin ($\underline{A_B}$) greater than A_B, α and β are empirically derived coefficient and exponent, respectively (Kefi et al., 2007; Scanlon et al., 2007; Rodriquez-Iturbe and Rinaldo, 1997; Rinaldo et al., 1993). The population is a truncated power law if it follows:

$$P(\underline{A_B} \geq A_B) = \alpha A_B^{-\beta} exp\{-A_B/A_X\} \tag{2.3}$$

where A_X marks the lower bound of increasing A_B values where $P(\underline{A_B} \geq A_B)$ is decreasing faster than power law form (Kefi et al., 2007). Discerning between the two types of relationships will help determine if there is an upper or lower bound to the geomorphic feature of interest within a given population.

A cumulative probability distribution is determined for drainage area (A_B) by ranking the population from smallest to largest, where the smallest A_B is assigned a value of 1 and the largest A_B is assigned the largest rank (N); the rank is divided by the total number (N). The same methods are followed for water surface area (A_S).

2.4.3 Determination of tidal range and tidal period

Tide stations are located around the CB; therefore, a tide station is used to estimate tidal ranges for numerous lagoons. Data compilations for tide stations operated by National Oceanic and Atmospheric Administration (NOAA) provide mean tidal range, spring tidal range and mean tidal level, for all CB lagoons and the oligohaline PR marshes (see Table 2.1). Tidal ranges for freshwater marshes are determined from data compiled by Maryland's Department of Natural Resources. Tidal range is defined as the difference in tidal stage (η) between high and low tide for a given tidal period (T).

Table 2.1: Tidal ranges in Chesapeake Bay at select NOAA tide stations

Region	Tide Station	Spring Range (m)	Mean Range (m)	Mean Tide Level (m)	Open or Intermittent Inlet-basin
CB W	North Point	0.35	0.31	0.23	Hines Pond
CB W	Mountain Point	0.27	0.24	0.18	Broadwater Road, Cape St Claire, Lake Claire, Morgan Drive
CB W	Annapolis	0.34	0.30	0.22	Big Pond, Blackwalnut, Chase Pond, Deep Pond, Heron Lake, Mezic Ponds, Sharps Point

CB W	Rose Haven	0.31	0.27	0.18	Herring Bay
CB W	Chesapeake Beach	0.34	0.30	0.21	Brownies Beach, North Beach, Sewage Plant Road
CB W	Cove Point	0.36	0.32	0.19	Calvert Cliffs North, Calvert Cliffs South, Camp Conoy, Cove Lake, Webster Ponds
CB W	Solomons	0.41	0.36	0.23	Aztec, Algonquin, Biscoe, Carroll, Cheyenne, Clubhouse, Drum Point, Far Cry Farm, Fresh Pond, Holly Drive, Lake Charming, Shaw Road, Long Lane, Long Neck, Massum Eyrie Road, Massum Eyrie Way, Murray Road, Norris Pond, Page Pond, Peters Pond, Shipwreck Way, Sivak Way, Spring Lake, St Clarence Middle, St Clarence North, St Clarence South, St James Church, Tippitt Pond
CB E	Tolchester	0.41	0.37	0.25	Bramble, Mendinhall, Stavley
CB E	Love Point	0.41	0.36	0.26	Love Point, River Shore
CB E	Matapeake	0.35	0.31	0.22	Bay Drive, Lake Cardoza, Price Creek, Price Farm, South Terrapin Beach, Wellman Way
CB E	Kent Point Marina	0.38	0.34	0.23	Bloody Point, Carter Creek, Holligans Snooze, Kent Fort Manor, Northwest, Scaffold Creek, Skove Lane
PR	Lower Marlboro	0.62	0.55	0.33	Oligohaline Marshes
PR	Jug Bay website	1.00	0.46	--	Freshwater Marshes

These tidal ranges are used to evaluate tidal prism at CB and PR sites. A frequency analysis of the Annapolis tide station shows that the spring tidal period (T) is ~24,000 s; this value is used for all tidal period analyses.

2.4.4 Watershed characteristics of Chesapeake Bay lagoons

A drainage basin is the total area that contributes to stream discharge; therefore in most cases, drainage basin area is proportional to streamflow. For watersheds in humid temperate regions, basin area is often the only parameter used in regional estimations of streamflow. For example, for most of Maryland, regional flood frequency relationships take the following form: $Q_B = \gamma(A_B)^{\lambda}$; where γ and λ are derived from gauged streams within a given region and A_B is drainage basin area (Dillow, 1996). For small, heterogeneous watersheds, other explanatory variables (e.g. percent forest, basin relief or runoff curve number) are included in multiple regression equations to estimate streamflow.

The coastal watersheds that directly contribute to CB lagoons are often small, and thus susceptible to the heterogeneity often observed for small watersheds. Several land-use categories have been identified as having significant effect on the hydrologic characteristics of a watershed (Birkshaw et al., 2011; Villarini and Smith, 2010; Dillow, 1996). In order to better understand the underlying controls on tidal prism for CB lagoons, the relationship between land-use characteristics and streamflow will be examined. Increased forest cover, in small basins, greatly increases storage and therefore decreases the rate of delivery of water to the lagoon, therefore a watershed with a significant area of forest (> 60%) will require a larger basin area to produce an equivalent peak flow discharge of an unaltered basin. Residential land-use, which occurs in many watersheds that contribute to CB lagoons, has the opposite effect; roads, roofs, and other impervious surfaces increase runoff, creating larger flows from a given drainage area (Dillow, 1996).

The state of Maryland is divided into five physiographic provinces (Fenneman, 1938); all CB lagoons lie within the Coastal Plain province. Dillow (1996) further divided the Coastal Plain into two regions (western and eastern) due to differences in elevation and stream discharge. Thus, in each region, different parameters influence runoff and thus are used in equations to estimate the magnitude and frequency of flood events. This study follows the guidelines established by the USGS for estimating peak-flow discharges (Dillow, 1996). Western shore peak flow discharges for the 2-year recurrence interval are determined from the following equation:

$$Q_2 = 1410A^{0.761}(F + 10)^{-0.782} \tag{2.4}$$

where A is the drainage area in square miles and F is the percent forest cover. These equations suggest that forested areas store runoff, but this mechanism becomes less effective for larger storm and flood events.

Eastern shore peak flow discharges for the 2-year recurrence interval are determined from the following equation:

$$Q_2 = 0.25A^{0.591}(RCN - 33)^{1.70}BR^{0.310}(F + 10)^{-0.464}(ST + 10)^{-0.148} \tag{2.5}$$

where RCN is the run-off curve number, BR is the basin elevation and ST is the percent storage. Drainage area (A), percent forest cover (F), percent storage and basin elevation are measured using MERLIN Online. Characterization of the 2-year peak-flow discharge for each region will allow determination of the role of streamflow in producing the water surface area and tidal prism.

An average value of forest cover is determined for the western shore so that a relationship between basin area and Q_2 can be determined for western shore lagoon watersheds. Similarly, average values of basin relief, percent storage, percent forest cover and a run-off curve number are used to determine a relationship between basin area and Q_2 for eastern shore lagoons. These relationships are then combined to produce one simple relationship for all CB lagoons:

$$Q_2 = 2.9AB^{0.71} \quad (R^2 = 0.99) \tag{2.6}$$

Where Q_2 is the 2-year peak discharge in cubic meters per second and A_B is basin area in square kilometers (Figure 2.2).

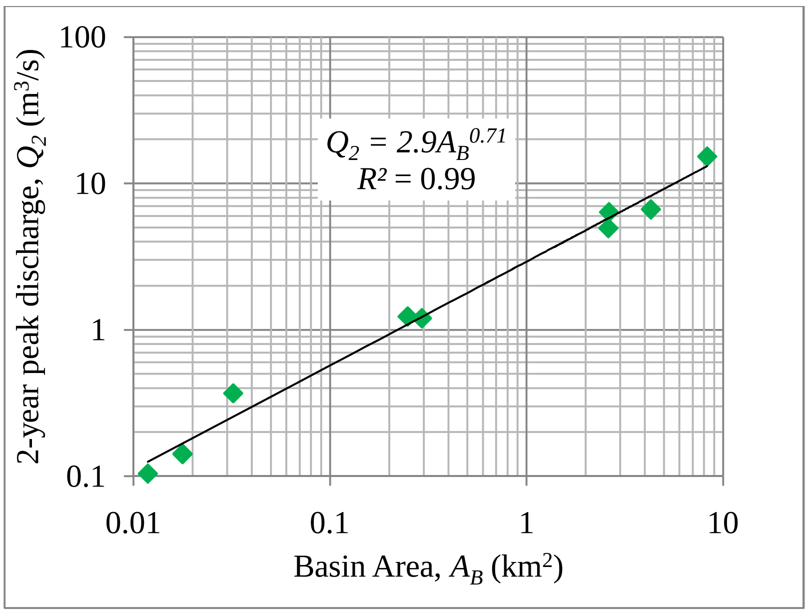

Figure 2.2: Relationship between the 2-year peak discharge and drainage basin area determined from Dillow (1996) for average CB lagoon watersheds.

With respect to river discharge and other geomorphic processes, Wolman and Miller (1960) found that low magnitude, high frequency events exhibit the largest amount of work, in the form of erosion and deposition, on the landscape. Subsequent work on river morphology has found a small range of recurrence intervals (from 1.5 to 5.0) that are associated with bankfull discharges (Simon et al., 2004; Williams, 1978; Leopold et al., 1964). In this study, the bankfull discharge is defined as the maximum discharge contained within a channel and is considered to be the most effective at forming and maintaining channel geometry (Simon et al., 2004; Leopold et al., 1964). Leopold et al.,

(1964) also found the 1.5-year recurrence interval discharge to best represent the bankfull discharge. Flood frequency equations for the Maryland Coastal Plain do not include a 1.5-year recurrence interval (Dillow, 1996); therefore the 2-year recurrence interval discharge will be used for estimating bankfull discharge from the watershed. The 2-year peak discharge (Q_2) will be tested against basin discharge (Q_B) values derived from bankfull inlet conditions (Equation 2.1) in a later chapter.

2.5 Results

2.5.1 The role of tidal forcing on Chesapeake Bay marsh and lagoon tidal prisms

The relationship between tidal range and water surface area for CB lagoons indicates wide variation in water surface area for a small range of values for tidal range (Figure 2.3). In comparison, PR tidal marshes experience a wide range of tidal ranges due to the larger tidal range (up to 1.2 m) and the variation in tidal range provided by the increase in inlet elevation with a decrease in inlet size. This creates a large range of tidal ranges and thus tidal marsh basin areas that have been formed by tidal processes alone.

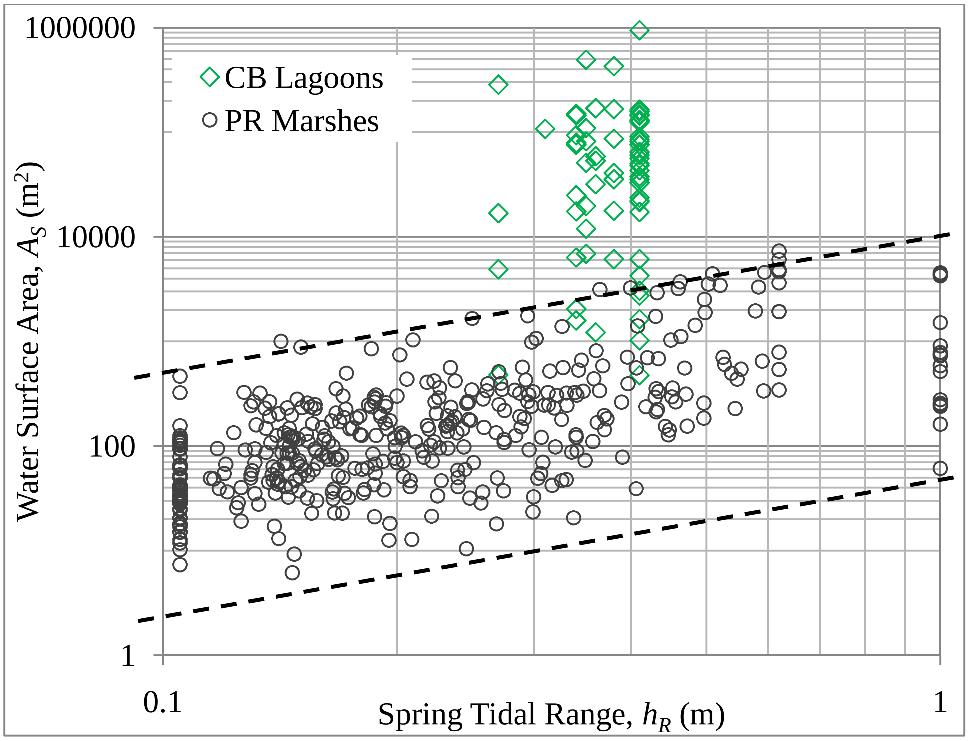

Figure 2.3: Water surface area plotted as a function of spring tidal range for PR marshes and CB lagoons.

Figure 2.3 also demonstrates that for a given tidal range, CB lagoons have much larger values of lagoon water surface area than the self-formed water surface areas of PR tidal marshes. These data support the hypothesis that the "tidal" lagoons of the CB are not formed by tidal processes alone but require streamflow inputs.

2.5.2 Geomorphic probability distributions for Chesapeake marshes and lagoons

Probability distributions for basin area and water surface area were determined for entire populations of both CB lagoons and PR tidal marshes. I present these as a comparison population study in order to determine tidal and streamflow controls on CB lagoon tidal prisms; in a further section I compare these new data to two other populations of geomorphic data obtained from studies in the UK (Davidson and Buck, 1997) and NSW, Australia (NSW Office of the Environment and Heritage, accessed October 2010).

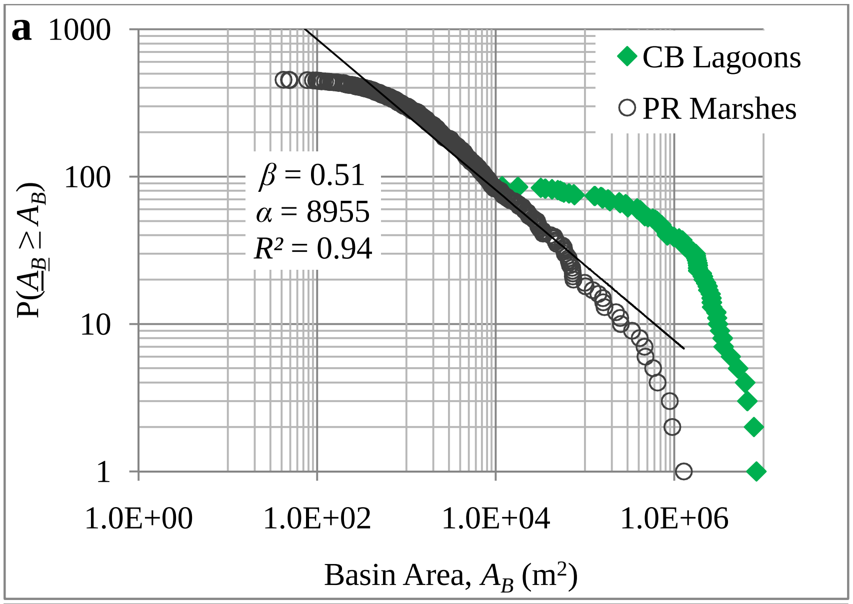

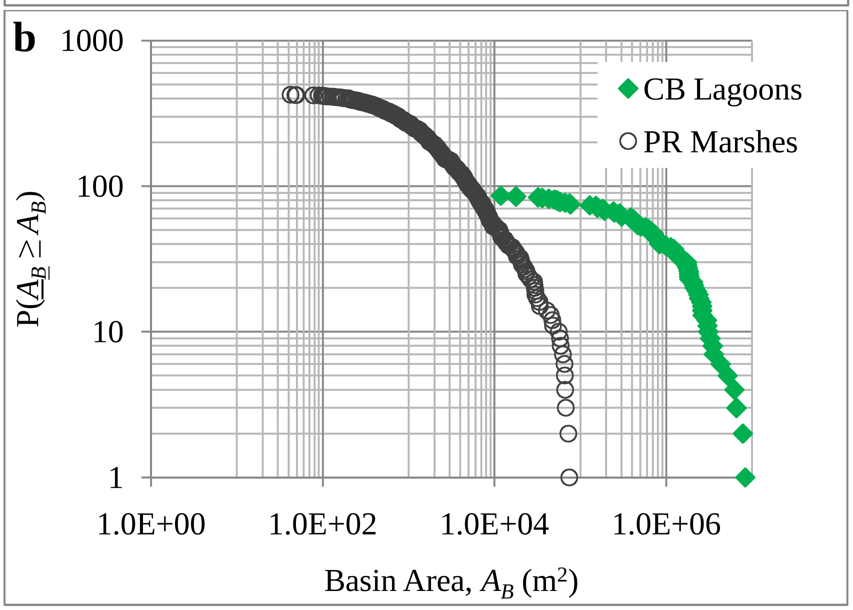

Figure 2.4: (a) PR marshes exhibit a power law relationship, with a lower bound of 42 m^2 and an upper bound of 1.3E6 m^2. Lagoons form in a subset of coastal watersheds with basin areas > 1E4 m^2 (0.01 km^2) and < 1E7 m^2 (10 km^2). (b) Same as (a), but PR marshes at the mouth of tributaries contributing to the PR have been removed, so that the upper bound is < 1E5 m^2.

The PR tidal marsh data set contains all oligohaline and freshwater marshes within the PR estuary and these data exhibit a power law for both basin area (Figures 2.4a and 2.5a) and water surface area (Figure 2.8a) when all PR tidal marshes are included, however when only self-forming basins, those that do not contain upland tributaries, are plotted alone, they exhibit a truncated distribution (Figures 2.4b and 2.8b). The basin area for self-forming marshes ranges from 40 m^2 to 74,300 m^2 (0.743 km^2). The smallest tidal marsh area is associated with the smallest tidal inlets that can be sustained during the growth of marsh vegetation, whereas the upper limit of tidal marsh area, for both self-forming and upland tributaries, may indicate the largest marshes that can form within the boundaries of the PR, by tidal range and inlet bed elevation. The upper bound is determined by travel times in a tidal cycle and the finite space within the PR Estuary. CB lagoons form within a subset of all coastal watersheds just as self-forming marshes are a subset of the PR tidal marshes along the PR estuary.

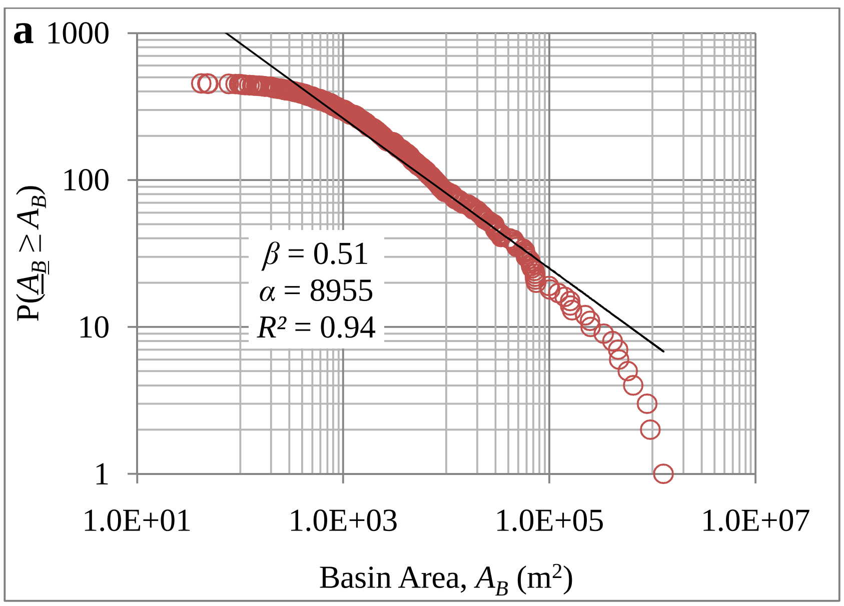

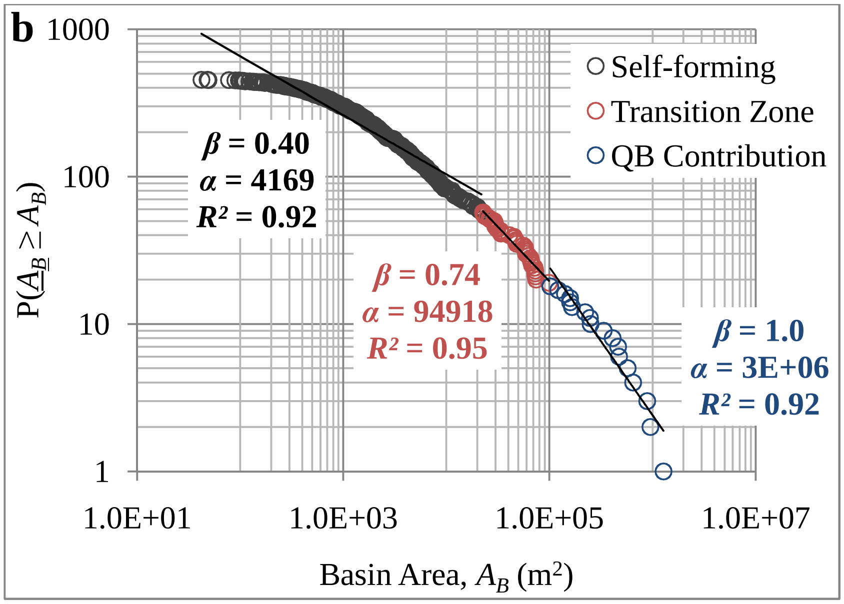

Figure 2.5: (a) Basin area (or marsh surface area) for the entire population of oligohaline and freshwater marshes along the PR estuary exhibits a power law relationship. (b) Identifying marshes at the mouth of upland tributaries shows a transition zone between 22,000 m^2 (0.022 km^2) and 100,000 m^2 (0.1 km^2).

The drainage basin areas that contribute to CB lagoons also exhibit a truncated power law distribution. Most research (Rodriguez-Iturbe & Rinaldo, 1997; Rodriguez-Iturbe et al., 1994; Rinaldo et al., 1993; Nakano, 1983) suggests that drainage basin areas usually exhibit power law distributions. Inclusion of all drainage basins that contribute to all embayments, lagoons and estuaries, in CB suggests that these power laws are truncated at both the upper and lower ends (Figure 2.6a). Further investigation indicates a transition for basin area sizes between 0.1 km^2 and 10 km^2 (Figure 2.6b) that separates lagoon data from open estuary data.

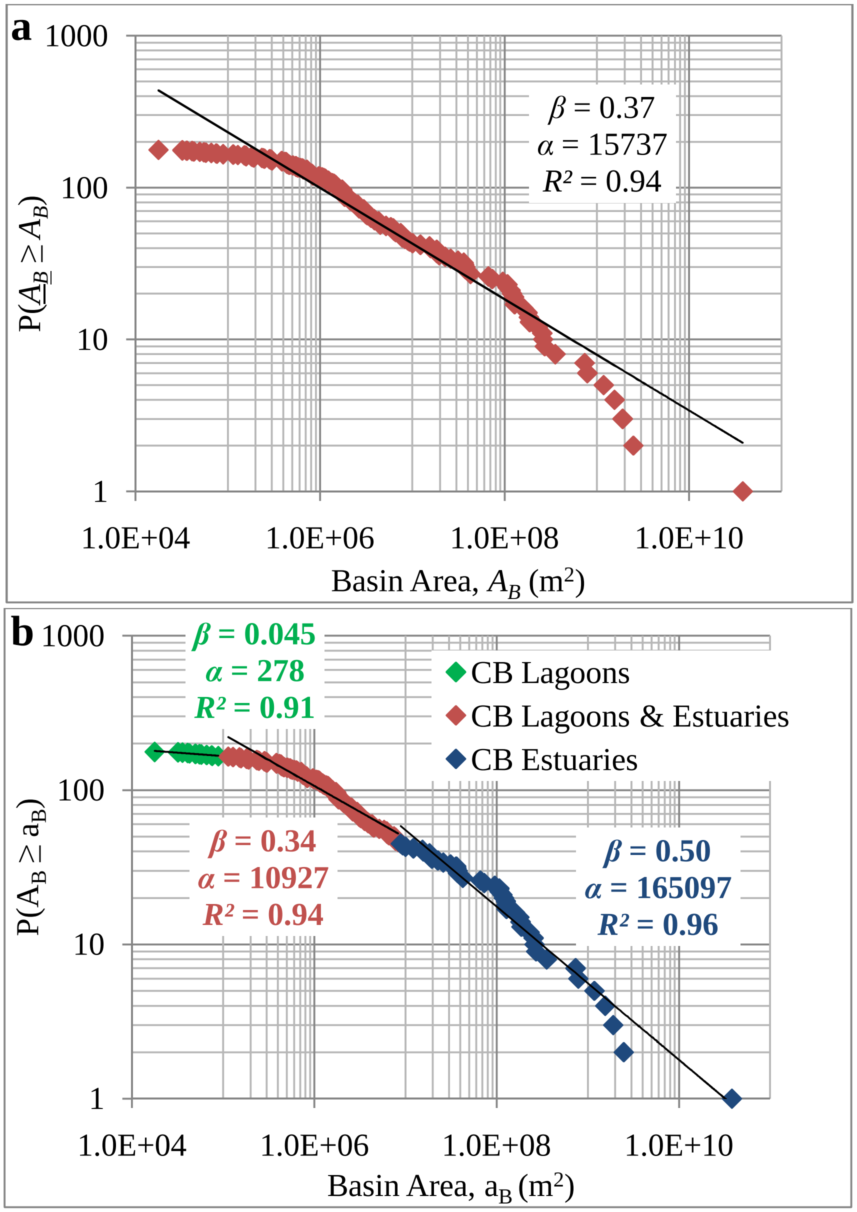

Figure 2.6: (a) Cumulative frequency for all inlet-basin systems in CB indicates power law behavior. (b) Identification of lagoons within the cumulative frequency indicates that lagoons have basin areas > 1.1E4 m^2 and the transition between lagoons and sub-estuaries occurs between basin area sizes of 1E5 m^2 (0.1 km^2) to 1E7 m^2 (10 km^2).

Mean basin area for CB lagoons (1,178,700 m^2) is three orders of magnitude larger than the mean basin area for self-forming PR tidal marshes (Figure 2.7). If tidal marshes with upland tributaries are included in the PR marsh population the difference in mean basin area remains the same order of magnitude (data not shown).

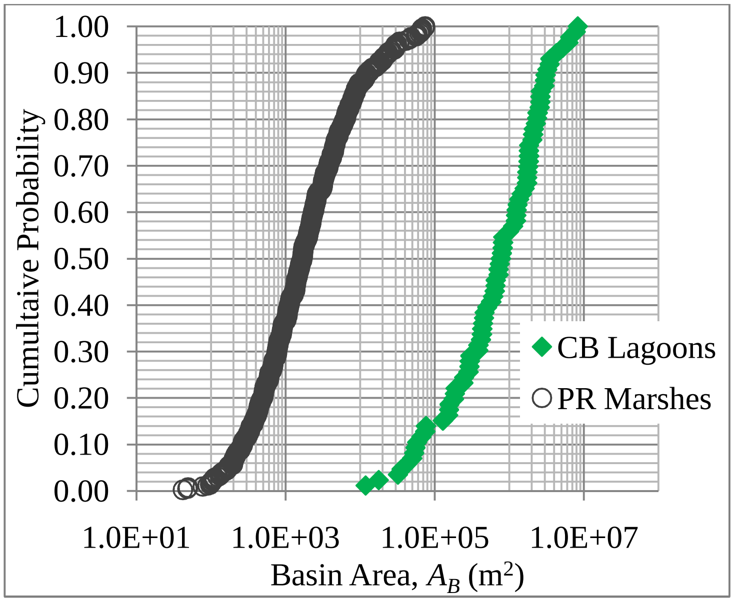

Figure 2.7: Cumulative probability distributions of basin area for CB lagoons and PR tidal marshes. Note the differences in maximum, minimum, and median basin size. Mean basin size (mean of 16th, 50th, and 84th percentiles) is significantly larger for lagoons (1,178,700 m^2 or 1.18 km^2) than tidal marshes (3,300 m^2 or 0.0033 km^2).

Tidal prism is a product of water surface area and tidal range; therefore in a regional study with similar tidal range, water surface area distributions are proxies for tidal prism distributions. The entire population of PR tidal marshes exhibit a power law for water surface area (Figure 2.8a), however, as before when marshes with upland tributaries are removed from the population, both PR marshes and CB lagoons exhibit truncated distributions (Figure 2.8b).

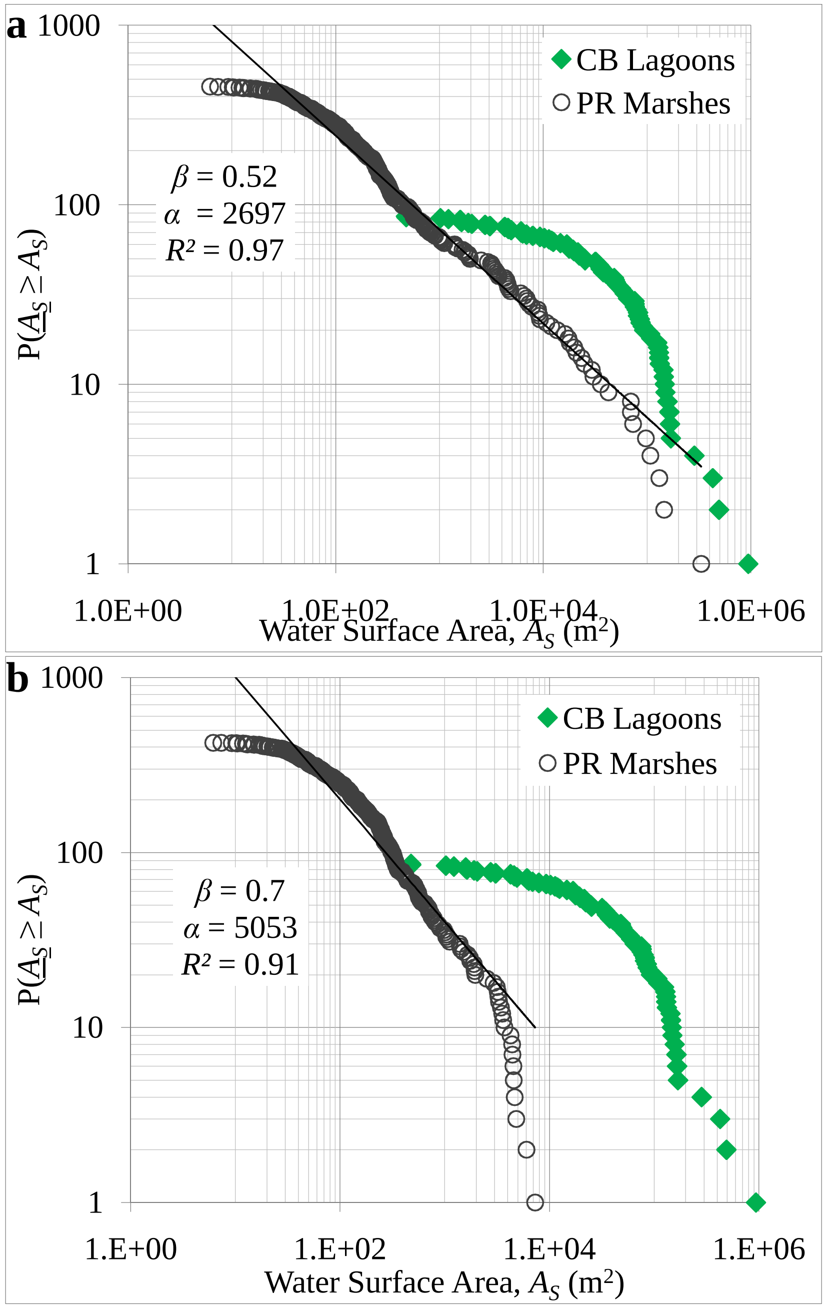

Figure 2.8: (a) PR marshes exhibit a power law relationship for water surface area, whereas CB lagoons do not. (b) When tidal marshes near terrestrial tributaries mouths are removed, the tidal marsh surface area shows a truncated distribution.

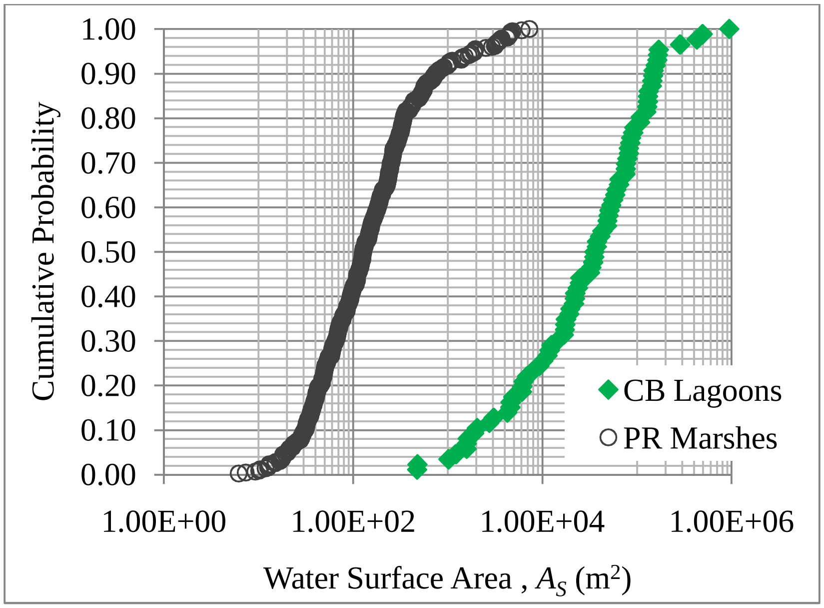

Figure 2.9: Cumulative probability distributions of water surface area for CB lagoons and PR tidal marshes. Note the differences in minimum, maximum, and median water surface area. Mean water surface area (mean of the 16th, 50th, and 84th percentiles) is 56,700 m^2 (0.0567 km^2) for lagoons and 210 m^2 (0.00021 km^2) for PR tidal marshes.

The mean surface area for CB lagoons is two orders of magnitude larger than the mean surface area for self-forming PR tidal marshes (Figure 2.9). Additionally, the minimum water surface area (475 m^2) necessary to form a CB lagoon is two orders of magnitude larger, indicating a threshold for formation.

Table 2.2: Bounding values for Chesapeake Bay lagoons and Patuxent River tidal marshes

	CB Lagoons			**Self-forming PR Marshes**		
	Lower Bound	Upper Bound	Range	Lower Bound	Upper Bound	Range
Basin Area (m^2)	11,835	8,308,059	8,296,224	42	74,300	74,258
Water Surface Area (m^2)	475	941,668	941,193	6	332,049	332,043
Spring Tidal Range (m)		0.41			1	

CB lagoons and PR tidal marshes not only show different types of distributions, for basin area and water surface area, but the data also have different ranges and bounding values (Table 2.2). The range of basin sizes that support CB lagoons is ~8,296,000 m^2; self-forming PR tidal marshes exist at a much smaller range of basin areas ~74,000 m^2. The ranges of water surface area values are on the same order of magnitude for both populations: ~941,000 m^2 for CB lagoons and ~332,000 m^2 for PR tidal marshes.

2.5.3 Comparison of geomorphic probability distributions for Chesapeake Bay and oceanic inlet-basin systems

Geomorphic data for oceanic inlet-basin systems are presented in this section and compared with data from CB marshes and lagoons. Both NSW and UK coastlines experience ocean waves, however tidal range for the two populations is very different. The southeast coast of Australia typically experiences a tidal range of 0.3 m (similar to CB) and almost never exceeds 0.5 m (Haines et al., 2006). Systems in the UK experience tides that range from micro-tidal (< 3 m) to supra-tidal (> 9 m), depending on location.

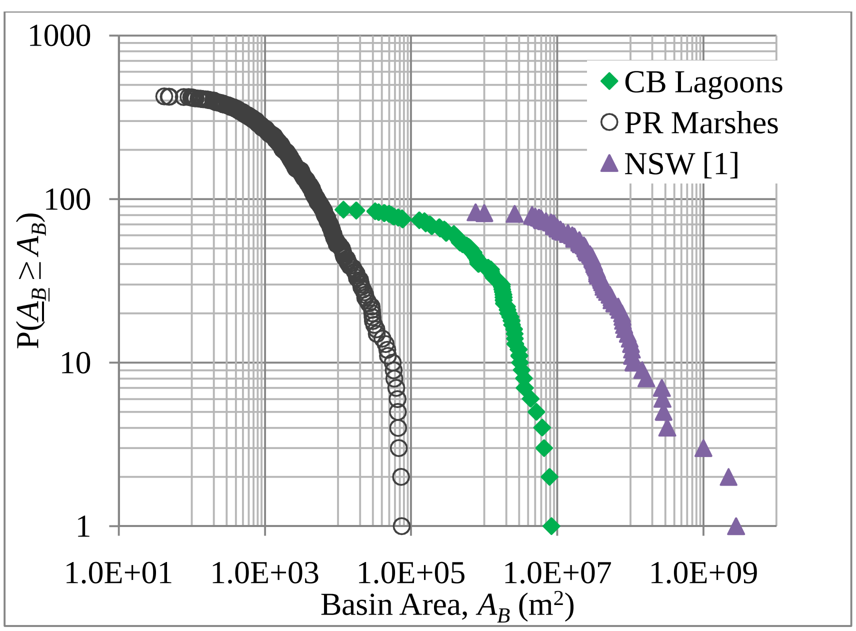

Figure 2.10: All populations show truncated distributions, indicating unique ranges of basin sizes for formation of each landscape type. [1]NSW data are from the NSW Office of the Environment and Heritage, accessed October 2010.

All three populations (Chesapeake lagoons, PR tidal marshes and NSW lagoons and creeks) exhibit truncated power law distributions for drainage basin area (Figure 2.10). NSW data have systematically larger basin areas than CB lagoons. The minimum basin area required for a NSW lagoon or creek to form is 760,000 m^2 (or 0.76 km^2), an order of magnitude larger than the minimum basin area required for a CB lagoon to form. Mean basin area is three orders of magnitude larger for NSW lagoons than CB lagoons (Figure 2.11). Basin area is often determined by regional geology and topography along with anthropogenic impacts such as storm water drains, channelization or damming. The variation in upper bounds on the basin area may be influenced by the size of the basin that can keep the waterway clear of sand in which an inlet might be constructed.

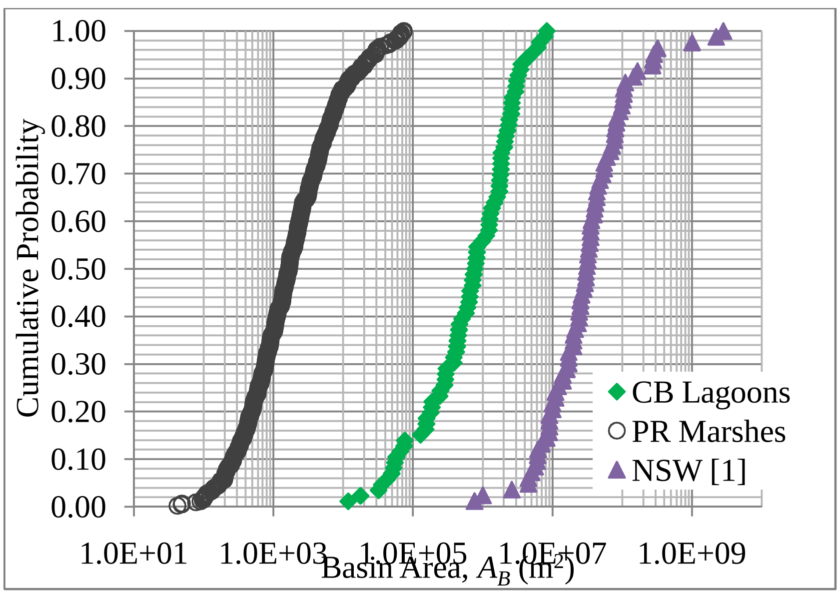

Figure 2.11: Cumulative probability plots show where the tails of the distributions overlap. There is a significant overlap between the large CB basins and small NSW basins. CB lagoons have a mean basin size (mean of the 16th, 50th, and 84th percentile) of 1,178,700 m^2 (1.179 km^2), PR marshes have a mean basin size of 3,300 m^2 (0.0033 km^2) and NSW have a mean basin size of 45,800,000 m^2 (45.8 km^2). [1]NSW data are from the NSW Office of the Environment and Heritage, accessed October 2010.

Comparison of water surface area distributions between CB lagoons and NSW data is useful because each experiences similar tidal ranges, but significantly different wave heights and periods. All populations show truncated power law distributions for water surface area (Figure 2.12). The bounding values for NSW water surface areas are 46,000 m^2 and 36,300,000 m^2. Estuaries in the UK exhibit a wide range of water surface areas from 180,000 m^2 to 666,540,000 m^2. CB lagoons overlap the smaller end-members of both of these populations, ranging from as small as 465 m^2 to 941,668 m^2.

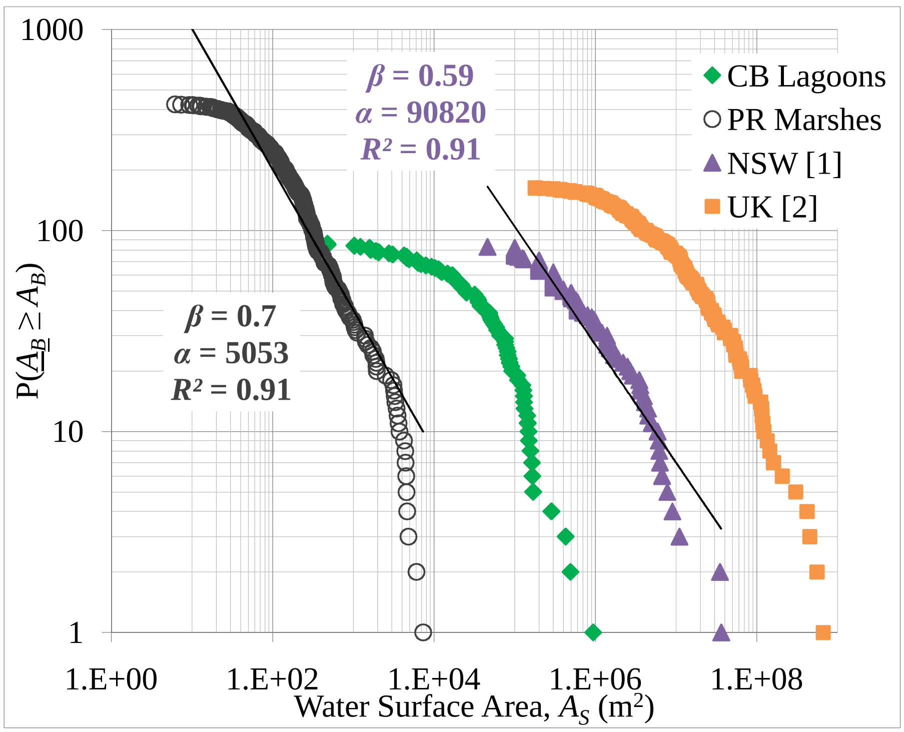

Figure 2.12: Water surface distributions for various inlet-basin populations' shows truncated distributions, indicating that there is a minimum water surface area necessary for formation. [1]NSW data are from the NSW Office of the Environment and Heritage accessed October 2010. [2]UK data are from Davidson and Buck (1997).

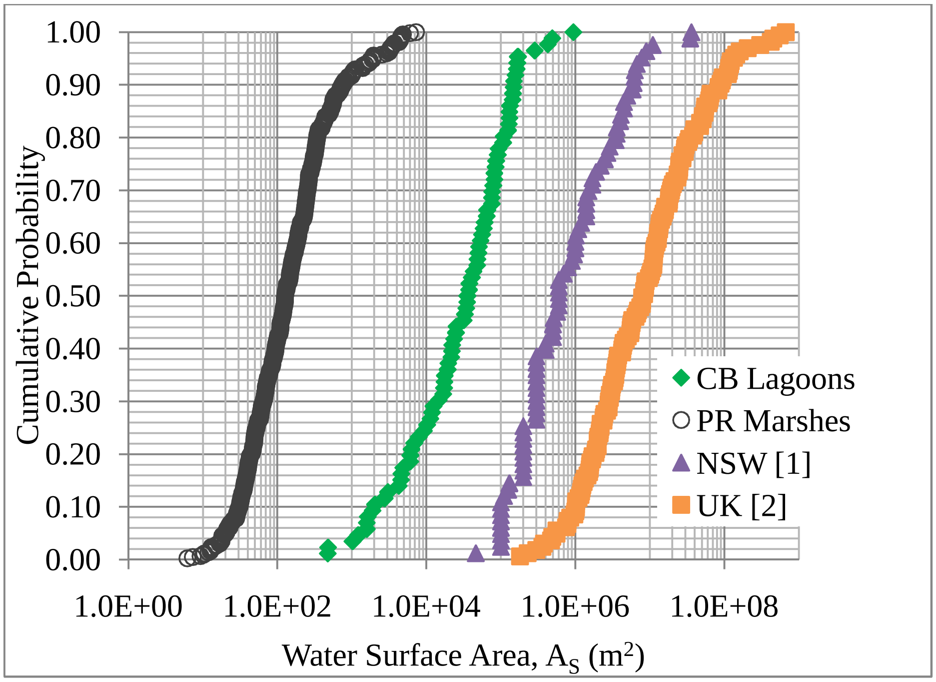

Figure 2.13: Cumulative probability plots for water surface area. CB lagoons have a mean water surface area (mean of the 16th, 50th, and 84th percentile) of 56,700 m^2 (0.0567 km^2), PR marshes have a mean water surface area of 210 m^2 (0.00021 km^2), NSW have a mean water surface area of 1,633,000 m^2 (1.63 km^2) and UK has a mean water surface area of 20,430,000 m^2 (20.4 km^2). [1]NSW data are from the NSW Office of the Environment and Heritage, accessed October 2010. [2]UK data are from Davidson and Buck (1997).

Mean surface area for UK estuaries is an order of magnitude larger than NSW lagoons and creeks and three orders of magnitude larger than CB lagoons (Figure 2.13). UK estuaries also experience the largest tidal ranges of all four populations; therefore it is expected that UK estuaries have the largest tidal prisms. NSW and CB experience similar spring tidal ranges, therefore lagoons and creeks along the NSW coast have larger tidal prisms than CB lagoons due to the relatively small water surface areas of CB lagoons. Additionally, because the spring tidal range is larger for PR tidal marshes than it is for CB lagoons, tidal prism should be larger for marshes with similar water surface areas as lagoons. Across all tidal range spectrums, inlet-basins with lagoons have larger water surface and larger basin areas than PR tidal marshes, which are formed by tidal inundation alone. This has implications for the role of drainage basin area and streamflow on controlling tidal prism for an inlet-basin.

2.5.4 Relationship of water surface area to basin area

The relationship between basin area (A_B) and water surface area (A_S) for CB tidal marshes and lagoons is shown in Figure 2.14. The relationship for self-formed tidal marsh systems is (Figure 2.14b):

$$A_S = 0.027 A_B^{0.83} \quad R^2 = 0.88 \tag{2.7}$$

and the relationship for CB lagoons is:

$$A_S = 0.038 A_B^{0.76} \quad R^2 = 0.49. \tag{2.8}$$

There is, however, wide scatter in this relationship, which is likely due to the heterogeneity of hydrologic response to land-use and soil type (Dillow, 1996) that may be enhanced by the small watershed sizes (< 10 km^2). Further investigation of causes of variation in this relationship will be conducted in Chapter 4, however the water surface areas that show significant variation are briefly examined here.

Ten lagoons with surface areas significantly smaller than the regional trend are shown in red on Figure 2.14b. These lagoons are from the eastern and western shore and have significant forest and/or wetland cover in the watershed or significant marsh vegetation encroachment into the lagoon. Seven of these lagoons have forest cover equal or greater than 80%; the remaining three have approximately 60-75% forest cover with significant marsh vegetation in the lagoon. Forest cover significantly reduces peak-flow estimates (Dillow, 1996), due to hydrologic storage in forested floodplains. Lagoons with water surface areas > 0.2 km^2 are also both western and eastern shore lagoons with a maximum of 30% forest cover (blue diamonds in Figure2.14b). Some of the lagoons with large water surface areas have significant agricultural and residential land-uses. This suggests that CB lagoons might respond to changes in land-use or climate that affect streamflow.

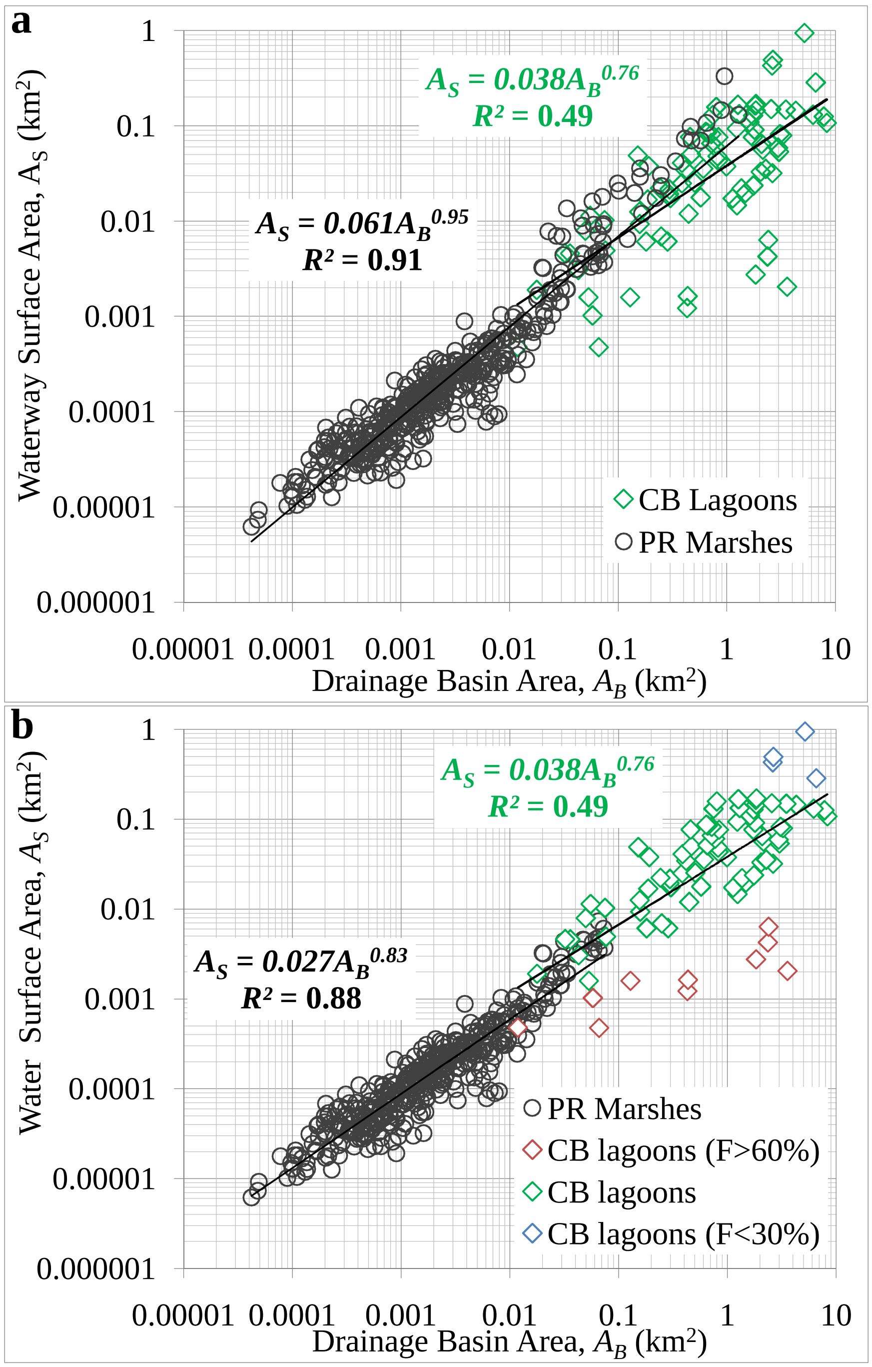

Figure 2.14: (a) Water surface area as a function of basin area for PR tidal marshes and CB lagoons. The PR marshes that overlap the CB lagoons have tributary basins. (b) PR marshes with upland tributaries have been removed from this plot.

These two regional populations show a transition from tidally dominated inlet-basins to tidal and streamflow dominated inlet-basins.

Some of the large PR tidal marshes ($A_B > 0.02$ km^2) have larger water surface areas than predicted by the power law: $A_S = 0.061 A_B^{0.95}$, therefore each of these marshes were examined individually for heterogeneities. The largest marshes are at the mouths of terrestrial tributaries, suggesting that these marshes receive streamflow runoff as well as tidal inflow. The tidal marsh data are provided as a comparison of water surface area created by tidal processes alone; therefore, these data were removed. The resulting transition from tidally-dominated end members with small water surface areas and streamflow-dominated lagoons with larger water surface areas is shown in Figure 2.14b.

CB lagoon and PR tidal marsh data were compared with data from NSW that have similar tidal ranges to CB lagoons (Table 2.3), but the NSW inlet-basins are oceanic lagoons that experience higher wave heights and longer wave periods. The relationship between drainage basin area and water surface area for NSW systems is:

$$A_S = 0.067 A_B^{0.71} \quad R^2 = 0.45. \tag{2.9}$$

Table 2.3: Bounding values for geomorphic populations

Basin Area, A_B (m^2)	**Lower Bound**	**Upper Bound**	**Range**
CB Lagoons	11,835	8,308,059	8,296,224
PR Marshes	42	1,277,976	1,277,934
NSW Lagoons & Creeks	760,000	2,800,000,000	2,799,240,000
Water Surface Area, A_S (m^2)	**Lower Bound**	**Upper Bound**	**Range**
CB Lagoons	475	941,668	941,193
PR Marshes	6	332,049	332,043
NSW Lagoons & Creeks	46,000	36,300,000	36,254,000
UK Estuaries	180,000	666,540,000	666,360,000
Spring Tidal Range, h_R (m)	**Lower Bound**	**Upper Bound**	
CB Lagoons	0.27	0.41	
PR Marshes	0.62*	1	
NSW Lagoons & Creeks	0.3	0.5	
UK Estuaries	< 3	> 9	

* lower effective tidal ranges are defined by the elevation of the tidal inlet.

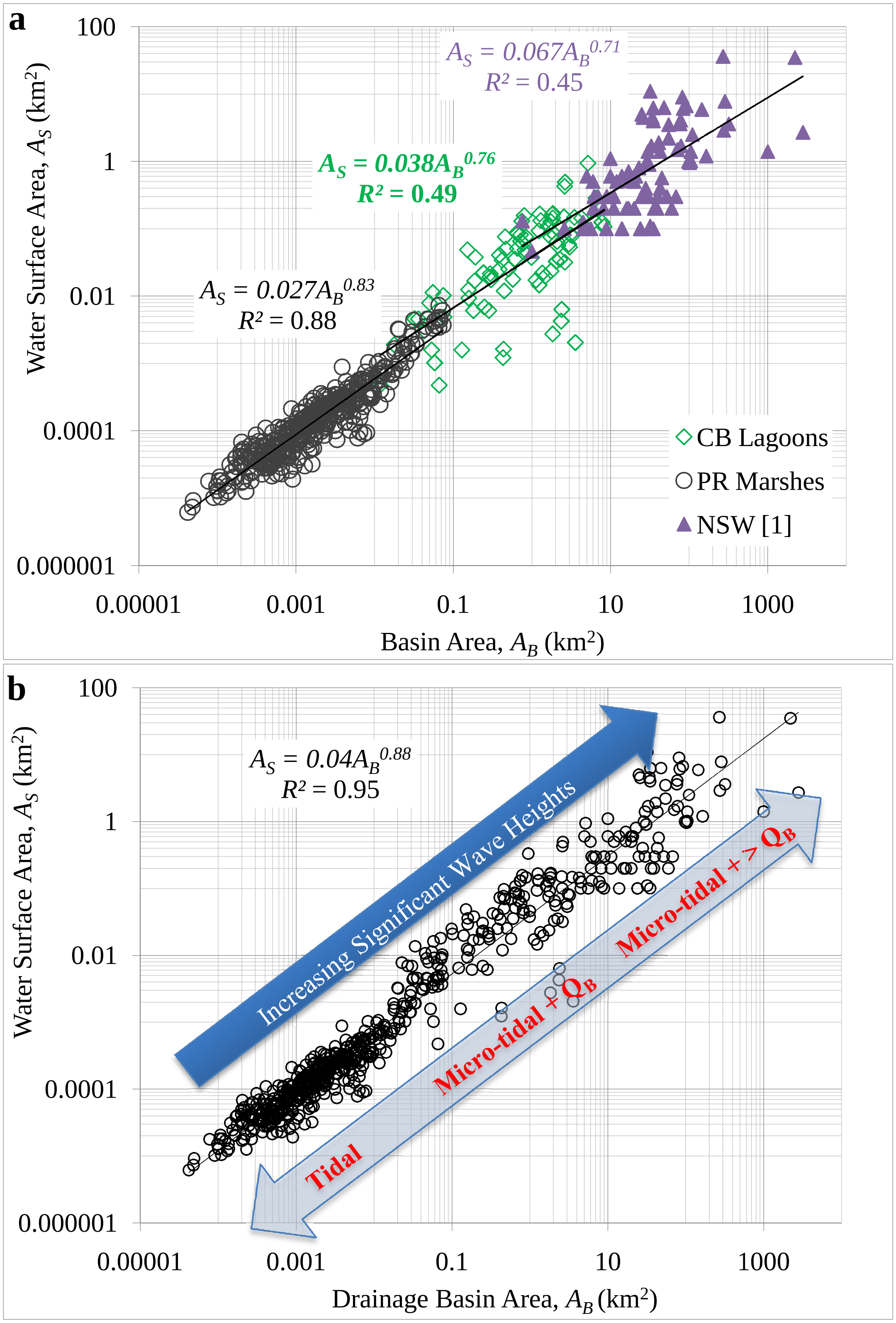

Figure 2.15: (a) Power law relationships between drainage basin area and water surface area, illustrating the range of each individual data set. (b) The general power law relationship for these systems with variations in wave, tidal and

streamflow characteristics. (NSW data are from the NSW Office of the Environment and Heritage, accessed October 2010).

The relationship for combined data for drainage basin area and water surface area for CB lagoons, PR tidal marshes and NSW lagoons is shown in Figure 2.15b. Each of the different systems occupies a separate portion of this graph (Figure 2.15a). The watershed area and lagoon water surface areas are considerably larger for NSW systems, but the relationship between water surface area and basin area for these systems is very similar (Figure 2.15). The general relationship exhibited between basin area (A_B) and water surface area (A_S) is:

$$A_S = 0.04 A_B^{0.88} \quad R^2 = 0.95. \tag{2.10}$$

This relationship suggests a strong relationship between drainage basin area and waterway area and is similar for streamflow prediction equations for many regions (Meigh et al., 1997; Dillow, 1996).

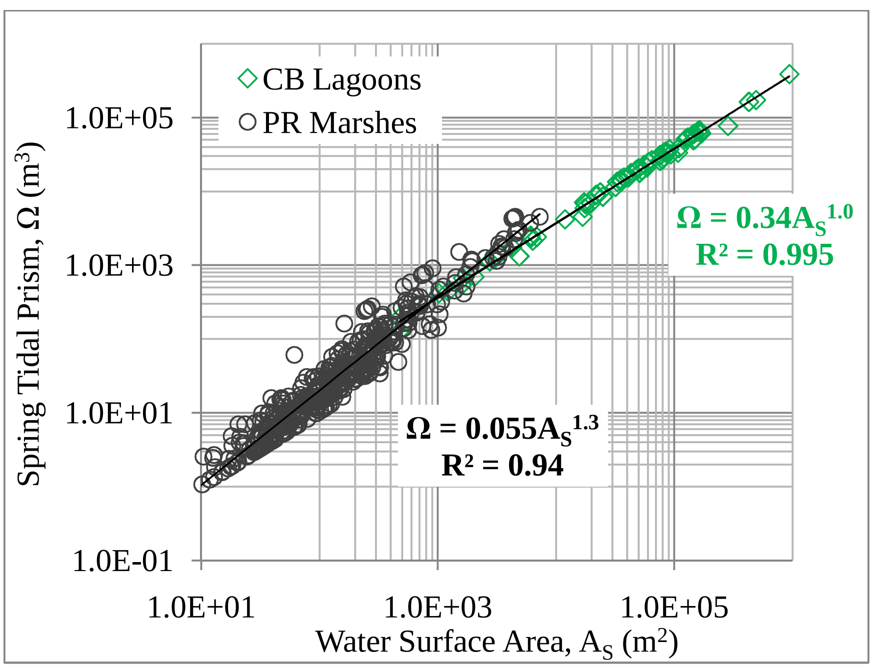

Figure 2.16: Spring tidal prism is plotted as a function of water surface area. For a given water surface area, PR marshes have a similar tidal prism to CB lagoons, but PR tidal marshes experiences a larger spring tidal range than CB.

The relative effect of tidal range and water surface area on the tidal prism can be investigated by plotting the spring tidal prism as a function of water surface area. These data for CB lagoons and PR tidal marshes are shown in Figure 2.16. The relationship that relates water surface area (A_S) to spring tidal prism (Ω) for CB lagoons is:

$$\Omega = 0.34A_S^{1.0} \quad R^2 = 0.995 \qquad (2.11)$$

and the relationship for PR tidal marshes is:

$$\Omega = 0.055A_S^{1.3} \quad R^2 = 0.94. \qquad (2.12)$$

CB lagoons have much smaller tidal ranges, and thus for a given water surface area would be expected to have a smaller tidal prism, however results show (see Figure 2.16) that tidal prisms are similar for CB lagoons and PR tidal marshes, with similar water surface areas.

2.6 Discussion

Previous work on coastal lagoons has focused on the relationship between tidal prism and inlet channel cross sectional area (e.g. Jarrett, 1976; O'Brien, 1976; 1931). This emphasis on tidal prism and "tidal" inlets has focused attention on the tidal component of lagoon formation and maintenance. In this study, I assumed that the area-prism relationship is an emergent property of inlet-basin systems and used a data-driven, downward modeling approach (Sivapalan, 2003; Klemes, 1983) to examine the components of tidal prism.

These data indicate a narrow range of values for both drainage basin area and water surface area in each population of inlet-basin systems. These boundaries are probably defined by underlying processes. Without significant wave action to fill tidal inlets, PR tidal inlets can be sustained at small dimensions (0.2 m in width) and these inlets form very small marsh drainage basins (~ 42 m^2). The upper bound for PR tidal marshes might be controlled by available riparian space or the distance water can travel into tidal marsh channels during a spring tidal cycle (Jenner, 2010).

Although CB and NSW systems have similar tidal ranges, the minimum drainage basin area for lagoon formation is much larger for NSW lagoons than CB lagoons. This suggests that the lower limit of supporting basin area is defined by a process, such as sediment transport by waves that truncates the lower portion of the geomorphic distribution. The upper bound may also be defined by wave transport. The upper bound of watershed areas associated with CB lagoons is a transition between drainage basins with coastal lagoons at their mouths and drainage basins with open sub-estuaries. These data suggest that stream discharge from larger watersheds can maintain inlet channel depths that are sufficiently large to prevent deposition of a beach across the channel inlet, through which a lagoon inlet channel could be built.

This research has generated an additional inter-regional, emergent relationship (the drainage basin-water surface area relationship) that appears to be as robust as the area-prism relationship for coastal lagoons. The inter-regional relationship illustrates the central tendency of these systems. Within a given region, such as the CB, the lagoon area to drainage basin area relationship indicates considerable scatter, which is consistent with the variability observed between stream discharge and basin area for small, Coastal Plain watersheds with heterogeneous topography, soils, and land-use (Birkinshaw et al., 2011; Daviau et al., 2000; Dillow, 1996).

2.7 Conclusions

The cumulative distribution of drainage basin areas contributing to PR tidal marshes, and the lagoon data for CB and NSW exhibit truncated power laws. These data indicate that the drainage basin area associated with each system (CB lagoons, PR tidal marshes, NSW lagoons) exist within a small window of drainage basin area. The sizes of self-formed drainage basins created by PR tidal marshes (42 to 7.3E4 m^2) are much smaller than the drainage basin areas that contribute to CB lagoons (1.1E4 to 8.3E6 m^2) or NSW lagoons and creeks (4.6E5 to 3.6E7 m^2). Examination of coastal watersheds in CB indicates that larger coastal watersheds are present, but coastal lagoons do not form at their mouths.

The size distribution of water surface areas also show relatively narrow ranges for each population. Each of these systems show upper and lower boundaries that restrict associated water surface areas to a narrow range of values.

The relationship between basin area and water surface area is similar across the three inlet-basin system populations that experience different tidal ranges, significant wave heights, and stream flow inputs. Each of these three populations (CB lagoons, PR tidal marshes, and NSW lagoons and creeks) occupies a different region of the emergent power law. Examined individually, the tidal marshes have higher exponents for the power law, than NSW and CB lagoons. The power law exponent for the drainage basin-water surface area relationship for CB lagoons is similar to that for drainage basin area – stream peak discharge relationships (Dillow, 1996), and the inter-regional relationship also has an exponent consistent with regional flood frequency relationships (Menabde and Sivapalan, 2001; Meigh et al., 1997), which suggests that this emergent relationship might be controlled by stream discharge.

Chapter 3: Inlet Cross Sectional Area and Sediment Characteristics

3.1 Introduction

Inlet channels that connect coastal lagoons to estuaries or oceans are found along coastlines around the world. Inlets to coastal lagoons have been examined along the U.S. Coastline and numerous studies (O'Brien, 1976; Johnson, 1973; Escoffier, 1940; O'Brien, 1931; LeConte, 1905) have developed and extended an empirical relationship between the inlet cross sectional area (A_C) and the tidal prism (Ω). Jarrett (1976) compiled available data for U.S. inlets and determined the following relationship: $A_C = 0.000158\ \Omega^{0.95}$. This relationship also applies to inlet data from the United Kingdom (UK), and New Zealand (NZ) oceanic coastlines (Townend, 2005; Hume and Herdendorf, 1993; 1992). Small tidal inlets, such as those along Chesapeake Bay (CB) shorelines however, appear to diverge from the area-prism relationship defined for inlets along oceanic coastlines (Hughes, 2002; Byrne et al., 1980).

Previous research on small inlets ($A_C < 100$ m^2) has shown that Jarrett's empirical area-prism relationship ($A_C = 0.000158\ \Omega^{0.95}$) under-predicts cross sectional area for small inlet-basin systems (Hughes, 2002; Seabergh et al., 2001; Byrne et al. 1980; Mayor-Mora, 1977). Bryne et al. (1980) found that CB inlets are larger than predicted from Jarrett's area-prism relationship. Previous research has attributed these deviations to the smaller waves, basin areas and tidal ranges that are found in CB. In the previous chapter, I evaluated the relationship between drainage basin area and water surface area and determined that CB systems follow similar relationships as other lagoon systems. This suggests that the differences in the area-prism relationship for CB systems may be caused by processes that control inlet cross sectional area. Figure 3.1 shows a lagoon inlet, viewed from two different directions.

Figure 3.1: Drum Point lagoon inlet. (a) Looking towards the bay, waves bring sand and gravel sized sediment into the inlet. Ebb-tidal currents must maintain a critical velocity in order to scour the inlet. (b) Looking landward, the inlet banks are stabilized as the inlet meanders through vegetation. Inlet cross sections were measured where the vegetation ends and the beach begins. Image taken May 21, 2011.

Byrne et al. (1980) examined small inlets in the CB and found that they have smaller width to depth ratios and small maximum tidal velocities compared with oceanic inlets. Hughes (2002), however, suggested that maximum velocity is not as useful of a parameter for determining inlet geometry equilibrium. Due to differences in tidal and streamflow conditions, maximum velocity at a single cross sectional area may vary by an order of magnitude, Hughes (2002) suggested a wide variety of factors, such as different primary flow channels, multiple inlets over time, or changes in littoral drift rates, that can affect inlet cross sectional area. Hughes developed a theoretical approach to predict equilibrium channel area, but in his analysis of CB inlets, he had to estimate sediment size. In this analysis, I propose that cross sectional area and its relationship to tidal prism might be influenced by streamflow and sediment size.

Byrne et al. (1980) suggested that the mean of the maximum flow velocities through CB inlets is approximately 0.35 m/s. This value was suggested as the lower limit of velocity required to transport medium to fine sand in the inlet and therefore it provides a lower limit of inlet stability. Coarse sediment in the CB, however, can be easily mobilized on beaches due to the short period waves with high local acceleration (Grasso et al., 2011). Therefore, sediment size may not be restricted to the sand sizes common on ocean beaches, and must be sampled.

In the previous chapter, I examined factors that control water surface area and thus tidal prism for tidal marsh and lagoon systems in CB and other select locations. In this chapter, I will examine factors that influence inlet cross sectional area. As in the previous chapter, the approach will be to measure or estimate parameters for the entire population of CB lagoon inlets and to compare these data to Patuxent River (PR) tidal marsh inlet channels and inlets from oceanic lagoon systems.

3.2 Hypotheses

i. Due to streamflow contributions from terrestrial watersheds, CB lagoon inlet widths will have larger average and maximum values than PR tidal marshes.

ii. Probability distributions of inlet width for CB lagoons and PR marshes can be expressed as power laws.

iii. Tidal inlet grain size for most inlets is larger than 0.25 mm, and grain size will provide an explanation for the larger cross sectional areas for CB lagoon inlets.

iv. Due to underlying contributions of streamflow discharge, inlet geometry data for a representative sample of lagoon inlets will behave as a homogeneous hydrological system as indicated by their hydraulic geometry relationships.

3.3 Methods

3.3.1 Measurement of channel width

CB lagoons and PR tidal marshes are first identified as permanent features in the landscape by viewing USGS air photo images from the period (1993 to 2011) accessed via Google Earth. Inlet widths were measured using a GIS program, MD MERLIN Online, which uses high-resolution photo images from April 2007. The inlet width will change over time due to natural or human-induced processes; therefore a common sampling date was used in this analysis. In addition, lagoon inlets have variable widths along their lengths, therefore all lagoon inlets were measured just landward of the beach. Lagoon channels at this location are typically stabilized by vegetation. Therefore, measurement of width at this location will provide a measurement of the equilibrium inlet width.

Cumulative distributions of inlet width will be compared for CB lagoon and PR tidal marsh data. If inlet width exhibits a power law distribution then it is *not* scale dependent, whereas if the population does not exhibit a power law, then different processes at different scales may control inlet width.

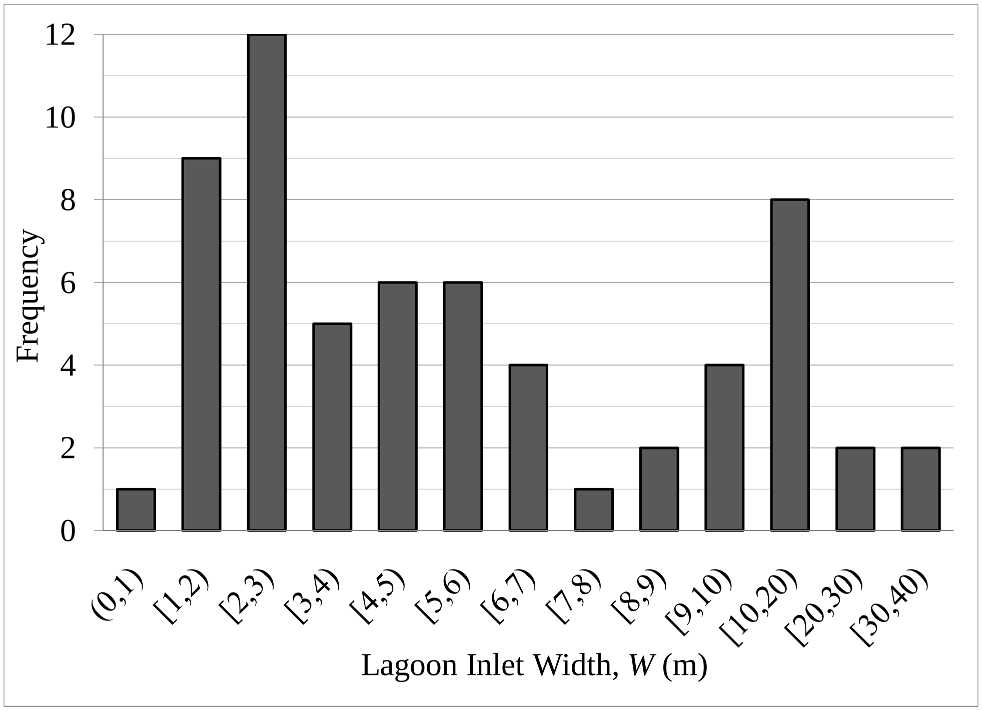

Figure 3.2: Inlet widths for CB lagoons were logarithmically binned in order to determine a sampling regime. Sites were chosen based on the width of the channel inlet and ease of access to the field site.

Sample sites for field measurement were chosen by logarithmically binning inlet width data to identify the distribution of inlet sizes (Figure 3.2). From these data, a sampling scheme was developed such that a proportional number of field sites were chosen from the bimodal distribution. The histogram indicates that over 80% of CB lagoon inlets are less than 10 m in width, therefore a proportional number of field sites were chosen to have widths less than 10 m. Of the 14 inlets chosen to measure, 12 (~86%) were less than 10 m wide and 2 (~14%) were greater than 10 m wide.

3.3.2 Field measurements of cross sectional area

Inlet cross sectional area was measured at 14 CB lagoon inlets sites and sediment samples were retrieved from 11 of these inlets. One cross section was measured at each field site, with an except for Brownies Beach where a foot bridge occupied the site where the cross section measure should be; therefore, cross section measurements were made above and below the bridge. A cross section for one of the larger inlets, at Price Creek, was obtained from NOAA Nautical Chart 12270. These additions provide 16 total cross sectional area measurements; 13 (~81%) inlets less than 10 m wide and 3 (~19%) inlets greater than 10 m wide.

Each cross section was measured from the left bank, facing shoreward toward the lagoon following the midsection method, outlined by the United States Geological Survey (USGS). The total cross sectional area is determined by first sectioning the width so that a rectangle is formed around each depth measurement (Buchanan and Somers, 1969). The area of each small rectangle is the product of the small width section (W_i) and the depth (D_i) that is bisecting the small width section (Figure 3.3). The total cross sectional area is the sum of these small areas:

$$A_C = \sum A_i = \sum W_i \, x \, D_i \tag{3.1}$$

Accurate measurement of the channel cross section requires measurement of sufficient verticals in a cross section. Although the number of measurements to define the cross section depend upon cross section complexity, 15-20 measurements within a simple channel, with a flat bed, are sufficient to define the channel.

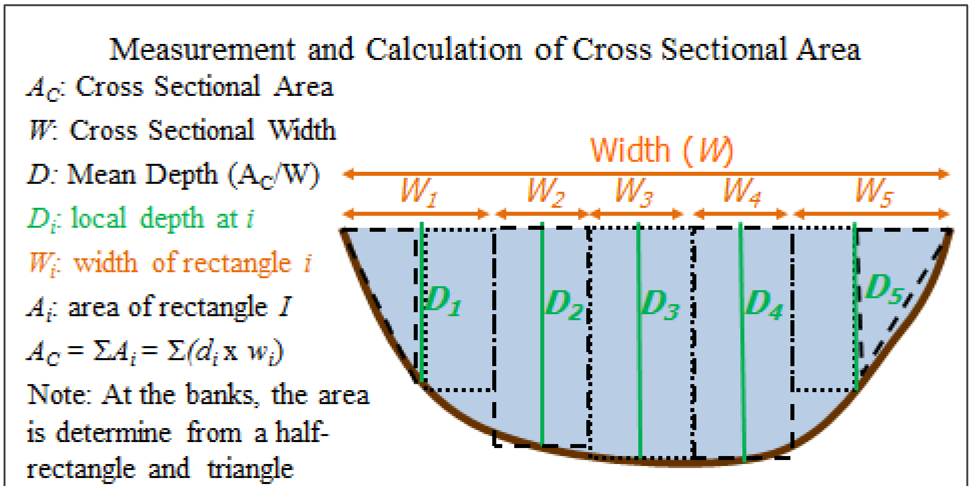

Figure 3.3: Definition sketch of cross sectional area. The cross sectional area is found by summing the rectangles (W_i x D_i) and outer triangles (½ W_i x D_i). Average depth is defined as the cross sectional area divided by the width.

3.3.3 Determination of relationships between inlet width and cross sectional area

Field measurements of cross sectional area were conducted on a representative sample of all inlets. These data were used to determine a relationship between inlet width and cross sectional area. This relationship is used to estimate inlet cross sectional area from channel width for inlets not measured in the field.

3.3.4 Inlet grain size distributions

Sediment samples from the bed of channel inlets were collected from 11 of the CB inlets for grain size analyses following the methods of Folk and Ward (1957). Before sieving, each sample was weighed and then sieved through -4 ϕ, -3 ϕ, -2 ϕ, -1 ϕ, 0 ϕ, 0.2 ϕ, 0.5 ϕ, 1 ϕ, 1.3 ϕ, 2 ϕ, 2.5 ϕ, 3 ϕ, and 4 ϕ sieves; the sediment caught by each sieve pan was weighed individually and recorded. Sieving was done in two steps: first the entire sample was sieved for 10 minutes through the -5 ϕ to 0.5 ϕ sieves and then the remaining sediment was sieved for 10 minutes through the 1 ϕ through 4 ϕ sieves. Grain size diameter (d) is reported in mm, where $\phi = -log_2(d)$. Cumulative weight percent is used to determine median grain size (d_{50}) and mean grain size (d_{MEAN}), defined as:

$$d_{MEAN} = \frac{d_{84} + d_{50} + d_{16}}{3} \tag{3.2}$$

where d_{84} is the 84th cumulative percentile, d_{50} is the 50th cumulative percentile and d_{16} is the 16th cumulative percentile (Prothero and Schwab, 1996).

<u>*3.3.5 Theoretical prediction of equilibrium inlet area (after Hughes, 2002)*</u>

Recently, Hughes (2002) derived a process-based relationship, which predicts cross sectional area (A_C) in the form of:

$$A_c = 0.87\left[\frac{W^{1/9}}{g(S_S - 1)^{4/9} d_{50}^{1/3} T^{8/9}}\right]\Omega^{8/9} \tag{3.3}$$

where W is the inlet width, g is the acceleration due to gravity, S_S is the sediment specific gravity (ρ_S/ρ_W; where ρ_S is the density of the sediment and ρ_W is the density of water), d_{50} is the median grain size diameter, T is the tidal period and Ω is the tidal prism ($\Omega = A_S h_R$; where A_S is water surface area and h_R is tidal range). The coefficient (0.87) was empirically derived to provide a best-fit area-prism relationship for small and large inlets. In his conclusions, however, Hughes (2002) acknowledges that the small CB inlets do not fit the proposed relationship. This result, however, could be due to an underestimation of grain size; Hughes (2002) used an estimated median grain size for CB inlets to be 0.25 mm. Actual values that are significantly coarser than this estimated size could affect the predictions.

In order to test the Hughes (2002) equation, I will use field measurements of inlet characteristics and actual values of grain size. An average grain size for each region of the CB (South West, Central West and Eastern) will be established and used for lagoons where sediment sampling was not conducted. The sediment specific gravity (S_S) of quartz (2.65) is used in all calculations, which is a reasonable estimate based on field observations.

3.3.6 Determination of tidal prism, tidal range and tidal period

The tidal prism is calculated as: $\Omega = A_S h_R$ where A_S is the water surface area and h_R is the tidal range. The tidal range for spring (high) tides is used to calculate tidal prism. Water surface area is measured using the GIS program MD MERLIN Online (http://www.mdmerlin.net/). Tidal data are retrieved from tide stations in CB, operated by National Oceanic and Atmospheric Administration (NOAA). Tidal period was found by analyzing an annual data series of tidal ranges and tidal periods from the NOAA Annapolis tide station. The average tidal period (24,000 s) associated with the average spring tidal range was chosen to represent the tidal period for spring tides for CB lagoons.

3.3.7 Determination of channel hydraulic geometry

Field measurements were used to determine “bankfull” width, depth, and channel area for selected CB lagoon inlets. These field measurements are also used to determine an estimate of maximum velocity (U_M), which was determined by assuming critical flow with a Froude number = 1:

$$U_M = \sqrt{gD} \tag{3.4}$$

where g is the acceleration due to gravity and D is mean inlet depth (Bruun, 1967; Henderson, 1966). This velocity is used to calculate inlet discharge (Q_M), defined as:

$$Q_M = U_M A_C \tag{3.5}$$

where U_M is mean channel velocity and A_C is cross sectional area.

The relationship of the hydraulic variables width, depth, and velocity to bankfull discharge is evaluated for the sites measured in the field. For river systems, width, depth, and velocity are expressed as power functions of discharge and the sum of exponents and product of coefficients are constrained by continuity and are equal to unity (Leopold and Maddock, 1953). Although there is not necessarily a continuity constraint among isolated lagoon inlet channels, width, depth, and velocity might exhibit hydraulic geometry relationships due to an underlying control of watershed discharge:

$$W = a(Q_M)^b \tag{3.6}$$

$$D = c(Q_M)^f \tag{3.7}$$

$$U_M = k(Q_M)^m \tag{3.8}$$

where W is inlet width, D is mean inlet depth, U_M is mean cross sectional velocity and b, f, and m and a, c, and k are empirically derived exponents and coefficients, respectively (Leopold and Maddock,1953). The inlet cross sectional area (A_C) can also be expressed as a power function of discharge (Q_M):

$$A_C = x(Q_M)^Z \tag{3.9}$$

such that x and z are also empirically-defined coefficient and exponent, respectively. For systems constrained by continuity, the coefficients $a*c*k = 1$ and exponents $b + f + m = 1$.

Channel morphology responds to two independent variables: discharge and sediment characteristics (Leopold et al., 1964). For lagoon inlet systems, discharge is from both tidal and watershed sources, while sediment characteristics at the inlet are primarily supplied by onshore transport by waves (Grasso et al., 2011; Hume and Herdendorf, 1992; Fitzgerald, 1988; Bruun, 1967). To incorporate sediment characteristics into regional assessments of hydraulic geometry, Parker (1979) developed dimensionless hydraulic geometry equations that are commonly used for regional assessments when grain size characteristics vary among systems with similar discharge. These, dimensionless hydraulic geometry parameters are:

$$W* = \frac{W}{d_{84}} \quad (3.10)$$

$$D* = \frac{D}{d_{84}} \quad (3.11)$$

$$Q* = \frac{Q_M}{\sqrt{gd_{84}}\, d_{84}^2} \quad (3.12)$$

where *W** is dimensionless inlet width, *D** is dimensionless inlet depth, d_{84} is the 84th cumulative percentile of grain size at the surface of the channel bed, *Q** is dimensionless discharge and *g* is the acceleration due to gravity (Parker et al., 2003; Ashmore and Parker, 1983; Parker, 1979). Leopold and Wolman (1957) found that flow resistance is often created by the grain size that is one standard deviation above mean grain size (84th percentile). Wiberg and Smith (1987) later confirmed this theory, demonstrating that sediment transport across a poorly-sorted, heterogeneous bed exhibits much different critical shear stresses than a well-sorted bed of uniform grain size. Therefore the grain size of morphological importance for this study is the d_{84} grain size.

3.4 Results

3.4.1 Inlet width probability distributions for Chesapeake Bay lagoons and Patuxent River tidal marshes

The inlet width was measured for the entire population of CB lagoons (Figure 3.4). The width characteristics were compared with the width measurements for the entire population of PR tidal marshes. These data were examined to determine upper and lower bounds, cumulative probability, and power law behavior.

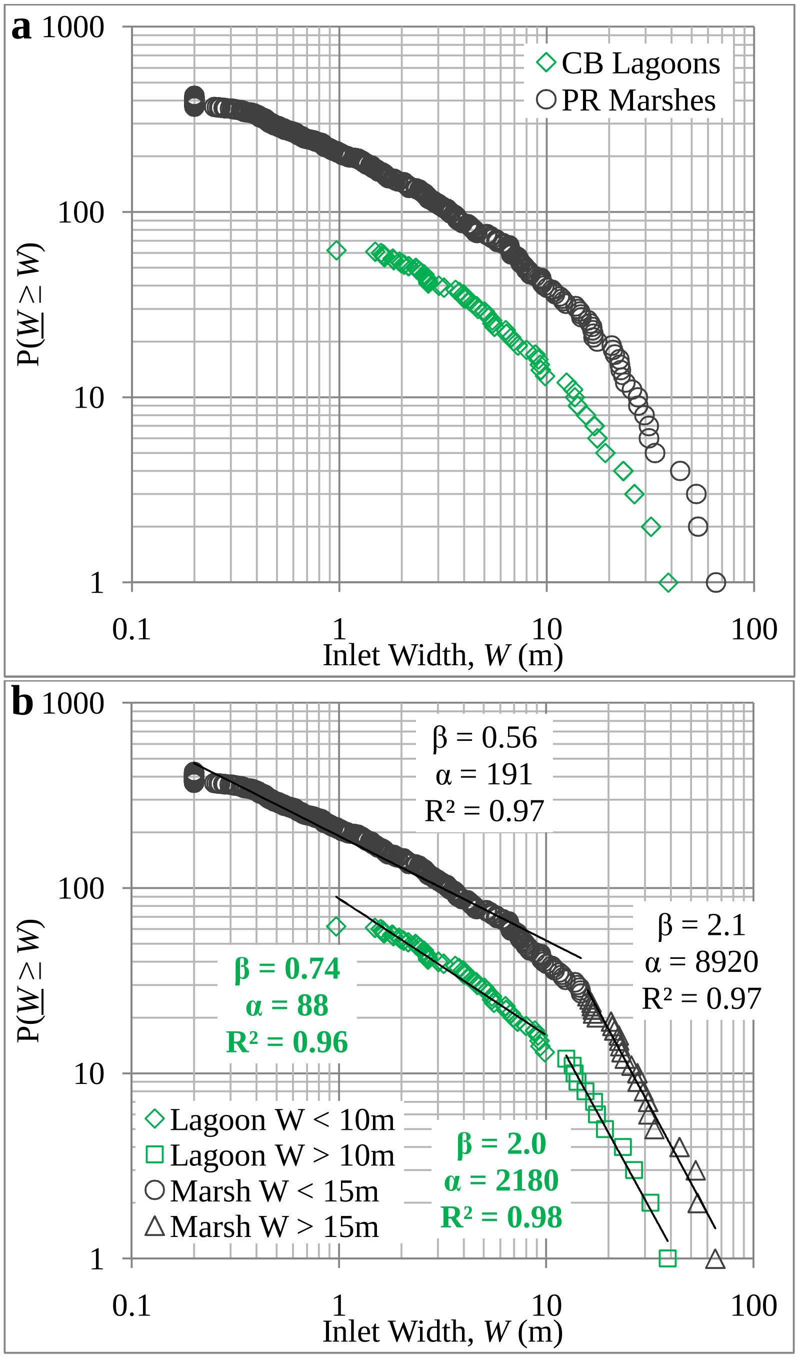

Figure 3.4: (a) CB lagoons and PR marshes do not exhibit a power law for the entire population of inlet widths; (b) however, both populations exhibit a bifractal distribution, with fractal dimensions of 2 for the larger inlet populations.

The power law equations for the two populations of inlet width data are similar. Neither population is a simple power law; therefore, these data were treated as a bifractal distribution where two power laws were used to explain each population of inlet width data. The breakpoint in each population was determined to be a function of inlet depth. Marshes with inlet widths less than 15 m experience a bankfull tidal range equal to their maximum depth, which is less than the full tidal range and they drain completely during spring low tides. Inlets with widths greater than 15 m experience the full tidal range and do not completely drain during low tides. The transition point between the two fractal distributions for lagoon inlet width occurs at 10 m. This break corresponds to a transition from predominately naturally opened inlets without jetties to predominately-altered inlets with one or two jetties. Systems that are engineered for navigation by jetties only include inlets that do not completely drain during most low tides. Jetties restrict width and thus increase depth and velocity for the same bankfull discharge. This reduces the width to depth (*W/D*) ratio. The value of the exponent (β) for the lagoon inlets with width greater than 10 m for CB lagoons and greater than 15 m for PR tidal marshes have values of β~2, which indicates a space filling feature (Rodriguez-Iturbe and Rinaldo, 1997; Tarboton et al., 1988; Mandelbrot, 1983).

Cumulative probability plots of inlet width (Figure 3.5) indicate upper and lower bounds, and median inlet width values for CB lagoon and PR tidal marsh inlets. Median inlet width is larger for CB lagoons than for PR tidal marshes, yet the largest PR marsh inlet width is greater than the largest CB lagoon inlet (Figure 3.5). There are proportionally more small tidal marsh inlets than there are small lagoon inlets.

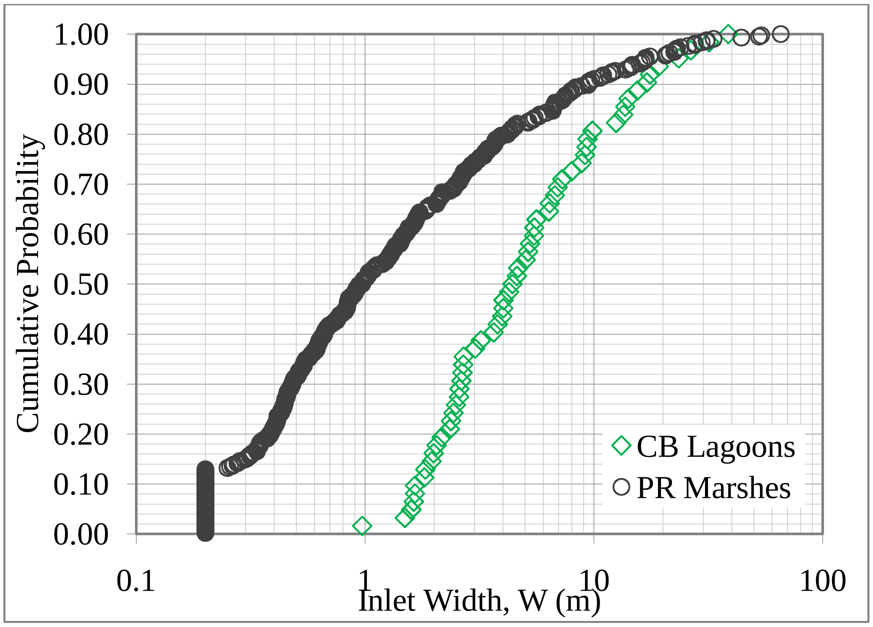

Figure 3.5: Cumulative probability distributions show where the tails of each distribution overlaps. Mean inlet size is determined by averaging the 16th, 50th, and 84th percentile. Lagoons have a mean inlet width of 6.6 m, whereas marshes have a mean inlet width of 2.4 m.

Upper and lower bounds of inlet width can also be determined from these probability distributions. Differences in tidal range, grain size, and significant wave height may play a role in the different bounding values for the two populations. The smallest CB lagoon inlet is 0.97 m wide, whereas the smallest PR tidal marsh inlet is 0.2 m wide. These lower bounds were validated with field measurements. The upper bound for PR tidal marshes (65.5 m) is greater than the upper bound for CB lagoon inlets (38.6 m), which represents a transition to a different type of inlet-basin system, such as an embayment, sub-estuary or marsh (Figure 3.5).

3.4.2 Morphology of Chesapeake Bay lagoon inlets

Field measurements of CB lagoon inlets provided morphologic data that are evaluated in this section to determine the range of characteristics and to identify controls on equilibrium channel cross sections (Table 3.1). These data were compared with similar data for CB inlets from Byrne et al. (1980) and are used to establish a relationship between inlet width and cross sectional area (Figure 3.6).

Table 3.1: Geometric characteristics of Chesapeake Bay lagoon inlets

No. Lagoon Name	Cross Sectional Area (m^2)	Width (m)	Depth (m)	*W/D* ratio
78 Bay Drive	0.99	7.92	0.12	64
45 Big Pond	3.55	8.84	0.40	22
12 Biscoe Pond	1.57	5.79	0.27	21
47 Blackwalnut	1.79	6.55	0.27	24
39 Brownies Down	0.06	2.13	0.03	78
39 Brownies Up	0.45	4.88	0.09	53
80 Carter Creek	10.52	17.98	0.59	31
49 Chase Pond	0.85	3.57	0.24	15
25 Drum Point	0.18	3.35	0.05	67
42 Herring Bay	9.49	12.19	0.78	16
60 Hines Pond	0.52	3.05	0.17	18
23 Long Lane	1.93	4.27	0.45	9
41 North Beach	0.41	1.86	0.22	8
79 Price Creek	20.193	26.50	0.76	35
13 St James Church	4.74	6.55	0.72	9
75 Terrapin South	3.28	7.62	0.43	18

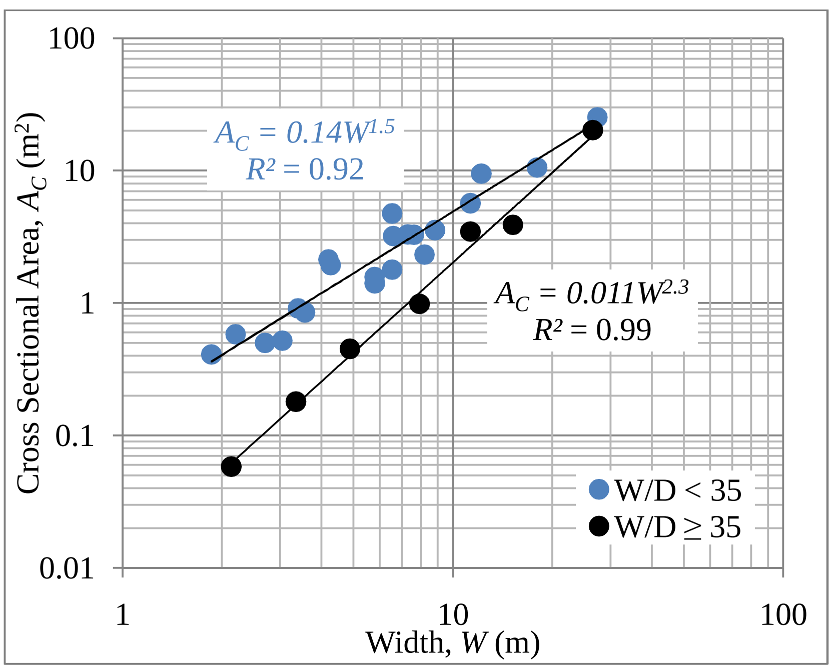

Figure 3.6: The relationship between inlet width and cross sectional area show two relationships. Data shown in blue have an average *W/D* ratio of 23 (*N* = 21), whereas data shown in black have an average *W/D* ratio of 56 (*N* = 7). The power

law represented by blue circles ($A_C = 0.14W^{1.5}$) can be used to estimate a streamflow-dominated cross sectional area. The power law exhibited by black circles ($A_C = 0.011W^{2.3}$) shows an alternative relationship for cross sectional area. Data are from this study and Byrne et al. (1980).

The channel width-cross sectional area data indicate two different relationships (Figure 3.6), which might be alternate stable states (Holling, 1973). As observed in most studies of inlet geometry (Townend, 2005; Hume and Herdendorf, 1992; Jarrett, 1976; O'Brien, 1976), there is a range of cross sectional area values for a given inlet width, which produces significant scatter in the cross sectional area data to be used in an area-prism relationship. The larger values of area measured in both this study and by Byrne et al. (1980), are interpreted to be the equilibrium cross sectional area formed during channel opening events. The alternative relationship with smaller cross sectional depths might represent the alternative channel morphology when the channel is altered by infilling sediment, transported by waves. The equation for the maximum channel areas is:

$$A_C = 0.14W^{1.5} \text{ for } W/D < 35 \quad R^2 = 0.92 \tag{3.13}$$

where A_C is cross sectional area, W is inlet width and D is inlet depth. This relationship is similar to the relationship derived from inlet geometry data from Byrne et al. (1980):

$$A_C = 0.15W^{1.5} \text{ for } W/D < 35 \quad R^2 = 0.94 \tag{3.14}$$

that was collected more than 30 years ago.

Inlets that have shallow depths (large width to depth ratios) exhibit a different power law relationship:

$$A_C = 0.11W^{2.3} \text{ for } W/D \geq 35 \quad R^2 = 0.99 \tag{3.15}$$

where A_C is cross sectional area, W is inlet width and D is inlet depth. These inlets have partially filled in with sediment transported into the inlet by waves (e.g. see Figure 3.1) and might be considered the wave-dominated stable state. Note that the two trends converge at the upper end of the width values, which is associated with lagoon inlets that are always open and do not close temporarily due to sediment transport by waves (Figure 3.6).

Plots of inlet width as a function of inlet depth also reveals two distinct states of inlet geometry (see Figure 3.7). Those inlets with width to depth ratios greater than 35 show a different relationship between width and depth, than inlets with width to depth ratios less than 35. This diagram also suggests that the width is a stable feature of the tidal inlet and that inlet depth shifts from one state to another, depending upon recent dynamic events.

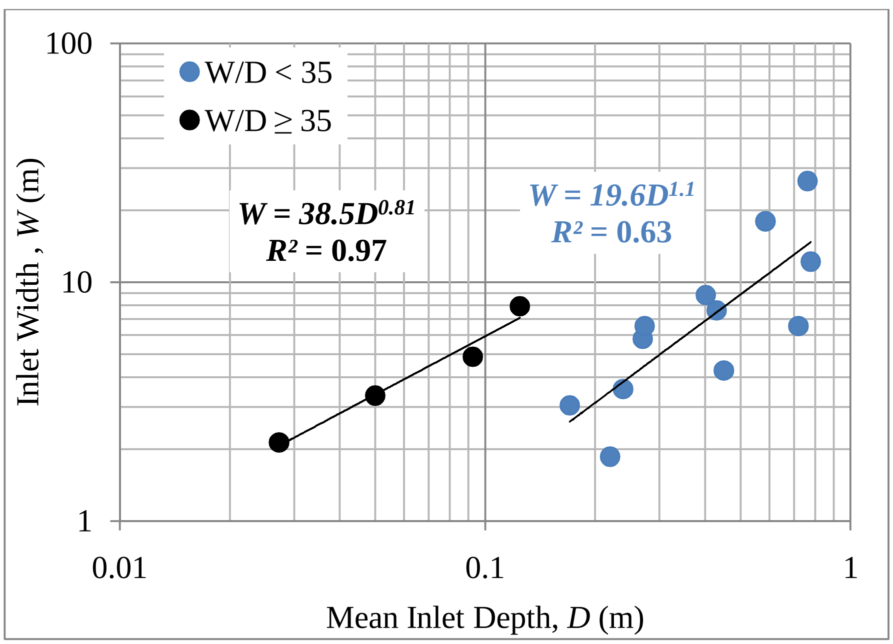

Figure 3.7: Inlet width plotted as a function of inlet depth shows a strong relationship for alternate stable state inlets with *W/D* ratios greater than 35.

3.4.3 Grain size analyses for Chesapeake Bay lagoon inlets

Sediment samples were sieved to determine grain size distributions for CB lagoon inlets (see Appendix A for cumulative grain size plots). Analysis shows that CB has a heterogeneous grain size distribution (see Table 3.2). The South Western shoreline of CB, which has 38 lagoons along its coast, has a median grain size (d_{50}) of 0.7 mm and a mean grain size (d_{MEAN}) of 1.2 mm. The Central Western shoreline, which has 25 lagoons, has a median grain size (d_{50}) of 0.5 mm and a mean grain size (d_{MEAN}) of 0.7 mm. Finally, the Eastern shore, which contains 22 lagoons, has a median grain size (d_{50}) of 0.7 mm and a mean grain size (d_{MEAN}) of 1.0 mm.

Table 3.2: Representative cumulative grain sizes for Chesapeake Bay lagoon inlets

Lagoon Name	d_{84} (mm)	d_{50} (mm)	d_{16} (mm)	d_{MEAN} (mm)
45 Big Pond	4.0	0.4	0.2	1.5
12 Biscoe Pond	1.6	0.6	0.2	0.8
47 Blackwalnut	0.5	0.3	0.3	0.4
39 Brownies Beach	0.7	0.5	0.2	0.4
80 Carter Creek	0.8	0.5	0.2	0.5
49 Chase Pond	0.4	0.3	0.2	0.3
25 Drum Point	1.0	0.7	0.5	0.7
23 Long Lane	2.0	0.4	0.2	0.9
41 North Beach	2.0	0.8	0.3	1.0
13 St. James Church	5.5	1.0	0.3	2.3
75 Terrapin South	2.9	0.9	0.5	1.4
South Western Average	2.5	0.7	0.3	1.2
Central Western Average	1.5	0.5	0.2	0.7
Eastern Average	1.9	0.7	0.3	1.0
Chesapeake Bay Average	1.9	0.6	0.3	0.9

All lagoons show a median grain size greater than 0.25 mm, which was used by Hughes (2002) to predict the cross sectional areas of CB inlets from Byrne et al. (1980). Grain size analyses show a median grain size of 0.3 mm or greater, with an average median grain size of 0.6 and a mean grain size of 0.9 mm. This indicates that CB lagoons must be in equilibrium with a dominantly coarse (0.5 – 1 mm) grain size in order to be open and functioning. Grain size is not closely related to cross sectional area for CB lagoon inlets (Figure 3.8). This suggests that grain size is an independent variable, controlled not by the channel flow, but by local sediment supply and transport conditions produced by waves.

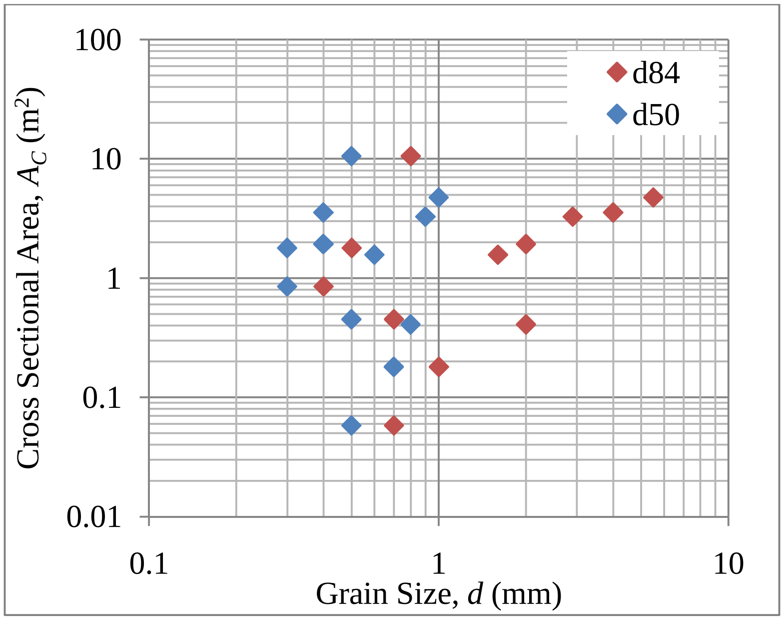

Figure 3.8: Cross sectional area as a function of grain size diameter shows no relationship; therefore grain size is an independent variable.

3.4.4 Measured cross sections compared to the Hughes (2002) equation

Calculation of the equilibrium cross sectional area from the Hughes (2002) process-based equation yields scatter above and below the 1:1 line when compared with field measurements (Figure 3.9). Scatter is skewed above the 1:1 line in Figure 3.9a, where field measurements were compared to the predicted area. The four field sites highlighted in orange are the sites that are experiencing infilling and therefore are not at equilibrium. In order to test the equilibrium area, I have used the field relationship between inlet width and cross sectional area to correct these alternate stable state inlets into equilibrium inlets, which I then compare to the predicted area in Figure 3.9b. Using the corrected cross sectional areas (in orange) in addition to the equilibrium cross sections (in black) shows equal scatter above and below the 1:1 line (Figure 3.9b), which indicates that when using correct grain size, the Hughes (2002) equation does not skew the data, but rather gives a predicted cross sectional area within 6 square meters of its measured value. The scatter in Figure 3.9 also reveals that larger inlets are better predicted than smaller inlets.

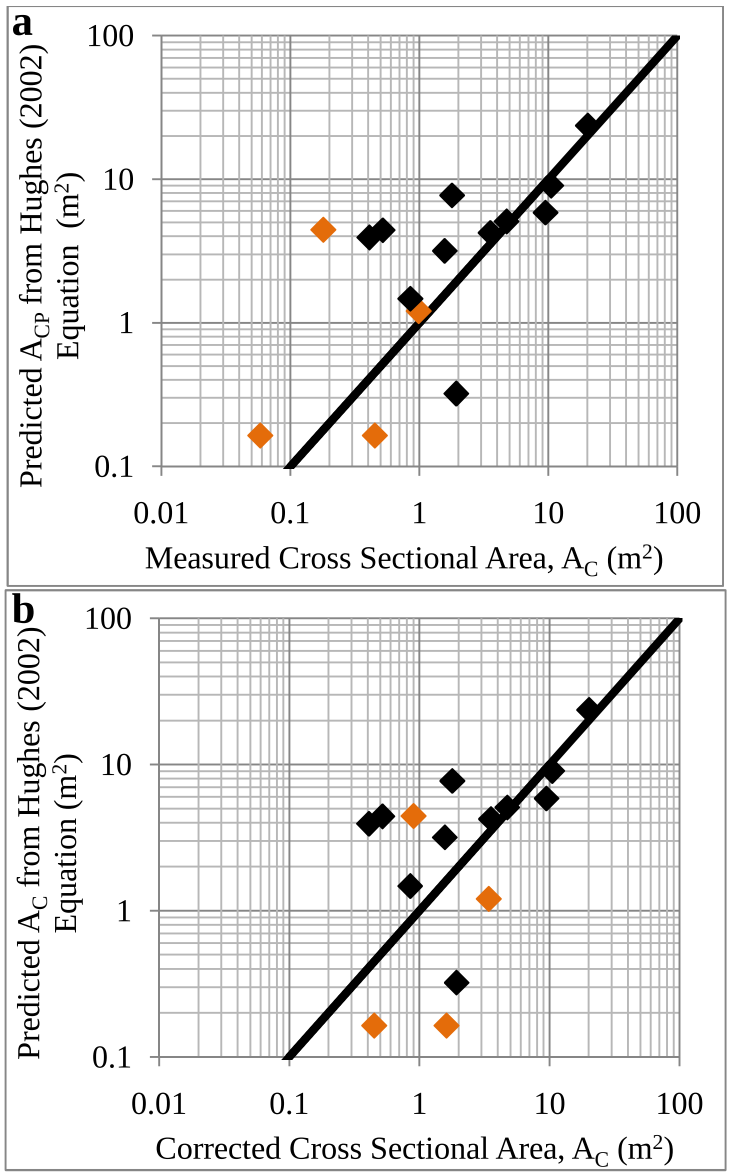

Figure 3.9: (a) Hughes (2002) equation was modified by including the correct grain size data and compared with field measurements. Data in orange are those field sites whose *W/D* ≥ 35. (b) These cross sections have been re-calculated using the

field relationship between width and area for *W/D* < 35. Both plots show scatter, however neither are skewed above or below the 1:1 line.

Using the field relationship (Equation 3.13) between inlet width (*W*) and cross sectional area (A_C), I have calculated cross sectional areas for the remaining inlets, whose inlet width was remotely sensed. I have chosen to only use Equation 3.13, as the other power law (Equation 3.15) represents an alternate stable state and I would like to test whether inlets in equilibrium can be predicted from the Hughes (2002) equations. Determination of the predicted area from the Hughes (2002) equation required grain size. Sediment samples were not taken at every site; therefore a spatial distribution of grain size was determined and applied to each lagoon. For example, all lagoons along the southwestern shoreline were assigned a median grain size, which is the average of the median grain sizes found at the sites sampled along the southwestern shoreline of CB.

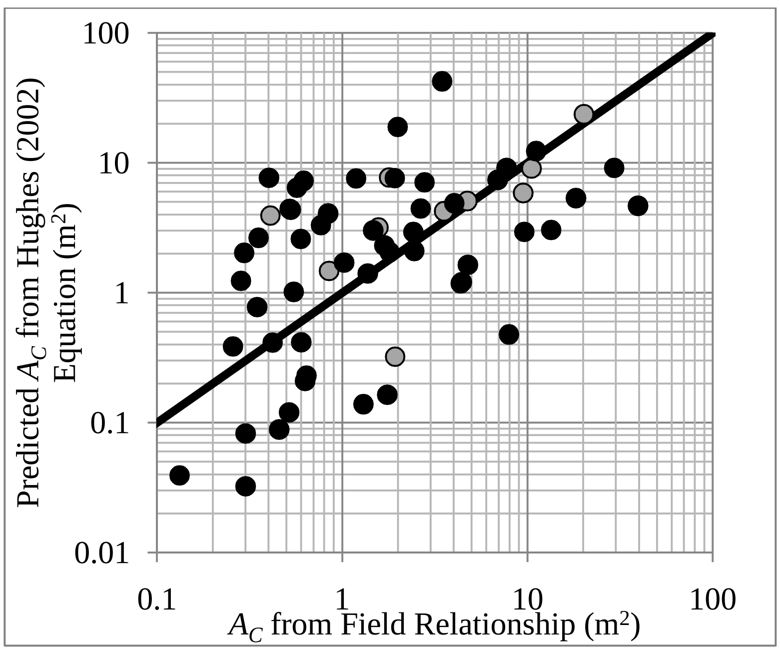

Figure 3.10: Cross sectional area (A_C) for the black circles is determined from the field relationship: $A_C = 0.14W^{1.5}$; where *W* is inlet width measured from air photo images. Gray circles represent field measurements. Comparison with predicted cross sectional areas calculated from the Hughes (2002) equations yields equal scatter above and below the 1:1 line.

To estimate cross sectional area for un-measured inlets, I used the upper relationship of width to cross sectional area measured in the field (Equation 3.13). These data for the entire population of open and intermittent lagoon inlet areas were compared to theoretical cross sectional areas determined from the Hughes (2002) equation. Although this comparison shows scatter above and below the 1:1 line (Figure 3.10) there appears to be no bias in using the Hughes (2002) equation, however it can under- or over-predict the cross sectional area by an order of magnitude.

3.4.5 Hydraulic geometry of Chesapeake Bay lagoon inlets

Hydraulic geometry parameters for lagoon inlets with $W/D < 35$ were plotted as functions of inlet discharge (Figure 3.11). These diagrams indicate the following relationships:

$$W = 3.0Q_M^{0.49} \quad R^2 = 0.89 \tag{3.16}$$

$$D = 0.22Q_M^{0.34} \quad R^2 = 0.90 \tag{3.17}$$

$$U_M = 1.5Q_M^{0.17} \quad R^2 = 0.90 \tag{3.18}$$

Note that $b + f + m = 1.00$ and $a*c*k = 1.0$, which suggests that these inlets function as a homogeneous hydrologic system. Additionally, the *b*, *f*, and *m* exponents are similar to exponents for downstream hydraulic geometry (Leopold and Maddock, 1953).

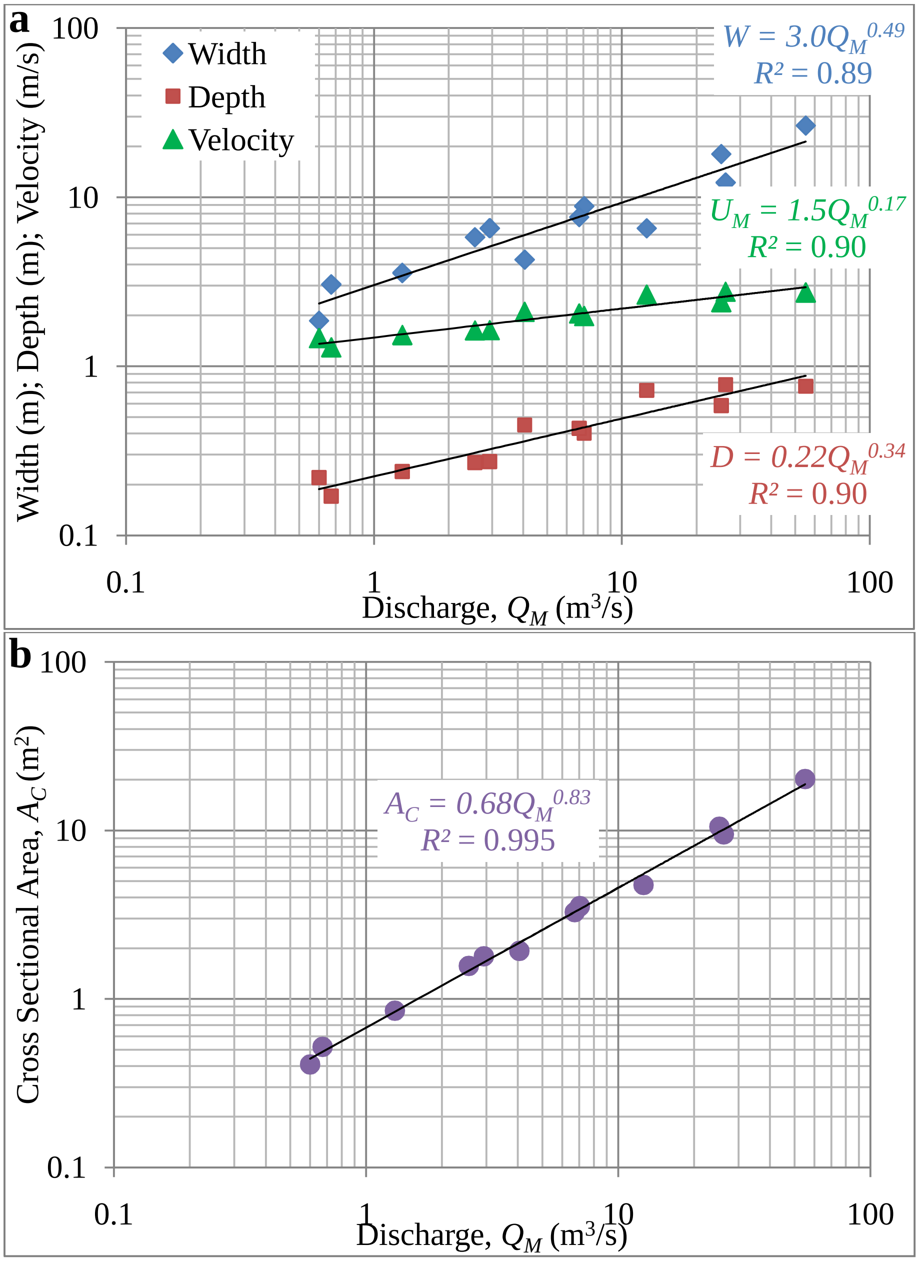

Figure 3.11: (a) Hydraulic geometry parameters (width, depth, velocity) are plotted as functions of discharge. (b) Relationship between inlet cross sectional area and discharge.

Although the inlets in this analysis are from different drainage basins, the product of the coefficients and sum of the exponents (in Figure 3.11a) do equal unity. The relationship between inlet cross sectional area (A_C) and discharge (Q) given by:

$$A_C = 0.38Q_M^{0.83} \quad R^2 = 0.995 \tag{3.19}$$

exhibits a significantly higher coefficient of determination (R^2) than the width and depth relationships ($R^2 \leq 0.90$). This suggests that parameters in addition to discharge influence channel shape. In the next section, I examine dimensionless hydraulic geometry relationships that incorporate bed grain size into the relationships.

3.4.6 Dimensionless hydraulic geometry for Chesapeake Bay lagoon inlets

Dimensionless hydraulic geometry relationships for lagoon inlets were determined to incorporate the effects of variations in grain size on channel inlet geometry (Figure 3.12). Dimensionless width ($W*$) and depth ($D*$) are plotted as functions of dimensionless discharge ($Q*$) for CB lagoons in Figure 3.12 and exhibit the following power law relationships:

$$W* = 842{,}630 Q*^{0.48} \quad R^2 = 0.96 \tag{3.20}$$

$$D* = 11{,}230 Q*^{0.35} \quad R^2 = 0.97 \tag{3.21}$$

where the grain size of morphologic importance is considered to be the d_{84} grain size (Wiberg and Smith, 1987; Leopold and Wolman, 1957). These dimensionless relationships exhibit stronger correlation coefficients than the hydraulic geometry relationships, suggesting that grain size controls some of the variation in channel morphology, which generates scatter in the hydraulic geometry relationships.

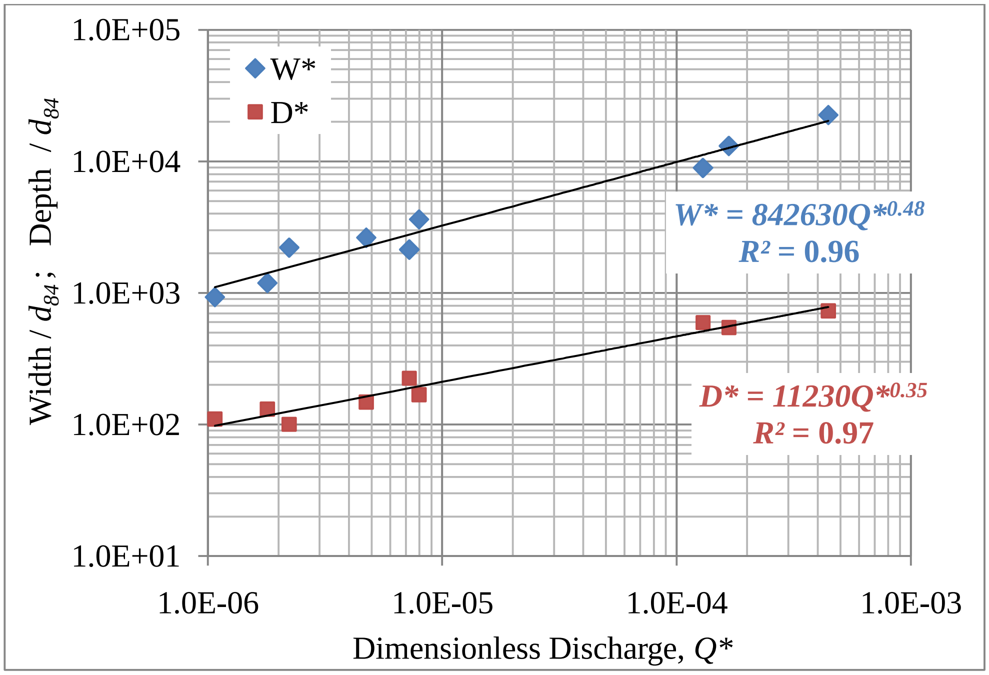

Figure 3.12: Dimensionless hydraulic geometry parameters, scaled by the d_{84} grain size show a stronger relationship than traditional hydraulic geometry parameters, therefore indicating that inlet hydraulics are dependent on grain size.

3.4.7 Area-prism relationship for Chesapeake Bay lagoons

Plotting the inlet cross sectional area and spring tidal prism for CB lagoons shows a similar relationship to the inlet-basins studied by Byrne et al. (1980); however this study's data set shows much more scatter (Figure 3.13). The resulting power law for CB lagoons is:

$$A_C = 0.0033\Omega^{0.63} \quad R^2 = 41. \tag{3.22}$$

This relationship describes the central relationship between inlet area and tidal prism for CB lagoon data, the Bryne et al (1980) equation is similar:

$$A_C = 0.0063\Omega^{0.67} \quad R^2 = 81 \tag{3.23}$$

and it describes the relationship for maximum channel areas (Figure 3.13).

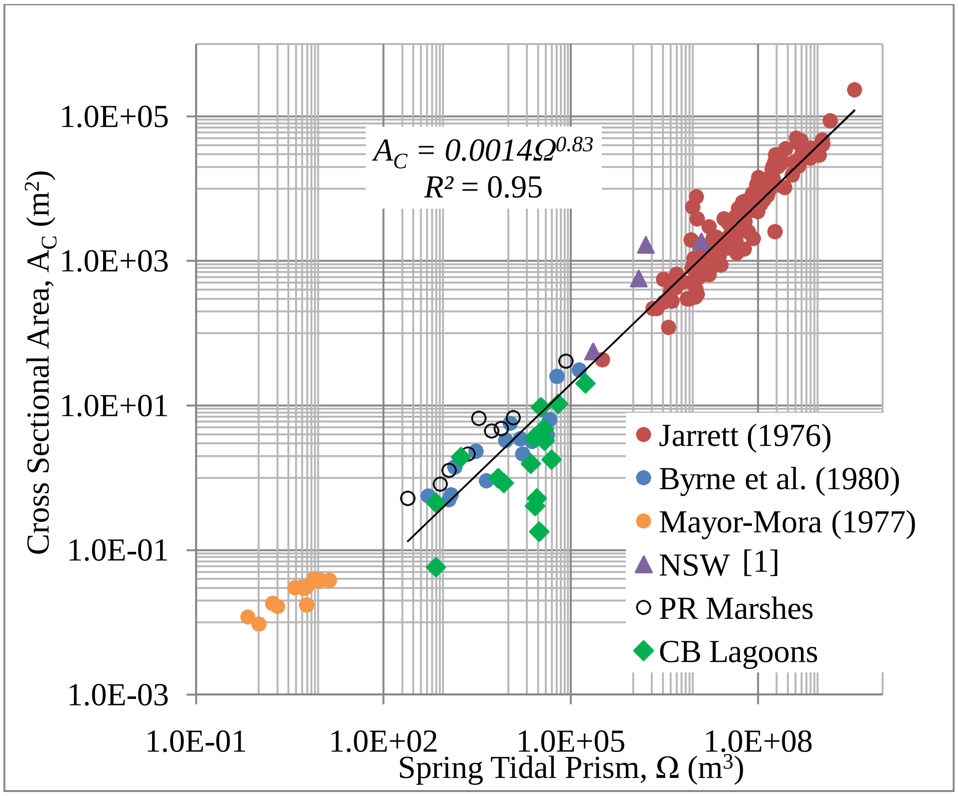

Figure 3.13: The area-prism data for CB lagoons from this study is plotted with the CB data of Byrne et al. (1980), PR marshes, NSW lagoons, the compilation by Jarrett (1976) and laboratory scale models by Mayor-Mora (1977). The power function includes combined data for all studies but excludes the laboratory models. [1]NSW data are from the NSW Office of the Environment and Heritage, accessed October 2010

Data from PR tidal marshes, NSW lagoons, laboratory models from Mayor-Mora (1977), CB lagoon data from this study and from Byrne et al. (1980) and the oceanic lagoon data compiled by Jarrett (1976) are shown in Figure 3.13b. Including all but laboratory model data yields a power law:

$$A_C = 0.0013\Omega^{0.83} \quad R^2 = 95. \tag{3.24}$$

This relationship extends over 8 orders of magnitude. The exponent is slightly different than Jarrett's (1976) relationship, but there is a significant change in the value of the coefficient from Jarrett's well-accepted empirical relationship; however this relationship better fits small and mid-ranged inlet-basin systems.

In previous compilations (e.g Hughes, 2002), data from laboratory experiments (Mayor-Mora, 1977) were included in the comparisons. When these data are included in the analysis the relationship becomes:

$$A_C = 0.0038\Omega^{0.77} \quad R^2 = 0.97. \tag{3.25}$$

Therefore, the inclusion of these laboratory data significantly modifies the exponent for the area-prism relationship. Data from Mayor-Mora (1977) were conducted with sediment that did not satisfy dimensional analysis. Therefore, these data should not be used in the comparisons of natural systems. This suggests that "small systems" are not significantly different than larger systems, but that non-scaled laboratory studies are different from natural systems. The scatter in the data from CB lagoons, however, suggests that small systems may be heterogeneous, a result also observed in the basin area and waterway surface area relationships.

3.5 Discussion

Previous research has suggested different mechanisms for the formation and maintenance of equilibrium lagoon inlet cross sectional areas. Elwany et al. (1998) and Prestegaard (1979) suggested that Southern California lagoons require river flooding events for channel maintenance, whereas in New Zealand, Hume and Herdendorf (1992) found that tidal currents are the dominant mechanism for transporting sediment out of the inlet. Kraus (2007) determined that diurnal tides and wind-driven tides are the two most important mechanisms for maintaining inlet stability along the Texas coast. The hydraulic geometry results and area-width lagoon inlet relationships suggest that CB lagoon inlets are formed by primarily streamflow and inlet depth can be altered by infilling sediment transported by waves.

Grain size analyses indicate that sediment in CB lagoon inlets is coarser than observed for many oceanic lagoon inlets. Previous studies have found that inlet size is not sensitive to grain size, but these studies primarily examined oceanic lagoons with sand-sized sediment, where flow resistance and sediment initiation conditions are more likely affected by sand bedforms rather than minor variations in grain size (Hughes, 2002; O'Brien, 1976; 1931). Short period waves, such as the 2-4 second period waves observed in the CB, are capable of moving gravel-sized sediment with small wave heights (Grasso et al., 2011). Therefore, CB lagoons are adjusted by both streamflow discharges and grain sizes found on Bay beaches. Similar constraints may apply to other inlets along bay, lake or other coasts with small fetches and thus short period waves and local sources of coarse sediment.

The hydraulic geometry relationships and the area-prism relationship might be useful as guidelines for management and restoration. In a study of intermittently open and closed lagoons in New South Wales, Australia, Haines and Thom (2007) postulated that sea level rise and changes in littoral transport and precipitation patterns may affect these vulnerable ecosystems. In stream flow-dominated lagoon inlets, changes in precipitation or runoff (caused by climate or land-use changes) may result in morphological responses at the lagoon inlet cross section, which may affect lagoon flushing times and water quality (Elwany, 2011). The dimensionless hydraulic geometry relationships could be particularly useful for management of lagoons in CB that experience anthropogenic or other changes that alter the size or supply of sediment. Field measurements of cross sectional area and sediment sampling could provide data for comparison with the dimensionless hydraulic geometry relationships established in this study.

Finally, although CB lagoons are consistent with inter-regional area-prism relationships, the local relationship derived for CB lagoons alone reflects variability related to: a) variations in inlet grain size; b) small watershed sizes leading to heterogeneous stream flow; c) land-use variations, and d) dynamic changes resulting from temporal variations in streamflow, wave characteristics, and sediment supply.

3.6 Conclusions

In this chapter, I investigated the factors that influence cross sectional area and the area-prism relationship for CB lagoons. I measured and compared CB lagoon inlet width data with a reference data set of tidal marsh inlets. The lagoon width data were used to identify representative field sites to characterize inlet geometry. Inlet channel morphology was measured in the field and bed sediment was sampled and sieved to obtain grain size distributions. Channel geometry data were used to determine hydraulic geometry and dimensionless hydraulic geometry relationships. Channel characteristics were also used in the evaluation of the channel area-tidal prism relationship for CB and other lagoons. The main conclusions are:

1. Inlet width data for all 86 CB lagoons indicates that these lagoons have a small range of inlet sizes. The largest CB lagoon inlets are significantly smaller than the largest Patuxent tidal marsh inlets.
2. Cross sectional area measurements indicated two relationships between inlet width and cross sectional area. Inlet width is a stable feature, but depth is

variable, probably due to infilling of channels by wave-induced sediment transport.

3. Sediment analyses indicate that CB lagoons inlets have coarser grain sizes than most oceanic lagoon inlets. Grain size was significantly larger than the value assumed by Hughes (2002), and Hughes' equation is in general agreement with measured channel cross sections.
4. The hydraulic geometry analysis suggests that lagoon inlet channels represent a homogenous hydrologic system. The hydraulic geometry exponents determined from this analysis are more similar to regional fluvial hydraulic geometry (Wolman, 1955; Leopold and Maddock, 1953), than to tidal marsh hydraulic geometry (Langbein, 1963; Myrick and Leopold, 1963). This suggests a central role of stream flow in forming and maintaining both lagoon surface area and tidal inlets. Dimensionless hydraulic geometry, which incorporates grain size, improves hydraulic geometry relationships and suggests that grain size explains some of the variability in inlet characteristics.
5. The area-prism relationship determined for CB lagoons exhibits a larger coefficient and smaller exponent than Jarrett's (1976) empirical relationship for oceanic inlets. The relationship derived by Byrne et al. (1980) defines the upper limit of channel areas for the combined CB lagoon data set. Comparison of these data with other lagoon inlets (Byrne et al., 1980; Jarrett, 1976) yields a power law relationship that extends over 8 orders of magnitude with an improved regression coefficient. The data from laboratory experiments (Mayor-Mora, 1977) of tidal inlets do not fit this empirical relationship.

Chapter 4: Geomorphic Characteristics of Chesapeake Bay Lagoons with Methods for Lagoon and Watershed Assessment

4.1 Introduction

Chesapeake Bay (CB) lagoons are small coastal ecosystems that exhibit a range of sizes, inlet conditions, and salinities (Bird, 1994; Kjerfve and Magill, 1989; Byrne et al., 1980). Coastal lagoons are important sites for primary productivity, biogeochemical processes and as hatcheries or habitat for aquatic species (Alvarez-Borrego, 1994; Knoppers, 1994; Yáñez –Arancibia et al., 1994). The biodiversity of a lagoon is influenced by water exchange between the lagoon and the bay, nutrient inputs, and turbulent mixing (Macedo et al., 2001; Bachelet et al., 2000). Lagoon geomorphic and hydraulic characteristics are influenced by tides, waves, and streamflow from lagoon watersheds (Elwany et al., 1998; Kraus, 1998; Gao and Collins, 1994; Bruun et al., 1978). These processes can be affected by local and regional land-use characteristics and lagoon inlet geometry (Haines and Thom, 2007; Roy et al., 2001; Lowrance and Leonard, 1988). Watershed runoff can be affected by both land-use changes and climate changes (Elwany, 2011; Haines and Thom, 2007; Sivapalan, 2003). Sea-level rise due to climate changes may also cause changes in lagoon and inlet morphology that may affect closure conditions, salinity, water quality, and coastal erosion.

To assess the response of these important coastal ecosystems to climate and anthropogenic changes, we need assessment tools that provide information on the governing processes of lagoon and inlet behavior. An area-prism relationship (e.g. Jarrett, 1976) has been developed for CB lagoons (Byrne et al., 1980), but while it can assess possible disequilibrium between lagoon water surface area and inlet characteristics, it provides little information as to underlying causes for disequilibrium. Therefore, the purpose of this paper is to examine geomorphic characteristics of CB lagoons, inlets, and associated watersheds, to develop predictive relationships between lagoon hydraulic and geomorphic characteristics, and to develop tools for watershed, lagoon, and inlet channel assessment.

4.2 Study sites and methods

CB lagoons were examined on USGS air photos for the period 1993-2011. From these air photos, 86 lagoon-inlet systems were identified in 3 regions of CB, Maryland (Figure 4.1). Inlet status (open, closed, intermittent) was assessed from these sequential air photos. The high-resolution photos from April, 2007 were chosen for measurement of geomorphic features. Inlet width (W) was measured from air photos; watershed area (A_B) and lagoon water surface area (A_S) were determined from air photo and topographic data using the GIS program MD MERLIN Online (http://www.mdmerlin.net/). Spring tidal range (h_R) was obtained from 11 National Oceanic and Atmospheric Administration (NOAA) tide gauges and used to determine spring tidal prism ($A_S h_R$) for each lagoon (Table 4.1). Inlet width data were used to develop a proportional sampling scheme for field data collection. The 86 inlet widths were binned into 10 logarithmic size classes from which 15 lagoon inlets were selected that represented the range of inlet channel sizes. Cross sections of these selected inlets were measured in the field. A relationship between cross sectional area and inlet width was developed from the field data and this relationship was used to estimate the cross sectional area of unmeasured inlets. Sediment samples of inlet bed sediment were obtained in the field for sieve analyses to determine sediment grain size. From these data, average grain size data were determined for each of the three regions shown in Figure 4.1. All measured and estimated data for each of the 86 lagoons is shown in Table 4.1.

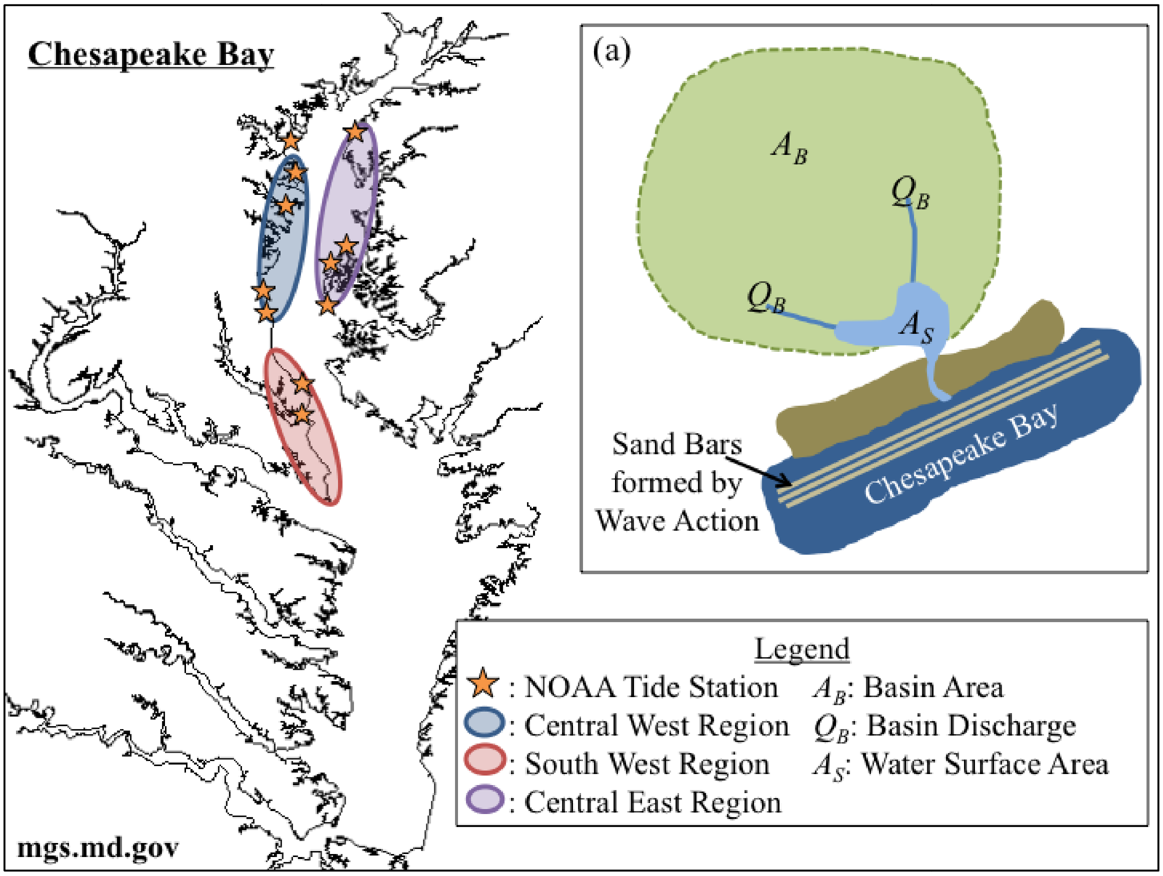

Figure 4.1: CB hosts 86 lagoons, which are clustered along three Maryland shorelines. Lagoons 1-38 are found along the Southwestern shoreline, lagoons 39-63 are found along the central western shoreline and lagoons 64-86 are found along the central eastern shoreline, numbers indicate lagoons listed in Table 1. Tide stations (stars) provided spring and mean tidal range data. Inset (a): definition sketch of lagoon and basin geomorphic variables.

Table 4.1: Measured and estimated data for Chesapeake Bay lagoons

No.	Region	Nat-ural*	Status	Inlet Width, W (m)	Inlet Length, L (m)	Inlet Area**, A_C (m^2)	Median Grain Size$^+$, d_{50} (mm)	Water Surface Area, A_S (m^2)	Spring Tidal Range, h_R (m)	Spring Tidal Prism, Ω (m^3)	Basin Area, A_B (m^2)	Basin Area, A (mi^2)	% Forest Cover, F	% Resi-dential Cover, R	% Ag cover, Ag	% Sto-rage cover, ST
1	SW	Y	I	8.0	377.4	3.46	0.7	941668	0.41	386084	5181783	2.001	20%		50%	30%
2	SW	Y	I	1.6	37.9	0.28	0.7	21552	0.41	8836	295984	0.114	10%		60%	30%
3	SW	Y	I	15.5	65.2	9.61	0.7	43086	0.41	17665	827932	0.320	80%		10%	10%
4	SW	Y	I	2.1	15.4	0.42	0.7	6102	0.41	2502	180670	0.070	90%			10%
5	SW	Y	I	6.4	51.5	2.42	0.7	48096	0.41	19719	818938	0.316	80%	10%		10%
6	SW	Y	C	2.0	135.0		0.7	34338			416692	0.161	80%			20%
7	SW	Y	I	13.4	15.9	7.71	0.7	157333	0.41	64506	798607	0.308	30%		40%	30%
8	SW	Y	I	2.4	54.7	0.53	0.7	84939	0.41	34825	658061	0.254	30%		40%	30%
9	SW	Y	I	6.9	127.9	2.78	0.7	127928	0.41	52451	1741362	0.672	20%		50%	30%
10	SW	Y	I	3.2	0.0	0.84	0.7	75778	0.41	31069	1733903	0.669	40%		40%	20%
11	SW	Y	I	2.5	26.6	0.57	0.7	130609	0.41	53550	6203718	2.395	50%		35%	15%
12	SW	Y	I	3.8	35.0	**1.57**	**0.6**	56025	0.41	22970	2141445	0.827	80%			20%
13	SW	Y	I	5.5	20.7	**4.74**	**1.0**	90931	0.41	37282	1793278	0.692	75%		5%	20%
14	SW	Y	C				0.7	12480			156245	0.060	85%	5%		10%
15	SW	Y	I			0.00	0.7	35335	0.41	14487	2274445	0.878	85%		5%	10%
16	SW	Y	I	1.6	46.4	0.30	0.7	37594	0.41	15414	989469	0.382	75%	15%		10%
17	SW	Y	I	9.8	48.3	4.77	0.7	23654	0.41	9698	1755108	0.678	85%		5%	10%
18	SW	Y	I	4.4	24.3	1.37	0.7	22033	0.41	9034	1359838	0.525	75%	10%		15%
19	SW	Y	I	4.3	19.1	1.30	0.7	1631	0.41	669	435377	0.168	85%		10%	5%
20	SW	Y	I	1.7	0.0	0.30	0.7	1023	0.41	419	57967	0.022	90%			10%
21	SW	Y	I	5.3	65.1	1.80	0.7	32885	0.41	13483	2047188	0.790	40%		40%	20%
22	SW	Y	I	2.7	14.2	0.63	0.7	2749	0.41	1127	1840060	0.710	70%		20%	10%
23	SW	Y	I	4.0	16.1	**1.93**	**0.4**	4253	0.41	1744	2365576	0.913	70%	20%		10%

No.	Region	Nat-ural*	Status	Inlet Width, W (m)	Inlet Length, L (m)	Inlet Area**, A_C (m^2)	Median Grain Size+, d_{50} (mm)	Water Surface Area, A_S (m^2)	Spring Tidal Range, h_R (m)	Spring Tidal Prism, Ω (m^3)	Basin Area, A_B (m^2)	Basin Area, A (mi^2)	% Forest Cover, F	% Resi-dential Cover, R	% Ag cover, Ag	% Sto-rage cover, ST
24	SW	N	O	12.5	57.0	6.90	0.7	124948	0.41	51229	7801683	3.012	30%	40%		30%
25	SW	Y	I	6.7	103.4	2.66	**0.7**	76293	0.41	31280	458233	0.177	60%	20%		20%
26	SW	N	I	3.0	20.7	0.77	0.7	60583	0.41	24839	772838	0.298	55%	20%		25%
27	SW	N	I	2.0	24.1	0.40	0.7	163634	0.41	67090	1826369	0.705	50%	20%		30%
28	SW	Y	I		17.1	0.00	0.7	17283	0.41	7086	1129896	0.436	65%	15%		20%
29	SW	Y	I	2.7	29.2	0.64	0.7	3059	0.41	1254	42842	0.017	80%			20%
30	SW	Y	I	1.0	25.5	0.13	0.7	475	0.41	195	66181	0.026	85%			15%
31	SW	N	I	3.6	37.5	1.02	0.7	31833	0.36	11460	2629683	1.015	75%	10%		15%
32	SW	Y	I	2.6	26.1	0.62	0.7	169461	0.36	61006	1851564	0.715	55%	15%		30%
33	SW	Y	C				0.7	1584			128657	0.050	85%			15%
34	SW	Y	I	2.6	57.5	0.60	0.7	53417	0.36	19230	3018020	1.165	75%	5%		20%
35	SW	Y	I	4.6	226.8	1.47	0.7	58865	0.36	21191	2955853	1.141	70%		10%	20%
36	SW	N	I	2.2	46.1	0.46	0.7	1222	0.36	440	430031	0.166	85%		10%	5%
37	SW	Y	C				0.7	1899			17762	0.007	85%			15%
38	SW	Y	C				0.7	22220			242584	0.094	80%			20%
39	CW	Y	I	5.2	20.7	1.75	**0.5**	2044	0.34	695	3579705	1.382	80%	10%		10%
40	CW	N	O	2.6	10.9	0.60	0.5	6344	0.34	2157	2401882	0.927	60%	25%		15%
41	CW	N	I	2.7	149.2	**0.41**	**0.8**	79174	0.34	26919	3245902	1.253	75%	15%		10%
42	CW	N	O	17.6	106.7	**9.49**	0.5	107445	0.31	33308	8308059	3.208	50%	10%	20%	20%
43	CW	Y	C				0.5	4577			35944	0.014	80%	5%		15%
44	CW	N	I		142.2	0.00	0.5	93435	0.34	31768	1230388	0.475	70%	10%		20%
45	CW	Y	O	7.3	165.7	**3.55**	**0.4**	75966	0.34	25829	836187	0.323	40%	30%		30%
46	CW	Y	C				0.5	7921			49790	0.019	60%	10%		30%
47	CW	Y	O	9.1	43.0	**1.79**	**0.3**	145001	0.34	49300	1842068	0.711	40%	30%		30%

No.	Region	Natural*	Status	Inlet Width, W (m)	Inlet Length, L (m)	Inlet Area**, A_C (m^2)	Median Grain Size$^+$, d_{50} (mm)	Water Surface Area, A_S (m^2)	Spring Tidal Range, h_R (m)	Spring Tidal Prism, Ω (m^3)	Basin Area, A_B (m^2)	Basin Area, A (mi^2)	% Forest Cover, F	% Residential Cover, R	% Ag cover, Ag	% Storage cover, ST
48	CW	Y	I	2.4	27.9	0.55	0.5	17481	0.34	5943	302006	0.117	40%	30%		30%
49	CW	Y	I	4.0	50.8	**0.85**	**0.3**	24934	0.34	8477	384650	0.149	30%	40%		30%
50	CW	Y	C				0.5	11341			55187	0.021	90%			10%
51	CW	Y	I	2.3	11.5	0.52	0.5	1588	0.34	540	53158	0.021	30%	30%	20%	20%
52	CW	N	C				0.5	130092			744713	0.288	30%	30%		40%
53	CW	N	O	31.9	301.4	29.37	0.5	149974	0.34	50991	2561220	0.989	30%	30%		40%
54	CW	N	O	17.0	201.6	11.13	0.5	285386	0.27	77054	6575682	2.539	30%	35%	5%	30%
55	CW	Y	O	1.8	81.6	0.35	0.5	16822	0.27	4542	186841	0.072	50%	30%		20%
56	CW	Y	I	1.7	28.4	0.30	0.5	479	0.27	129	11835	0.005	80%	5%		15%
57	CW	Y	I			0.00	0.5	4899	0.27	1323	76393	0.029	40%	20%	10%	30%
58	CW	Y	C				0.5	9310			157728	0.061	80%			20%
59	CW	Y	C				0.5	65587			717979	0.277	60%	15%		25%
60	CW	N	O	4.7	97.9	**0.52**	0.5	81813	0.35	28635	718013	0.277	60%	20%		20%
61	CW	Y	C				0.5	19273			293390	0.113	55%	10%	20%	15%
62	CW	Y	C				0.5	10242			74831	0.029	75%			25%
63	CW	N	C				0.5	48657			151372	0.058	60%	10%		30%
64	CE	N	I	4.0	102.3	1.19	0.7	147928	0.41	60650	3484611	1.345	10%		70%	20%
65	CE	Y	C				0.7	132514			1296254	0.500	40%		40%	20%
66	CE	Y	I	8.8	45.8	4.03	0.7	81884	0.41	33572	3082919	1.190	25%		55%	20%
67	CE	N	O	5.5	86.7	1.92	0.7	143598	0.41	58875	4300763	1.661	50%		30%	20%
68	CE	N	C				0.7	14650			1239006	0.478	20%		65%	15%
69	CE	Y	C				0.7	37770			190943	0.074	20%		70%	10%
70	CE	Y	O	38.6	78.0	39.52	0.7	64666	0.41	26513	2091429	0.808	20%		55%	25%
71	CE	Y	O	1.8	248.0	0.35	0.7	49990	0.41	20496	467024	0.180	40%	20%		40%

No.	Region	Natural*	Status	Inlet Width, *W* (m)	Inlet Length, *L* (m)	Inlet Area**, A_C (m^2)	Median Grain Size+, d_{50} (mm)	Water Surface Area, A_S (m^2)	Spring Tidal Range, h_R (m)	Spring Tidal Prism, Ω (m^3)	Basin Area, A_B (m^2)	Basin Area, *A* (mi^2)	% Forest Cover, *F*	% Residential Cover, *R*	% Ag cover, *Ag*	% Storage cover, ST
72	CE	Y	I	1.5	31.0	0.26	0.7	6891	0.35	2412	248632	0.096	15%		75%	10%
73	CE	Y	C				0.7	25235			506578	0.196	30%	10%	30%	30%
74	CE	Y	C				0.7	4616			32150	0.012	60%		10%	30%
75	CE	Y	I			**3.28**	**0.9**	109401	0.35	38290	1613042	0.623	40%	10%	40%	10%
76	CE	N	I	19.2	84.4	13.42	0.7	51073	0.35	17875	653797	0.252	20%	60%		20%
77	CE	Y	I			0.00	0.7	11948	0.35	4182	444856	0.172	80%	5%		15%
78	CE	Y	I	9.4	87.3	4.42	0.7	19725	0.35	6904	1482208	0.572	30%	20%	30%	20%
79	CE	N	O	26.5	96.0	**20.19**	0.7	492255	0.35	172289	2652033	1.024	10%	20%	30%	40%
80	CE	N	O	14.1	193.3	**10.52**	**0.5**	166245	0.38	63173	1260186	0.487	20%	25%	25%	30%
81	CE	Y	I	9.3	11.7	4.36	0.7	17741	0.38	6742	573789	0.222	80%			20%
81	CE	Y	I	5.6	195.4	1.99	0.7	428551	0.38	162849	2611819	1.008	30%	25%	5%	40%
83	CE	Y	O	23.4	518.1	18.27	0.7	86555	0.38	32891	638586	0.247	20%		20%	40%
84	CE	Y	O	13.7	13.5	7.95	0.7	6113	0.38	2323	284543	0.110	15%		60%	25%
85	CE	Y	O	5.0	5.4	1.69	0.7	40815	0.38	15510	386563	0.149	15%		55%	30%
86	CE	Y	O	6.4	6.7	2.45	0.7	35531	0.38	13502	607559	0.235	20%		50%	30%

SW: south western shoreline; CW: central western shoreline; CE: central eastern shoreline; I: intermittent; O: open; C: closed

*Natural refers to the presences of jetties or groins; a natural inlet has no coastal engineering structures and is assigned a Y for yes.

**Cross sectional area is determined by field measurements or by the field relationship: $A_C = 0.14W^{1.5}$

+The average median grain size for each region (SW, CW, CE)

Note: Remote measurements are from April 2007 high-resolution aerial photography; values in **bold** are from field measurements.

Coastal lagoons are physical systems with four main controlling variables. These variables: drainage basin discharge (Q_B), water surface area (A_S), cross sectional area (A_C) and tidal stage (η), determine the total flux (Q_M) through the lagoon inlet. Although each of these variables change with time, they are components of a continuity equation, which when expressed in terms of lagoon inlet velocity (U_M) produces the following equation (Gao and Collins, 1994; Bruun et al., 1978):

$$U_M = \left(\frac{A_S}{A_C}\right)\left(\frac{d\eta}{dt}\right) + \left(\frac{Q_B}{A_C}\right). \quad (4.1)$$

This equation indicates that both stream discharge and tidal forcing govern inlet velocity and thus discharge through the lagoon inlet.

In this study, streamflow discharge (Q_B) is estimated from two different procedures. The first is by solving the above continuity equation for Q_B, and making the assumption that maximum inlet velocity (U_M) occurs when the Froude number = 1. All other terms in Equation 4.1 are measured. Maximum inlet velocity (U_M) is calculated as:

$$U_M = \sqrt{gD} \quad (4.2)$$

where g is the acceleration due to gravity and D is mean inlet depth. Solving Equation 4.1 for basin discharge and substituting the spring tidal range (h_R) and tidal period (T) into the expression yields the following relationship:

$$Q_B = U_M A_C - A_S\left(\frac{h_R}{T}\right), \quad (4.3)$$

which was solved for all 15 measured inlet cross sections. Note that $U_M A_C$ is the total discharge from all sources that moves through the tidal inlet. This discharge will be referred to as inlet maximum discharge Q_M.

Although basin discharge would be best determined by physical measurements of stream discharge into the lagoons, none of the lagoon watersheds and contributing streams are gauged. Therefore, stream discharges are estimated from regional flood frequency equations constructed for the CB region (Dillow, 1996). We make the assumption that inlet channels are in dynamic equilibrium (supported by historical air photo data) and like terrestrial streams, they are built and maintained by high frequency, low magnitude floods (1.5-2 year recurrence interval events; Leopold et al., 1964; Wolman and Miller, 1960; Leopold and Maddock, 1953). Therefore, regional flood frequency relationships were used to determine peak discharges (Q_2) for the 2-year recurrence interval flood (Dillow, 1996). Dillow provides a series of relationships in which Q_2 is determined primarily by basin area sizes, with modifications due to percent forest cover, runoff curve number, topography, and soil characteristics for Coastal Plain watersheds (Table 4.1). We used land-use and other characteristics for CB watersheds that contribute to lagoons (Table 4.1) and defined a simple, average scaling relationship for these small (<10 km^2) Coastal Plain watersheds to provide an estimation of Q_2 :

$$Q_2 = 2.9 A_B^{0.71} \qquad (4.4)$$

where Q_2 is the 2-year peak discharge in m^3/s and A_B is the basin area in km^2.

4.3 Geomorphic characteristics of Chesapeake Bay lagoons and watersheds

In this section, we present the geomorphic characteristics of 86 CB lagoons and their associated watersheds. Lagoon water surface area, drainage basin area, and inlet width data for all the lagoons are presented in Figure 4.2 as cumulative probability distributions. These data are used to obtain upper and lower bounds, median, and mean values for each geomorphic feature (Table 4.2). Remotely-sensed and field geomorphic data were used to develop the following relationships: a) inlet channel width to cross sectional area, which can be used to estimate cross sectional area for unmeasured channels; b) drainage basin area to water surface area; c) water surface area to tidal prism; and d) inlet channel area to tidal prism.

4.3.1 Cumulative distributions of geomorphic data

Geomorphic data were measured and these data are expressed as two different types of cumulative probability distributions (Figure 4.2). The first diagram (Figure 4.2a) is a plot of the rank of each lagoon (rank of 1 = largest) versus cumulative water surface area. This diagram indicates that the largest 10 lagoons (ranks 1 through 10) encompass 50% of the total water surface area of all 86 lagoons. The other three diagrams (Figures 4.2b-d) are cumulative probability distributions of the contributing drainage basin area, lagoon water surface area, and inlet channel width for CB lagoons. These cumulative probability distributions are used to determine upper and lower bounds, median, and mean for each geomorphic parameter (Table 4.2). These statistics indicate that these geomorphic parameters encompass relatively narrow ranges; less than two orders of magnitude for each parameter. These geomorphic data are not normally or log-normally distributed; they represent truncated power law distributions with a large number of small systems and relatively few large ones. This is also illustrated in Figure 4.2a, which indicates that the 45 smallest lagoons (half of the population) provide less than 10% of the total lagoon water surface area provided by all 86 CB lagoons.

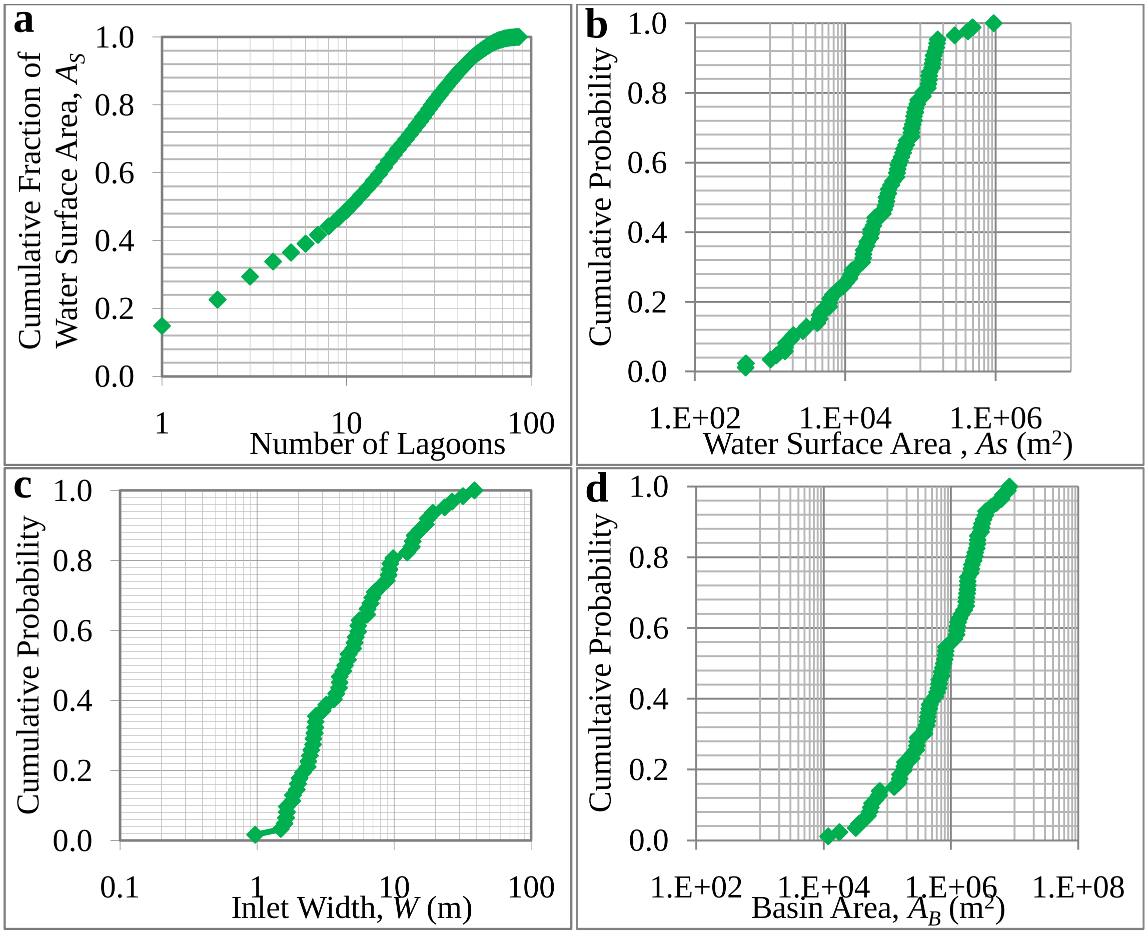

Figure 4.2: (a) Lagoon rank (largest =1) versus cumulative fraction of lagoon water surface area. (b-d) Cumulative probability distributions of geomorphic data for 86 CB coastal lagoons: (b) Watershed area, (c) Inlet width, (d) Lagoon surface area.

Table 4.2: Statistics for geomorphic features

Geomorphic Feature	Median	Mean	Lower bound	Upper bound
Basin Area (m^2)	772,840	1,178,700	11,835	3,208,060
Water Surface Area (m^2)	35,530	56,700	475	941,670
Inlet Width (m)	4.4	6.6	0.97	38.6

4.3.2 Relationship between channel width and channel cross sectional area

Field measurements of inlet cross sectional area were combined with the previous measurements of inlet geometry obtained by Byrne et al., (1980) on protected CB shorelines (Figure 4.3a). These combined data yield two distinct equations: inlets with width to depth ratios < 35 exhibit the following relationship:

$A_C = 0.14W^{1.5}$ ($R^2 = 0.92$) (4.5)

where A_C is cross sectional area and W is inlet width. Inlets with width to depth ratios $\geq$ 35 exhibit the following relationship:

$A_C = 0.011W^{2.3}$ ($R^2 = 0.99$). (4.6)

This relationship merges with the previous relationship at the upper limits of both inlet width and cross sectional area. These two distinct relationships may indicate two alternate states that reflect the local effectiveness of streamflow, wave, and tidal processes that transport sediment into or out of the lagoon inlet.

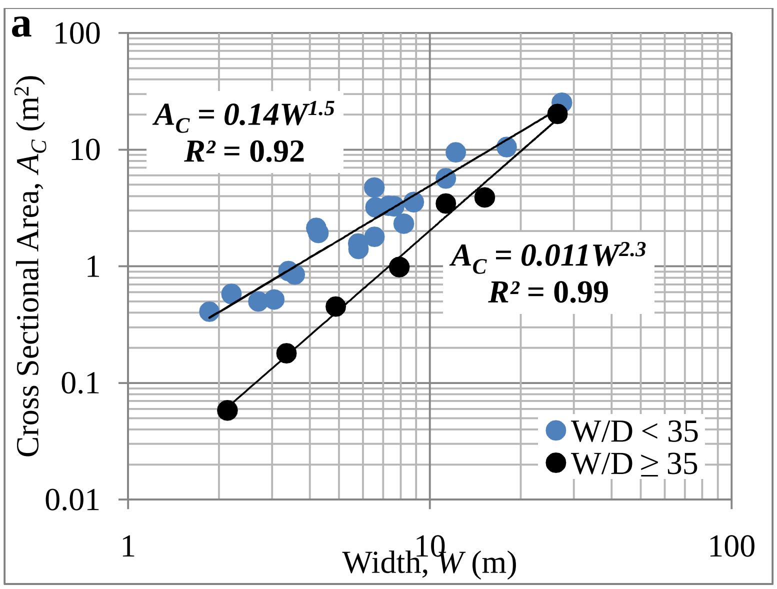

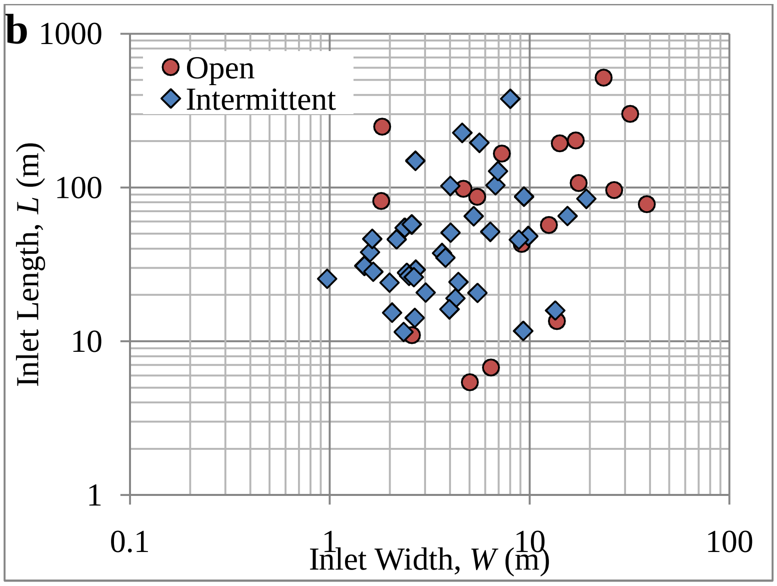

Figure 4.3: Relationship between lagoon inlet width and (a) inlet cross sectional area and (b) inlet length for CB lagoons.

Inlet channel length is plotted as a function of inlet width in Figure 4.3b. Assessment of inlet status (intermittent, open) indicates that inlet length is independent of inlet width and appears to have no bearing on inlet closure. Inlets that are always open tend to have inlet widths greater than 15-20 meters, which is the range of inlet widths where the two alternate states in Figure 4.3a converge.

4.3.3 Relationship of lagoon water surface area to drainage basin area

Data on basin area (A_B) and water surface area (A_S) for CB lagoons were used to develop the following relationship (Figure 4.4):

$$A_S = 0.038 A_B^{0.76} \quad R^2 = 0.49. \qquad (4.7)$$

This relationship shows significant scatter and relatively low R^2 values. The value of the exponent, however, is similar to the exponent in regional flood frequency equations for the Maryland Coastal Plain (Dillow, 1996), in which stream discharge is expressed as a power function of basin area. The average exponent for basin area (A_B) in the flood frequency relationship (Equation 4.4) for lagoon watersheds is 0.71, which is very similar to the exponent between water surface area and basin area (Equation 4.7). Investigation of the scatter in this relationship indicates that it may be related to land cover variability observed in these watersheds (Table 4.1). Watersheds with >80% forested area have proportionally smaller 2-year floods and the lagoon surface area in this watersheds falls below the regional trend on Figure 4.4. Urban or agricultural land-uses increase runoff, and watersheds with significant proportions of these land-uses fall above the regional trend in Figure 4.4.

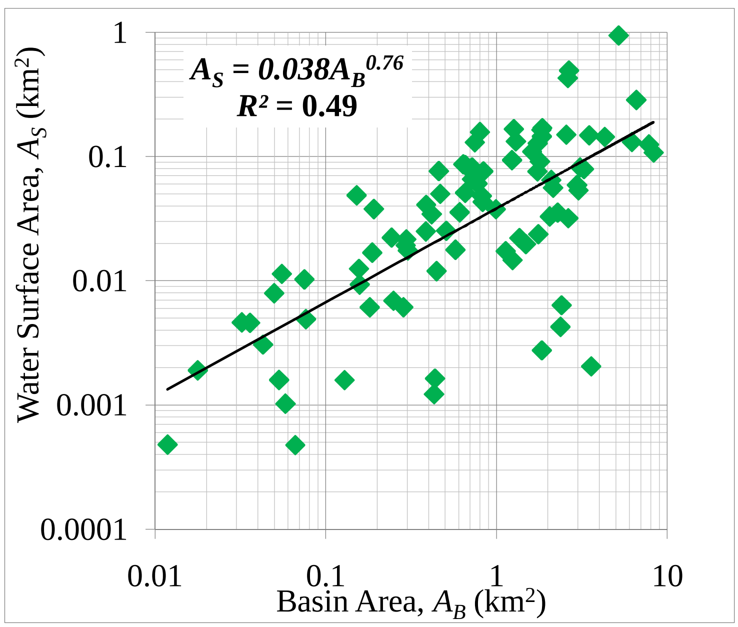

Figure 4.4: Relationship of watershed area (A_B) to lagoon water surface area (A_S) for CB lagoons.

<u>*4.3.4 Relationship between water surface area and tidal prism*</u>

The relative effect of tidal range and water surface area on the tidal prism can be investigated by plotting the spring tidal prism as a function of water surface area. These data for CB lagoons are shown in Figure 4.5a. Tidal range was determined from 11 tidal gauges located in proximity to the lagoon channels. The relationship between water surface area (A_S) and spring tidal prism (Ω) for CB lagoons is:

$$\Omega = 0.34 A_S^{1.0} \quad R^2 = 0.995 \qquad (4.8)$$

This relationship is linear (exponent of 1.0) and it indicates little variation in spring tidal range in regions of the CB where lagoons are found. The average spring tidal range for all of the lagoons is 0.34 m.

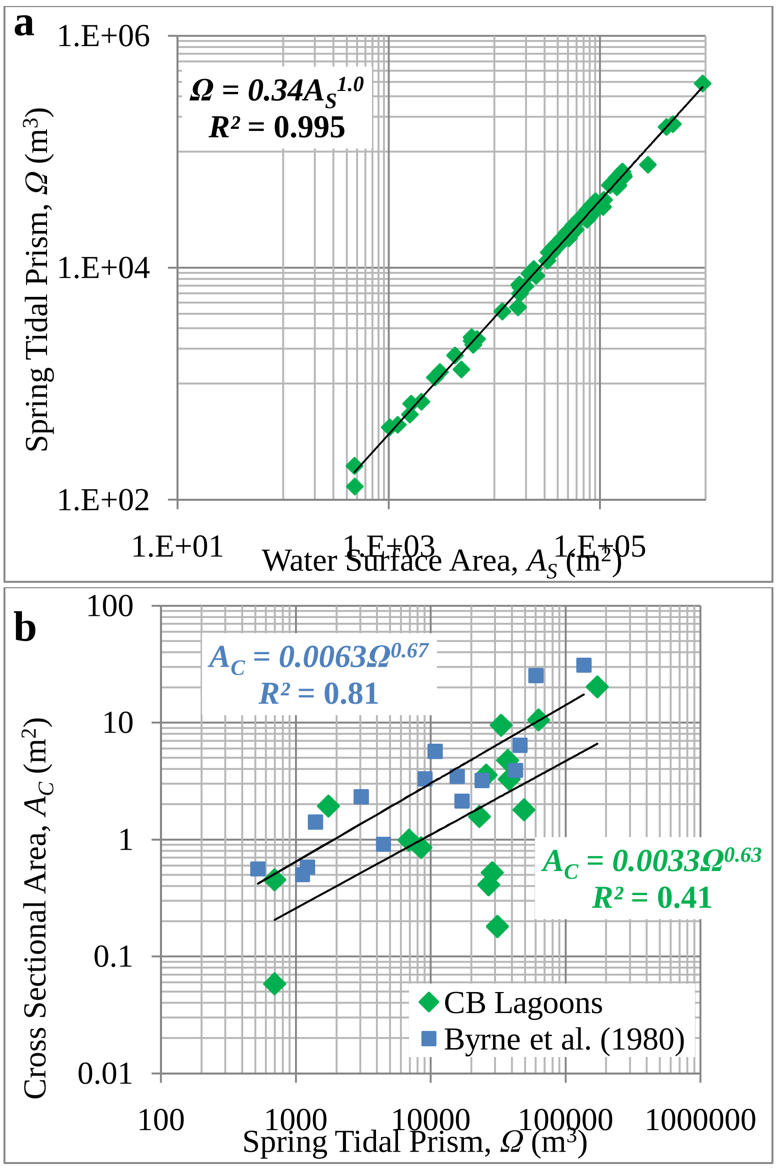

Figure 4.5: (a) Relationship between lagoon water surface area and spring tidal prism for CB lagoons; (b) Relationship between spring tidal prism and inlet cross sectional area for CB lagoons and inlet-basins measured by Byrne et al. (1980).

4.3.5 Inlet area-tidal prism relationship

The data on inlet channel area and tidal prism were used to develop an area-prism relationship exhibited by CB lagoons, which is:

$$A_C = 0.0033\Omega^{0.63} \quad R^2 = 0.41 \tag{4.9}$$

where A_C is inlet cross sectional area (m^2) and Ω is tidal prism (m^3; Figure 4.5b). This relationship is poorly defined (R^2 = 0.41), which might be expected due to the dependence of tidal prism on water surface area, and the heterogeneity of the watershed characteristics that provide underlying controls on lagoon water surface area. The upper boundary of these data is consistent with the area-prism relationship defined by Byrne et al. (1980) for sheltered CB inlets:

$$A_C = 0.0063\Omega^{0.67} \quad R^2 = 0.81. \tag{4.10}$$

Due to the small tidal range, tidal prism is defined primarily by lagoon water surface area for CB lagoons. Therefore, the area-prism relationship reflects both the heterogeneity of runoff from small drainage basins and the independent variation in inlet grain size and other factors that affect inlet morphology. These processes might lead to the considerable variation observed in the area-prism relationship for CB lagoons.

4.3.6 Comparison of basin discharge (Q_B) to 2-year R.I. peak discharge (Q_2)

In this section, I compare results from the two methods used to determine discharge from the contributing watershed (Q_B and Q_2) and then compare this discharge to the maximum bankfull discharge for the lagoon inlet (Q_M). Basin discharge (Q_B) was calculated by solving Equation 4.3 (the continuity equation) for basin discharge, where cross sectional area (A_C) and water surface area (A_S) are measured values, maximum velocity (U_M) is estimated from a Froude number = 1, and spring tidal range (h_R) and period (T) are determined from nearby NOAA tide stations. This calculation was made for all 15 measured inlet cross sections and yielded both positive and negative basin discharge values. Negative or zero values of Q_B indicate that the tidal prism ($A_S h_R$) is large in proportion to the inlet geometry and predicted stream discharge. Most of the basin discharge values were positive and the proportion of velocity contributed by the basin discharge is: U_B/U_M where U_B is the velocity of the basin discharge, defined as: Q_B/A_C and the total inlet velocity (U_M) is obtained from the critical Froude number estimation. Results indicate that for most of the lagoons, at least 60% of the total inlet velocity is from basin discharge contributions. Data for water surface area (A_S) and basin discharge (Q_B) from the continuity equation (Equation 4.3) is shown in Figure 6.

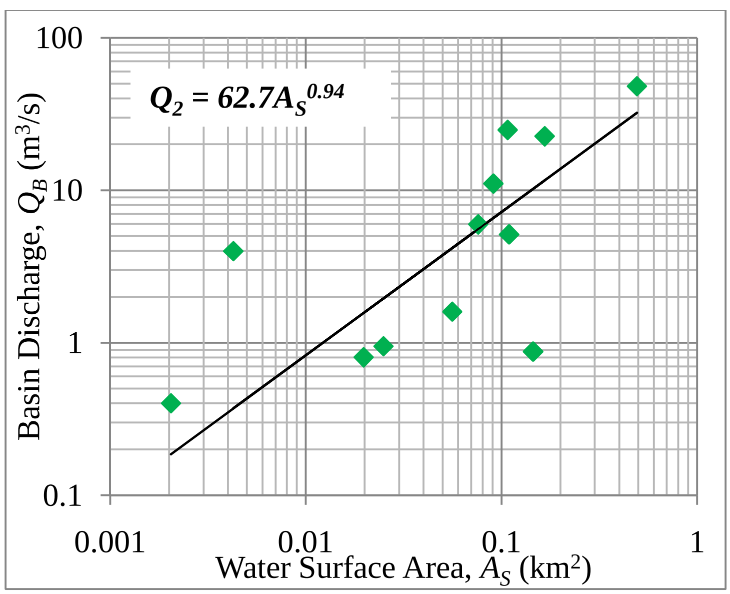

Figure 4.6: Relationship between water surface area and basin discharge derived from the continuity equation (see text). The solid line on this diagram is the 2-year peak discharge (Q_2) predicted from the average regional flood frequency relationship for Coastal Plain streams.

The contributions of basin discharge derived from the inlet continuity equation can be compared with the 2-year flood discharge by expressing both discharges (Q_2 and Q_B) as functions of equilibrium lagoon surface area (A_S). The empirical relationship between water surface area and drainage basin area (Figure 4.4) is given by Equation 4.7 and the relationship between the 2-year peak discharge (Q_2) and drainage basin area derived from flood frequency equations for Maryland coastal watersheds is given by Equation 4.4. Thus, these two equations and three variables (Q_2, A_B, A_S) can be manipulated to solve for an additional equation between the 2-year peak discharge (Q_2) and lagoon water surface area (A_S), which is the equation and solid line shown in Figure 4.6; a figure in which the basin discharge Q_B was determined from continuity considerations. First, each equation is solved for A_B:

$$A_B = \left(\frac{A_s}{0.038}\right)^{1.3} \tag{4.11}$$

$$A_B = \left(\frac{Q_2}{2.9}\right)^{1.4} \tag{4.12}$$

and then set equal to one another:

$$\left(\frac{A_s}{0.038}\right)^{1.3} = \left(\frac{Q_2}{2.9}\right)^{1.4}. \tag{4.13}$$

Solving for Q_2 I find:

$$Q_2 = 62.7A_S^{0.94} \tag{4.14}$$

where Q_2 is measured in m^3/s and A_S is in km^2. This relationship and its agreement with data (Figure 6) justifies the simplifying assumption of using a Froude number of 1 to estimate maximum average velocity for the lagoon inlet. These results also suggest that inlet channel formative velocities are predominately from basin discharge sources.

4.3.7 Relationship of Q_M to inlet channel geometry

Lagoon channels with large width to depth ratios are interpreted to have shoaled due to landward transport of sediment by waves. This wave-modified inlet geometry, however, should not be used to estimate channel forming discharges, which suggests that the relationship of channel width to discharge (Figure 4.7a), rather than cross sectional area to discharge (Figure 4.7b) provides a more accurate procedure for the estimation of channel-forming inlet discharge (Q_M).

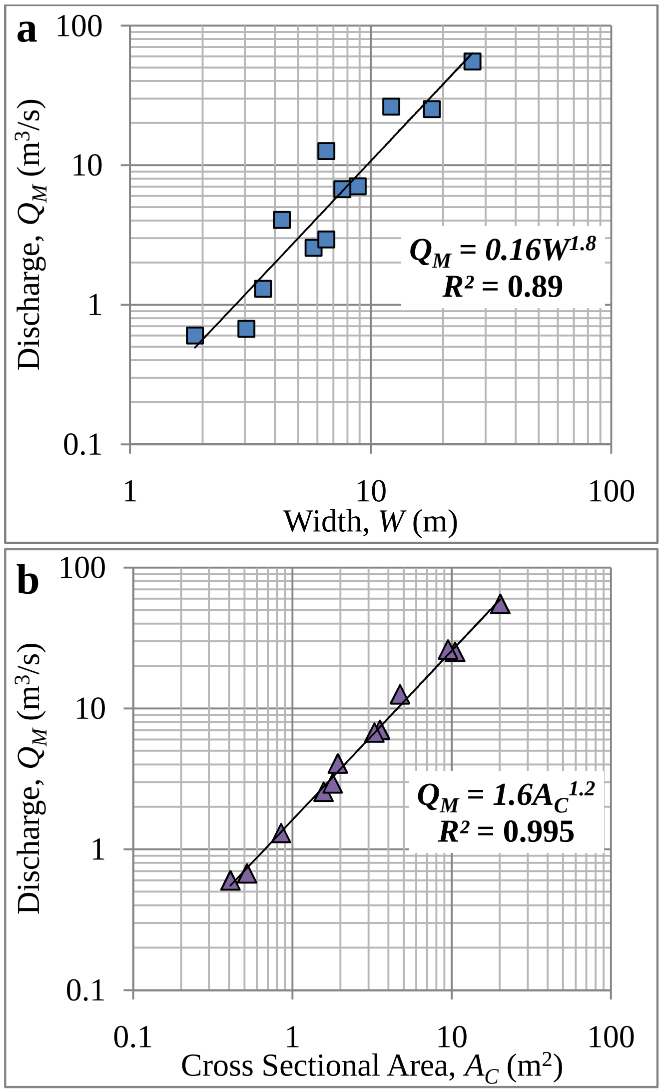

Figure 4.7: (a) Relationship between inlet width and maximum inlet discharge. (b) Relationship between cross sectional area and maximum inlet discharge for CB lagoons.

4.4 Lagoon and watershed assessment procedures

The classic approach to assess lagoon characteristics (tidal prism and inlet characteristics) has been provided by the area-prism relationship (e.g. Jarrett, 1976). This relationship includes water surface area (a component of tidal prism), inlet cross sectional area, but it only includes discharge from drainage basin sources indirectly through the controls of basin area on lagoon water surface area. This provides significant limitations on the usefulness of the area-prism relationship in identifying sources of disequilibrium among components of lagoon-watershed systems. We suggest that the area-prism relationship identified by Byrne et al. (1980) should be used as a first step to identify disequilibrium between water surface area and inlet characteristics.

If the area-prism relationship suggests disequilibrium or if you wish to predict changes due to climate or land-use changes, we suggest a series of assessment procedures based on lagoon, watershed, and inlet characteristics. If the area-prism relationship implies disequilibrium, these procedures can be used to identify controlling variables that affect the area-prism relationship.

Lagoon–inlet systems in equilibrium should have similar Q_B and Q_2 values, where Q_B is obtained from continuity considerations of lagoon and inlet characteristics and Q_2 is determined from watershed characteristics and regional flood frequency equations. The assessment procedures are provided in two flow charts (Figure 4.8). The first flow chart is designed to assess basin discharge. It begins with basin characteristics and uses the average regional relationship (Equation 4.4) for lagoon watersheds to estimate the 2-year peak flow from drainage basin area data (Figure 4.8a). If the watershed under evaluation is significantly different from the average coastal plain watersheds, then more detailed flood frequency relationships defined by Dillow (1996) should be used for analysis. The results of the drainage basin analysis can be compared with the water surface area-basin area relationship (Equation 4.7) to determine whether the water surface and thus tidal prism are in equilibrium with the contributing drainage basin area.

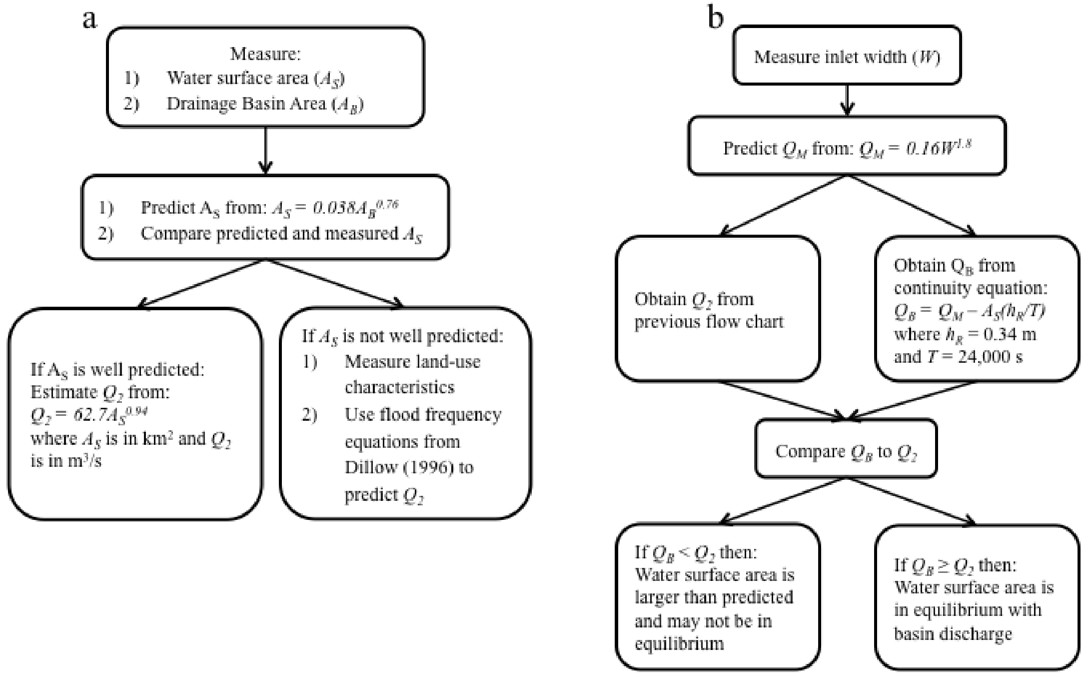

Figure 4.8: Flow diagram for (a) watershed assessment and (b) lagoon inlet assessment for CB lagoons.

The second flow chart begins with inlet geometry characteristics (Figure 4.8b) and uses inlet hydraulic relationships as well as the 2-year peak discharge to determine the proportion of streamflow-derived velocity in the inlet. Results from this study indicate that maximum channel velocities are largely due to streamflow-derived velocities.

If a lagoon-inlet system is consistent with: a) the area-prism relationship, b) the drainage-basin water surface relationship, and c) tidal and drainage basin discharge are sufficient to maintain inlet morphology, then the system is considered at equilibrium; this does not, however, ensure that the inlet will be maintained in an open condition. Intermittent lagoon closure is a natural phenomenon; most of the inlet channels with widths less than 15m are susceptible to temporary closure conditions. The relationships between inlet width and inlet cross sectional area (Figure 4.3a) indicate at any given time, inlet channel morphology can take one of two alternate stable states (Holling, 1973), due to recent streamflow or wave transport events.

4.5 Discussion

In this study, I have captured a snapshot of lagoon geomorphic characteristics for 86 lagoons, which provides a robust data set for comparison with other geomorphic populations. The "alternate states" observed in the inlet channel area provides a cautionary note for the measurement and assessment of inlet channel area and its relationship to underlying processes. Data from intermittent and open lagoons indicate that inlet length is independent of inlet width and appears to have no bearing on inlet closure. Most inlets that are always open have inlet width greater than 15-20 meters. Widening a channel to 20 m, however, will not create an open inlet unless this inlet can be maintained by combined tidal discharge and stream discharge from small, frequent floods.

This project, however, was not designed to evaluate temporal changes in inlet characteristics or water surface areas. Future research on CB lagoons could identify the frequency of closure for various lagoons under different scenarios of waves and flood events. Field study of a set of lagoons that represent the population distribution could provide important information on these sediment transport processes and feedbacks among stream discharge, inlet morphology, tidal flow, and sediment transport by waves.

The assessment procedures described here are preliminary and assessment by empirical equations should be accompanied by air photo and field measurements to assess watershed and lagoon changes over time. Many small lagoon inlets are naturally dynamic and will periodically open and close, depending on the sequences of sediment transport events (e.g. streamflow, waves). A lagoon that is intermittently open may provide unique habitats where small fish and crustaceans can escape predators, and these intermittently lagoons may be important for the CB ecosystem (Roy et al., 2001; Yáñez – Arancibia et al., 1994). The duration of opening and closing may change due to changes in wave climate due to changes in sea-level or storminess (Haines and Thom, 2007). Inter-annual variations in streamflow may be increasing, with more frequent floods and droughts (Kaushal et al., 2008; Acker et al., 2005; Neff et al., 2000); which may lead to significant changes in inlet behavior, salinity, or other drivers of ecosystem change.

These small coastal ecosystems, however, are particularly vulnerable to climate change and anthropogenic changes in lagoon watersheds due to their dependence on streamflow generation processes that can be highly variable and because of their intermittent connection to CB (Elwany, 2011; Haines and Thom, 2007; Kemp et al., 2005; Roy et al., 2001). One of the most important results of this research is that the heterogeneity of the contributing drainage basins leads to variable hydrologic responses that may directly impact lagoon morphology and function. The small size of these watersheds make them particularly vulnerable to land-use changes (Birkinshaw et al., 2011; Villarini and Smith, 2010; Gupta, 2004; Dillow, 1996), which could affect basin contributions to streamflow that in turn may affect lagoon inlet status (i.e. open, closed, intermittent).

This research indicates that lagoons occupy a narrow range of small watersheds that are responsive to changes in land-use. Although sea level is rising, population growth in CB coastal communities continues to increase, which puts additional pressure on these small coastal ecosystems. For example, increases in urban and residential land-uses may result in higher peak flows that may result in increases in lagoon water surface area. Erosion of lagoon shorelines may have direct impacts on the people who have built along the shorelines. Alternatively, truncation of watersheds by roads, ponds, and other structures may limit streamflow contributions to lagoons, which may result in low water levels during dry periods and limit the peak flows that maintain inlet morphology. Positive feedbacks among anthropogenic changes in lagoon watersheds and lagoon morphological responses may create disequilibrium conditions that are difficult to correct.

These changes in land-use and lagoon characteristics have been observed at Northwest Creek lagoon, located on the western shore of Kent Island. The lagoon was bulldozed shut in the 1970s to enhance the beach. Wave erosion has significantly expanded the lagoon surface area; a processes that has been enhanced by variable water levels and removal of marsh vegetation along the shoreline. Roads, dams and other structures have decreased streamflow discharge into the lagoon. These series of changes have created a lagoon water surface area that is significantly larger than predicted from the area-prism relationship and the basin area-lagoon surface area relationship presented in this paper. The lagoon cannot be restored by merely re-opening the channel inlet. Restoration procedures would require changes in the water surface area, restoration of marsh vegetation along the shorelines, and finding the best compromise to equilibrium conditions among the system components.

4.6 Conclusions

Lagoons in the CB region represent a unique ecosystem that has formed within a narrow range of geomorphic conditions that are constrained by streamflow, tidal, and wave processes. These processes act with and against one another over time, creating both open and closed inlet conditions and a range of lagoon and inlet characteristics. The results of this study indicate that for CB lagoons, stream discharge is the dominant driver of both lagoon surface area and inlet cross section morphology; however, inlet characteristics can be altered by wave sediment transport. Results from this study indicate that streamflow-dominated lagoon inlets derive at least 60% of their inlet velocity from the basin discharge velocity. Finally, the two alternate inlet states suggest that large inlets tend to remain open, whereas smaller inlets are more susceptible to intermittent closure, which depends on whether streamflow can maintain inlet depth during prevailing wave conditions.

In this study, I have derived a number of relationships for watershed and lagoon assessment that can be used to predict responses to watershed or sea level changes and to assess the success of management efforts. Evaluation of lagoon characteristics through the series of empirical relationships that I have derived will provide information on processes that control the area-prism relationship. These empirical relationships can be used to find disequilibrium among lagoon system components and identify restoration strategies.

Appendix A: Chesapeake Bay Lagoon Data

No.	Name of Lagoon	No.	Name of Lagoon	No.	Name of Lagoon
1	Long Neck Creek	31	Cove Lake	61	Curtis Bay Pleasure S.
2	Holly Dr	32	Webster Ponds	62	Curtis Bay Pleasure N.
3	Fresh Pond	33	Cove Point Rd	63	Fort Smallwood Park
4	Murray Road	34	Calvert Cliffs S.	64	Stavley Pond
5	Peters Pond	35	Calvert Cliffs N.	65	Big Fairlee Pond
6	Filbert Pond	36	Camp Conoy Rd	66	Mendinhall Lake
7	St. Clarence Creek S.	37	Todds Pond	67	Bramble Lake
8	St. Clarence Creek M.	38	Flag Ponds	68	Hinchingham Lane
9	St. Clarence Creek N.	**39**	**Brownies Beach Rd**	69	Cabin Cove
10	Shipwreck Way	40	Sewage Plant Rd	70	River Shore Lane
11	Carroll Pond	**41**	**North Beach**	71	Love Point
12	**Biscoe Pond**	**42**	**Herring Bay**	72	Price Farm Lane
13	**St. James Church Rd**	43	Beverly Beach Park	73	Terrapin Beach Park N.
14	Elms Environmental	44	Deep Pond	74	Terrapin Beach Park M.
15	Spring Lake Dr	**45**	**Big Pond**	**75**	**Terrapin Beach Park S.**
16	Page Pond	46	Southbreeze Lane	76	Wellman Way
17	Tippitt Pond	**47**	**Blackwalnut Creek**	77	Lake Cardoza
18	Norris Pond	48	Heron Lake	78	Bay Dr
19	Far Cry Farm Lane	**49**	**Chase Pond**	79	Price Creek
20	Massum Eyrie Way	50	W Road	**80**	**Carter Creek**
21	Sivak Way	51	Sharps Point Rd	81	Bloody Point Rd
22	Massum Eyrie Rd	52	Westinghouse Bay	81	Northwest Creek
23	**Long Lane**	53	Mezick Ponds	83	Holligans Snooze
24	Shaw Rd	54	Cape St Claire	84	Skove Lane
25	**Drum Point Pond**	55	Lake Claire	85	Scaffold Creek
26	Lake Charming	56	Morgan Dr	86	Kent Fort Manor
27	Clubhouse Dr	57	Broadwater Rd		
28	Cheyenne Lane	58	Downs Park		
29	Algonquin Trail	59	Kurtz Ave		
30	Aztec Trail	**60**	**Hines Pond**		

Field measurements were made at the **bolded** lagoons.

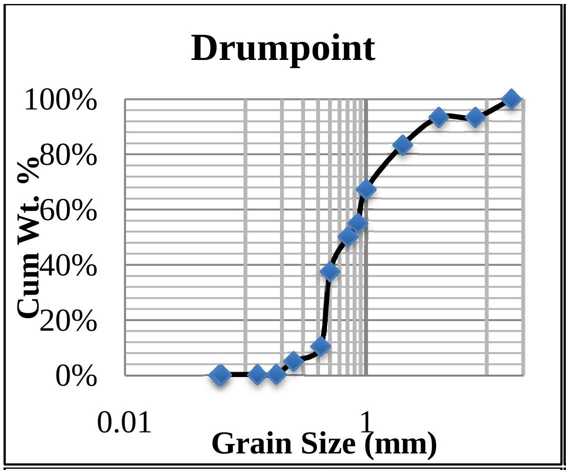
Drumpoint
100%
80%
60%
40%
20%
0%
Cum Wt. %
0.01
1
Grain Size (mm)

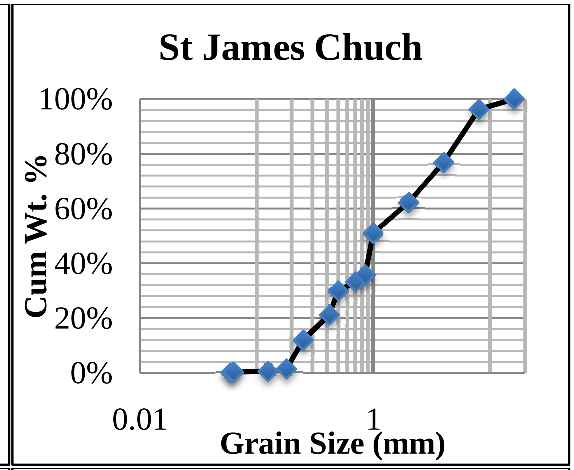
St James Chuch
100%
80%
60%
40%
20%
0%
Cum Wt. %
0.01
1
Grain Size (mm)

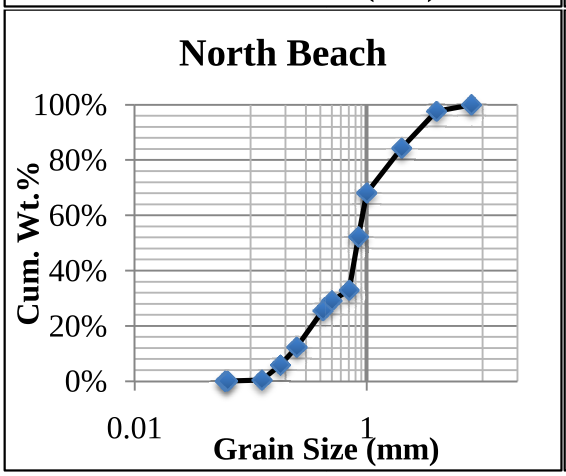
North Beach
100%
80%
60%
40%
20%
0%
Cum. Wt.%
0.01
1
Grain Size (mm)

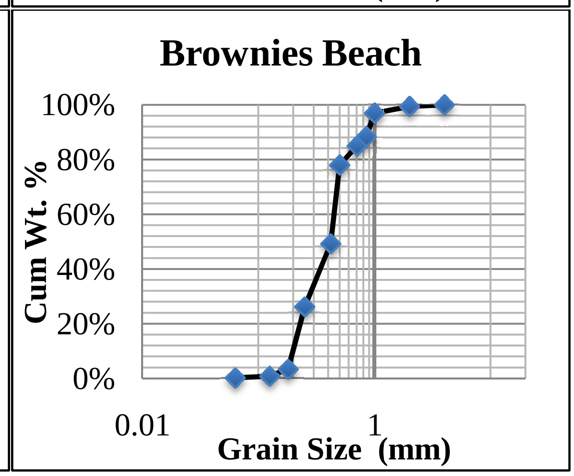
Brownies Beach
100%
80%
60%
40%
20%
0%
Cum Wt. %
0.01
1
Grain Size (mm)

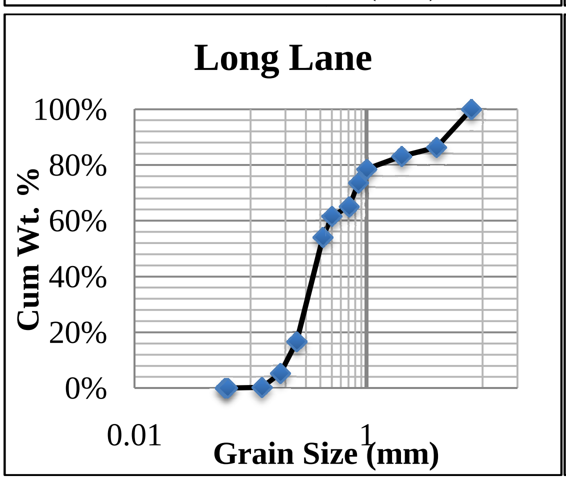
Long Lane
100%
80%
60%
40%
20%
0%
Cum Wt. %
0.01
1
Grain Size (mm)

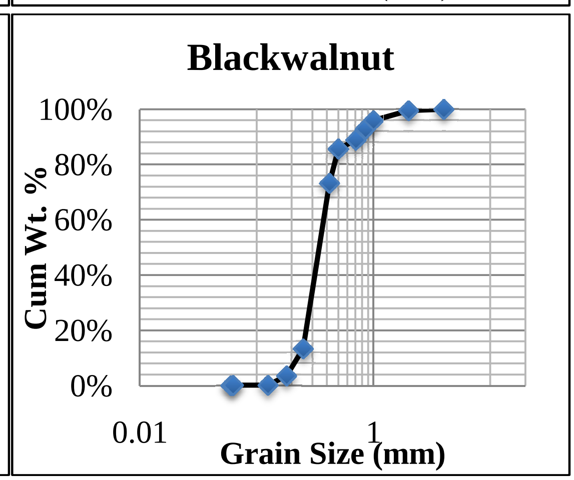
Blackwalnut
100%
80%
60%
40%
20%
0%
Cum Wt. %
0.01
1
Grain Size (mm)

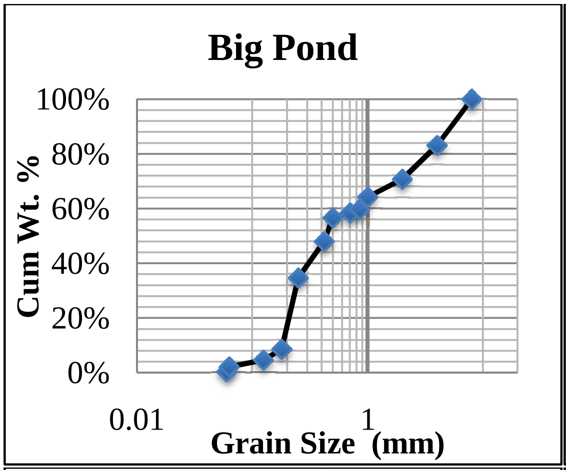
Big Pond
100%
80%
60%
40%
20%
0%
Cum Wt. %
0.01
1
Grain Size (mm)

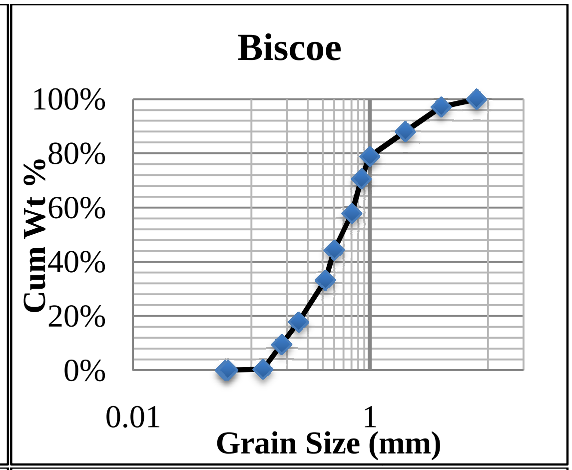
Biscoe
100%
80%
60%
40%
20%
0%
Cum Wt %
0.01
1
Grain Size (mm)

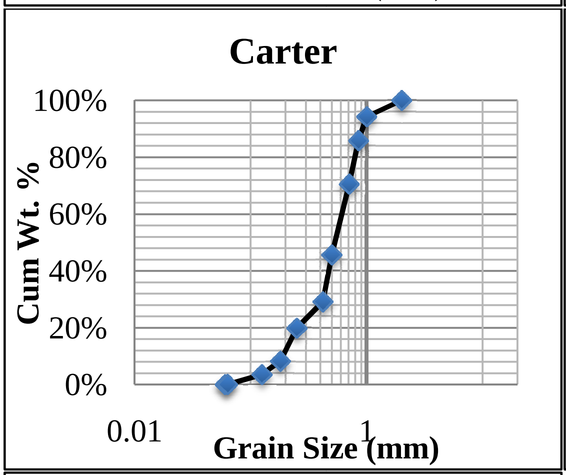
Carter
100%
80%
60%
40%
20%
0%
Cum Wt. %
0.01
1
Grain Size (mm)

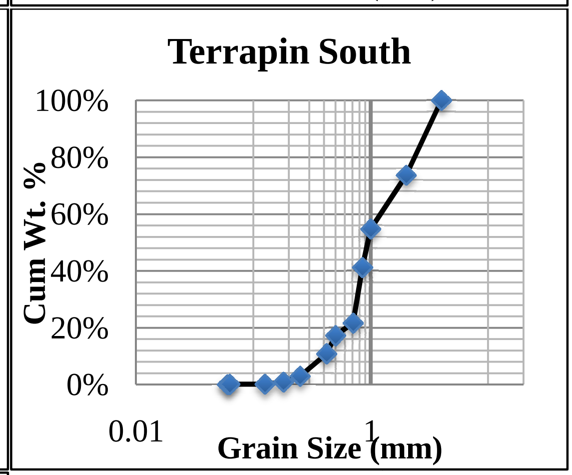
Terrapin South
100%
80%
60%
40%
20%
0%
Cum Wt. %
0.01
1
Grain Size (mm)

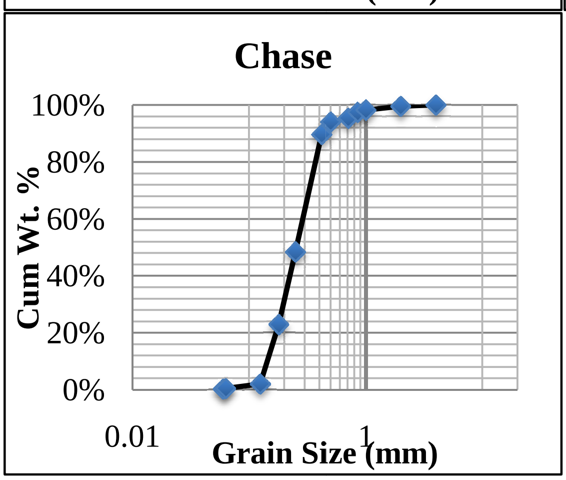
Chase
100%
80%
60%
40%
20%
0%
Cum Wt. %
0.01
1
Grain Size (mm)

Appendix B: Patuxent River Tidal Marsh Data

Channel ID	Marsh Basin Area, A_B (m^2)	Water Surface Area, A_S (m^2)	Spring Tidal Range, h_R (m)*	Spring Tidal Prism, Ω (m^3)	Inlet Width, W (m)	Cross Sectional Area, A_C (m^2)+
			Self-forming tidal marshes			
63	515	61	1.00	61	16.8	10.5
64	876	212	0.43	91	6.6	2.9
65	20336	3197	0.46	1470	7.8	3.6
66	3191	342	0.28	97	2.3	0.7
67	2427	325	0.31	102	3.0	0.9
68	388	70	0.31	22	2.9	0.9
70	7847	343	0.25	86	1.7	0.4
71	5875	394	0.26	103	1.9	0.5
72	1667	138	0.23	32	1.4	0.3
73	3146	264	0.19	49	0.8	0.2
75	42	6	0.15	1	0.5	0.1
76	48	7	0.11	1	0.2	0.0
77	3919	301	0.20	60	1.0	0.2
78	203	17	0.14	2	0.4	0.1
79	49	9	0.15	1	0.5	0.1
80	105	18	0.20	4	0.9	0.2
81	411	49	0.30	15	2.8	0.8
82	1364	142	0.45	64	7.3	3.3
83	4334	544	0.55	302	12.4	6.9
84	1698	148	0.18	26	0.7	0.1
85	2213	166	0.19	32	0.9	0.2
86	3249	239	0.30	71	2.7	0.8
87	1061	110	0.22	24	1.3	0.3
88	789	50	0.24	12	1.5	0.4
89	1714	134	0.27	36	2.0	0.5
90	5979	495	0.54	267	11.6	6.2
91	230	13	0.20	2	0.9	0.2
92	888	90	0.34	31	3.7	1.3
93	494	21	0.22	5	1.3	0.3
94	674	92	0.30	27	2.6	0.8
95	3684	292	0.43	126	6.6	2.8

Channel ID	Marsh Basin Area, A_B (m^2)	Water Surface Area, A_S (m^2)	Spring Tidal Range, h_R (m)*	Spring Tidal Prism, Ω (m^3)	Inlet Width, W (m)	Cross Sectiona l Area, A_C (m^2)$^+$
96	137	13	0.21	3	1.1	0.2
97	268	18	0.27	5	2.1	0.6
99	7001	585	0.37	215	4.5	1.6
100	264	23	0.30	7	2.7	0.8
101	342	32	0.14	5	0.4	0.1
102	110	10	0.25	3	1.6	0.4
103	90	10	0.11	1	0.2	0.0
104	2601	205	0.19	39	0.9	0.2
105	101	13	0.11	1	0.2	0.0
106	131	12	0.11	1	0.2	0.0
107	7632	745	1.00	745	16.5	10.3
108	1140	120	0.20	24	1.0	0.2
109	1576	146	0.19	28	0.9	0.2
110	852	67	0.12	8	0.3	0.0
111	853	110	0.16	18	0.6	0.1
112	2408	237	0.42	99	6.2	2.6
113	1656	238	0.19	44	0.8	0.2
114	311	60	0.24	15	1.6	0.4
115	2478	255	0.25	63	1.6	0.4
116	742	72	0.22	16	1.3	0.3
118	1190	83	0.16	13	0.6	0.1
119	97	15	0.11	2	0.2	0.0
120	551	47	0.15	7	0.5	0.1
121	1849	196	0.37	72	4.5	1.7
122	337	69	0.25	17	1.7	0.4
123	107	21	0.34	7	3.6	1.2
124	1154	183	0.29	53	2.5	0.7
125	1298	128	0.34	44	3.7	1.3
126	135	15	0.11	2	0.2	0.0
127	100	13	0.14	2	0.4	0.1
128	419	28	0.26	7	1.8	0.5
129	224	21	0.19	4	0.8	0.2
131	78	18	0.11	2	0.2	0.0
132	123	17	0.11	2	0.2	0.0
133	198	50	0.27	13	2.1	0.6
134	2470	289	0.23	66	1.3	0.3

Channel ID	Marsh Basin Area, A_B (m^2)	Water Surface Area, A_S (m^2)	Spring Tidal Range, h_R (m)*	Spring Tidal Prism, Ω (m^3)	Inlet Width, W (m)	Cross Sectional Area, A_C (m^2)$^+$
135	544	35	0.17	6	0.7	0.1
136	31318	4392	1.00	4392	65.5	70.9
137	3987	259	0.19	50	0.9	0.2
139	1390	95	0.23	22	1.4	0.3
140	467	32	0.25	8	1.7	0.4
141	2281	337	0.59	200	14.6	8.7
142	2237	228	0.54	124	11.9	6.5
143	1284	155	0.47	73	8.3	3.9
144	8464	560	0.41	227	5.7	2.3
145	29833	1956	0.58	1131	13.8	8.0
146	9632	605	0.53	319	11.0	5.8
147	6788	588	1.00	588	17.6	11.2
148	112	18	0.11	2	0.2	0.0
149	5026	440	0.36	158	4.2	1.5
150	4534	429	0.29	126	2.5	0.7
151	166	20	0.11	2	0.2	0.0
152	1738	151	0.26	39	1.9	0.5
153	2122	232	0.32	74	3.1	1.0
154	612	33	0.30	10	2.7	0.8
155	2581	171	0.24	40	1.5	0.3
156	512	59	0.24	14	1.5	0.4
157	433	39	0.41	16	5.7	2.3
158	17884	1512	1.00	1512	31.1	24.9
159	3163	436	0.55	239	12.0	6.6
160	57920	4256	1.00	4256	44.0	40.6
161	6494	155	0.44	68	7.1	3.1
162	1565	55	0.31	17	2.8	0.9
163	440	37	0.27	10	2.2	0.6
164	1350	162	1.00	162	23.1	16.4
165	6401	248	1.00	248	21.3	14.7
166	1428	116	0.27	32	2.2	0.6
167	1284	108	0.27	30	2.2	0.6
168	220	41	0.24	10	1.5	0.4
169	3393	168	0.36	61	4.3	1.6
170	393	28	0.13	4	0.4	0.0
171	437	36	0.26	9	1.9	0.5

Channel ID	Marsh Basin Area, A_B (m^2)	Water Surface Area, A_S (m^2)	Spring Tidal Range, h_R (m)*	Spring Tidal Prism, Ω (m^3)	Inlet Width, W (m)	Cross Sectiona l Area, A_C (m^2)$^+$
172	7666	567	0.29	164	2.5	0.7
175	5716	265	0.22	59	1.3	0.3
177	9130	406	0.22	89	1.2	0.3
178	2104	98	0.24	24	1.6	0.4
179	4665	260	0.25	64	1.7	0.4
180	3545	313	0.47	147	8.3	3.9
181	1937	128	0.45	57	7.3	3.2
182	1672	90	0.22	19	1.2	0.3
183	655	28	0.11	3	0.2	0.0
184	1377	108	0.11	11	0.2	0.0
185	12247	648	0.59	383	14.5	8.5
186	8178	334	0.35	116	3.9	1.3
187	2525	129	0.18	23	0.8	0.1
188	4074	203	0.14	29	0.4	0.1
189	10489	557	0.47	261	8.2	3.8
190	13544	906	1.00	906	20.6	14.0
191	4514	282	0.19	53	0.8	0.2
192	2628	219	0.27	60	2.2	0.6
193	1429	62	0.11	7	0.2	0.0
194	447	37	0.11	4	0.2	0.0
195	451	28	0.11	3	0.2	0.0
196	471	30	0.11	3	0.2	0.0
197	335	35	0.13	5	0.3	0.0
198	766	99	0.17	16	0.6	0.1
199	214	54	0.14	7	0.4	0.1
200	174	40	0.11	4	0.2	0.0
201	598	46	0.14	6	0.4	0.1
202	806	86	0.14	12	0.4	0.1
203	6689	264	0.46	120	7.7	3.5
204	2341	110	0.36	39	4.2	1.5
205	356	41	0.14	6	0.4	0.1
206	424	37	0.15	6	0.5	0.1
207	2237	146	0.24	35	1.6	0.4
208	256	59	0.16	9	0.5	0.1
209	212	49	0.13	6	0.3	0.0
210	197	32	0.15	5	0.5	0.1

Channel ID	Marsh Basin Area, A_B (m^2)	Water Surface Area, A_S (m^2)	Spring Tidal Range, h_R (m)*	Spring Tidal Prism, Ω (m^3)	Inlet Width, W (m)	Cross Sectiona l Area, A_C (m^2)$^+$
211	268	42	0.11	4	0.2	0.0
212	317	51	0.15	8	0.5	0.1
213	961	94	0.13	12	0.3	0.0
214	920	92	0.13	12	0.3	0.0
215	895	110	0.21	23	1.1	0.2
216	1742	197	0.15	29	0.5	0.1
217	343	33	0.11	4	0.2	0.0
218	449	53	0.15	8	0.5	0.1
219	1377	125	0.16	20	0.6	0.1
220	1998	173	0.16	29	0.6	0.1
221	1925	233	0.15	35	0.5	0.1
222	2338	243	0.13	31	0.3	0.0
223	891	48	0.12	6	0.3	0.0
224	2144	236	0.15	37	0.5	0.1
225	1249	147	0.15	21	0.4	0.1
226	1340	230	0.14	31	0.4	0.1
227	1032	151	0.16	24	0.6	0.1
228	438	45	0.14	6	0.4	0.1
229	248	29	0.12	4	0.3	0.0
230	467	47	0.14	7	0.4	0.1
231	710	50	0.14	7	0.4	0.1
232	3579	266	0.14	36	0.4	0.1
233	2222	240	0.19	46	0.9	0.2
234	6255	562	0.23	132	1.5	0.3
235	4439	420	0.24	100	1.5	0.4
236	26259	1755	0.29	517	2.6	0.8
237	777	53	0.11	6	0.2	0.0
238	1385	119	0.11	13	0.2	0.0
239	45133	3536	0.50	1778	9.7	4.9
240	3734	281	0.15	42	0.5	0.1
241	4686	326	0.13	41	0.3	0.0
243	1551	277	1.00	277	33.3	27.5
246	19981	3255	0.40	1300	5.5	2.2
247	1461	125	0.11	13	0.2	0.0
248	1157	101	0.11	11	0.2	0.0
249	3200	171	0.17	29	0.6	0.1

Channel ID	Marsh Basin Area, A_B (m^2)	Water Surface Area, A_S (m^2)	Spring Tidal Range, h_R (m)*	Spring Tidal Prism, Ω (m^3)	Inlet Width, W (m)	Cross Sectional Area, A_C (m^2)$^+$
250	5202	266	0.29	78	2.6	0.8
251	11366	1069	0.30	323	2.7	0.8
252	13228	743	0.20	150	1.0	0.2
253	691	70	0.20	14	1.0	0.2
254	3754	282	0.26	73	1.9	0.5
255	5234	498	0.17	86	0.7	0.1
256	3856	884	0.15	133	0.5	0.1
257	334	36	0.18	6	0.8	0.1
258	582	62	0.18	11	0.8	0.1
259	2651	249	0.16	39	0.5	0.1
260	3766	320	0.13	43	0.4	0.0
261	3117	207	0.17	35	0.6	0.1
262	2200	205	0.22	46	1.3	0.3
263	8322	1031	0.45	464	7.4	3.3
264	3401	257	0.50	128	9.4	4.7
265	3277	245	0.33	81	3.4	1.1
266	1002	78	0.22	17	1.2	0.3
267	11317	700	0.42	294	6.2	2.6
268	8835	660	0.35	228	3.8	1.3
269	7179	514	0.27	139	2.1	0.6
270	2593	223	0.43	97	6.7	2.9
272	7280	89	0.16	14	0.5	0.1
273	2436	116	0.16	19	0.6	0.1
274	5269	163	0.16	25	0.5	0.1
275	6535	465	0.11	49	0.2	0.0
276	20935	1005	0.14	142	0.4	0.1
278	763	71	0.19	14	0.9	0.2
279	24983	1034	0.21	217	1.1	0.2
280	1574	156	0.11	16	0.2	0.0
282	1071	74	0.16	12	0.6	0.1
284	755	64	0.15	10	0.5	0.1
285	2648	179	0.33	58	3.3	1.1
286	1176	77	0.17	13	0.6	0.1
287	1028	66	0.11	7	0.2	0.0
288	1059	110	0.11	12	0.2	0.0
289	666	51	0.20	10	1.0	0.2

Channel ID	Marsh Basin Area, A_B (m^2)	Water Surface Area, A_S (m^2)	Spring Tidal Range, h_R (m)*	Spring Tidal Prism, Ω (m^3)	Inlet Width, W (m)	Cross Sectiona l Area, A_C (m^2)$^+$
290	1698	77	0.20	15	1.0	0.2
291	911	60	0.14	8	0.4	0.1
292	4858	102	0.22	23	1.3	0.3
293	14260	353	0.17	59	0.6	0.1
294	7172	229	0.16	36	0.5	0.1
296	788	42	0.11	4	0.2	0.0
297	1618	100	0.15	15	0.4	0.1
298	3520	255	1.00	255	16.8	10.5
299	372	48	0.33	16	3.4	1.1
300	7180	516	1.00	516	31.1	25.0
301	5110	240	1.00	240	22.8	16.1
302	11725	786	1.00	786	16.6	10.4
303	2067	155	0.23	36	1.4	0.3
304	288	38	0.18	7	0.8	0.1
305	611	41	0.21	9	1.1	0.2
306	2353	126	0.18	23	0.8	0.1
307	1813	126	0.14	18	0.4	0.1
308	371	33	0.11	3	0.2	0.0
309	4432	295	0.45	133	7.4	3.4
310	3095	204	0.14	29	0.4	0.1
312	680	47	0.33	15	3.3	1.1
313	6081	78	0.39	30	5.2	2.0
314	17108	731	1.00	731	25.8	19.2
315	1385	134	0.12	17	0.3	0.0
317	5513	418	0.22	93	1.3	0.3
318	6100	521	0.31	164	3.0	1.0
319	1788	147	0.14	20	0.4	0.1
320	3333	339	0.36	123	4.4	1.6
321	1703	308	0.34	105	3.7	1.3
322	48096	4518	1.00	4518	52.7	52.3
323	7924	94	0.16	15	0.5	0.1
324	600	40	0.13	5	0.3	0.0
325	2592	143	0.37	53	4.5	1.7
326	5125	397	0.27	108	2.1	0.6
327	2419	185	0.50	92	9.4	4.7
328	6458	437	0.21	90	1.1	0.2

Channel ID	Marsh Basin Area, A_B (m^2)	Water Surface Area, A_S (m^2)	Spring Tidal Range, h_R (m)*	Spring Tidal Prism, Ω (m^3)	Inlet Width, W (m)	Cross Sectional Area, A_C (m^2)$^+$
329	16586	684	0.43	297	6.8	2.9
330	1473	51	0.11	5	0.2	0.0
331	4724	134	0.24	32	1.5	0.4
332	2168	158	0.22	34	1.2	0.3
333	1137	107	0.14	15	0.4	0.1
334	774	54	0.13	7	0.3	0.0
335	524	55	0.12	7	0.3	0.0
336	162	21	0.11	2	0.2	0.0
337	33884	1924	0.62	1193	27.6	21.1
338	13485	853	0.19	158	0.8	0.2
339	1018	67	0.19	13	0.8	0.2
340	246	49	0.11	5	0.2	0.0
341	403	59	0.15	9	0.5	0.1
342	11684	246	0.31	76	2.9	0.9
343	18221	814	0.36	294	4.3	1.5
344	1042	37	0.12	4	0.3	0.0
345	5547	265	0.13	35	0.3	0.0
346	20596	1115	0.46	517	8.0	3.7
347	807	70	0.13	9	0.3	0.0
348	58897	3628	0.62	2250	22.4	15.8
349	809	39	0.12	5	0.3	0.0
350	499	36	0.17	6	0.6	0.1
351	6709	191	0.29	55	2.4	0.7
352	521	61	0.18	11	0.7	0.1
353	11936	395	0.40	156	5.4	2.1
354	3155	99	0.20	20	1.0	0.2
355	3319	74	0.17	12	0.6	0.1
356	2298	85	0.15	13	0.5	0.1
358	603	43	0.19	8	0.8	0.2
359	318	52	0.17	9	0.6	0.1
360	1737	81	0.17	14	0.7	0.1
361	1351	124	0.15	18	0.5	0.1
362	505	95	0.12	11	0.3	0.0
363	153	24	0.11	3	0.2	0.0
364	10743	984	0.30	293	2.7	0.8
365	1673	55	0.19	10	0.8	0.2

Channel ID	Marsh Basin Area, A_B (m^2)	Water Surface Area, A_S (m^2)	Spring Tidal Range, h_R (m)*	Spring Tidal Prism, Ω (m^3)	Inlet Width, W (m)	Cross Sectiona l Area, A_C (m^2)$^+$
366	2013	129	0.14	19	0.4	0.1
367	1393	84	0.19	16	0.8	0.2
368	8721	563	0.33	184	3.3	1.1
369	1067	122	0.34	41	3.7	1.3
370	21943	789	0.62	489	53.8	53.8
371	2027	175	0.25	44	1.7	0.4
372	2224	179	0.25	44	1.7	0.4
373	2758	330	0.30	99	2.7	0.8
375	5579	126	0.20	26	1.0	0.2
376	16147	533	0.34	182	3.8	1.3
377	6509	96	0.23	22	1.4	0.3
378	9655	353	0.43	152	6.6	2.9
379	7412	538	0.62	334	15.8	9.7
380	18224	1660	0.25	415	1.7	0.4
381	1495	98	0.32	31	3.2	1.0
382	3358	263	0.39	102	5.1	2.0
384	763	42	0.32	13	3.1	1.0
385	65396	7300	0.62	4526	29.6	23.3
386	247	40	0.11	4	0.2	0.0
387	1066	117	0.15	17	0.5	0.1
388	3028	120	0.20	24	1.0	0.2
389	1521	160	0.13	21	0.4	0.0
390	1728	152	0.29	44	2.5	0.7
391	33486	1927	0.62	1195	27.6	21.1
392	14567	705	0.53	370	10.9	5.7
393	11921	707	0.40	280	5.4	2.1
394	1521	73	0.35	25	3.9	1.4
395	4461	319	0.29	92	2.4	0.7
396	3823	249	0.27	67	2.1	0.6
398	695	50	0.17	9	0.7	0.1
399	652	23	0.17	4	0.7	0.1
400	1603	32	0.17	6	0.7	0.1
401	2073	358	0.45	162	7.5	3.4
402	944	30	0.11	3	0.2	0.0
403	62730	4655	0.62	2886	23.9	17.3
404	1864	147	0.17	26	0.7	0.1

Channel ID	Marsh Basin Area, A_B (m^2)	Water Surface Area, A_S (m^2)	Spring Tidal Range, h_R (m)*	Spring Tidal Prism, Ω (m^3)	Inlet Width, W (m)	Cross Sectiona l Area, A_C (m^2)$^+$
406	9629	344	0.62	213	22.5	15.9
408	844	79	0.16	13	0.6	0.1
409	1462	175	0.20	34	0.9	0.2
410	1167	146	0.22	32	1.2	0.3
411	688	69	0.15	10	0.5	0.1
413	1557	182	0.37	68	4.6	1.7
414	7822	337	0.26	88	1.9	0.5
415	428	31	0.17	5	0.6	0.1
419	386	32	0.11	3	0.2	0.0
420	482	65	0.11	7	0.2	0.0
421	512	38	0.19	7	0.9	0.2
422	3178	349	0.27	95	2.1	0.6
423	40807	3141	0.36	1145	4.4	1.6
424	8360	308	0.19	58	0.8	0.2
425	28861	1403	0.41	572	5.8	2.4
426	746	65	0.11	7	0.2	0.0
427	66639	4834	0.62	2997	20.9	14.3
428	65774	3444	0.52	1794	10.6	5.5
429	8156	325	0.34	110	3.7	1.2
430	67678	4425	0.51	2253	10.0	5.1
431	22789	1391	0.33	454	3.3	1.1
432	4177	324	0.11	34	0.2	0.0
433	5915	293	0.19	55	0.8	0.2
434	4360	301	0.17	51	0.7	0.1
435	4687	321	0.33	106	3.4	1.1
436	9202	309	0.30	91	2.6	0.8
438	906	19	0.13	2	0.3	0.0
439	788	86	0.14	12	0.4	0.1
440	1341	68	0.14	10	0.4	0.1
441	4828	194	0.23	45	1.4	0.3
442	5122	267	0.25	66	1.7	0.4
443	4154	331	0.43	144	6.8	2.9
444	1090	41	0.15	6	0.5	0.1
445	595	43	0.14	6	0.4	0.1
446	571	23	0.17	4	0.6	0.1
447	506	47	0.21	10	1.1	0.2

Channel ID	Marsh Basin Area, A_B (m^2)	Water Surface Area, A_S (m^2)	Spring Tidal Range, h_R (m)*	Spring Tidal Prism, Ω (m^3)	Inlet Width, W (m)	Cross Sectiona l Area, A_C (m^2)$^+$
448	929	88	0.34	29	3.6	1.2
449	909	47	0.23	11	1.4	0.3
450	831	26	0.12	3	0.3	0.0
451	2498	187	0.17	32	0.7	0.1
452	1291	30	0.16	5	0.5	0.1
453	4181	134	0.14	19	0.4	0.1
454	4639	235	0.23	55	1.5	0.3
455	55803	3308	0.58	1931	14.1	8.2
456	8704	362	0.23	82	1.4	0.3
457	144	31	0.11	3	0.2	0.0
458	285	25	0.11	3	0.2	0.0
459	3802	190	0.24	45	1.5	0.4
460	47270	4575	0.59	2717	14.7	8.7
461	410	110	0.11	12	0.2	0.0
462	920	94	0.11	10	0.2	0.0
463	614	79	0.11	8	0.2	0.0
464	1731	248	0.18	46	0.8	0.1
465	597	113	0.11	12	0.2	0.0
466	23596	1740	0.43	749	6.6	2.8
467	724	86	0.15	12	0.4	0.1
468	2005	225	0.17	39	0.7	0.1
469	265	38	0.11	4	0.2	0.0
470	214	18	0.11	2	0.2	0.0
471	644	60	0.18	11	0.8	0.1
472	1131	72	0.20	15	1.0	0.2
473	174	29	0.11	3	0.2	0.0
474	275	64	0.14	9	0.4	0.1
475	204	68	0.14	10	0.4	0.1
476	2964	232	0.14	34	0.4	0.1
477	2146	126	0.28	36	2.4	0.7
478	206	31	0.11	3	0.2	0.0
479	303	49	0.12	6	0.3	0.0
480	23571	1892	0.50	943	9.5	4.7
481	201	33	0.23	8	1.3	0.3
482	198	42	0.11	4	0.2	0.0
483	29268	2521	0.50	1254	9.5	4.7

Channel ID	Marsh Basin Area, A_B (m^2)	Water Surface Area, A_S (m^2)	Spring Tidal Range, h_R (m)*	Spring Tidal Prism, Ω (m^3)	Inlet Width, W (m)	Cross Sectional Area, A_C (m^2)$^+$
485	310	87	0.14	12	0.4	0.1
486	272	36	0.11	4	0.2	0.0
487	2036	166	0.23	39	1.5	0.3
488	2748	257	0.15	39	0.5	0.1
489	72591	6058	0.62	3756	16.2	10.0
490	169	39	0.17	6	0.6	0.1
491	1102	122	0.15	18	0.5	0.1
492	29884	2928	0.43	1266	6.7	2.9
493	519	73	0.15	11	0.5	0.1
494	4472	248	0.31	78	3.0	0.9
495	1471	133	0.20	27	1.0	0.2
496	2293	127	0.19	24	0.8	0.2
497	888	114	0.11	12	0.2	0.0
498	4179	193	0.18	35	0.8	0.1
499	29513	1425	0.48	690	8.9	4.3
500	764	94	0.11	10	0.2	0.0
501	74290	3712	0.46	1717	7.9	3.7
502	1959	158	0.23	37	1.4	0.3
503	1058	68	0.16	11	0.6	0.1
504	803	119	0.15	17	0.5	0.1
505	369	23	0.16	4	0.5	0.1
506	548	58	0.13	8	0.3	0.0
507	1820	121	0.31	37	2.9	0.9
508	328	34	0.11	4	0.2	0.0
509	679	106	0.14	15	0.4	0.1
511	8790	306	0.32	98	3.2	1.0
512	381	61	0.11	6	0.2	0.0
513	1108	130	0.15	20	0.5	0.1
514	680	111	0.15	17	0.5	0.1
515	2543	191	0.19	36	0.9	0.2
516	1104	191	0.14	26	0.4	0.1
517	1718	185	0.18	33	0.7	0.1
518	530	36	0.14	5	0.4	0.1

Channel ID	Marsh Basin Area, A_B (m^2)	Water Surface Area, A_S (m^2)	Spring Tidal Range, h_R (m)*	Spring Tidal Prism, Ω (m^3)	Inlet Width, W (m)	Cross Sectional Area, A_C (m^2)$^+$
Tidal marshes located at the mouths of Patuxent River tributaries						
69	27037	6971	0.73	5089	12.2	6.7
74	99042	24963	1	24963	20.7	14.1
98	576617	69865	1	69865	44.0	40.6
117	59324	9179	0.73	6701	14.6	8.7
130	45370	10724	1	10724	26.7	20.2
138	250574	23337	1	23337	49.0	47.2
173	336147	42452	1	42452	47.5	45.3
174	72657	8880	1	8880	43.9	40.4
176	1277976	130682	1	130682	71.5	80.2
242	22698	7768	1	7768	93.4	116.7
271	221996	17406	0.73	12707	14.8	8.8
277	121618	6493	0.73	4740	5.4	2.1
281	474169	69865	1	69865	28.7	22.3
283	887812	146007	1	146007	26.3	19.7
295	141167	19779	1	19779	31.9	25.9
311	650234	107676	1	107676	77.0	89.1
316	47033	8988	1	8988	58.7	60.9
357	101667	20836	0.62	12918	15.2	9.1
374	71607	18018	0.62	11171	41.5	37.5
383	159233	35688	0.62	22127	48.8	47.0
397	464596	97538	0.62	60474	54.8	55.2
405	952879	332049	0.62	205870	102.1	132.3
407	409666	73177	0.62	45369	43.5	40.0
412	57946	16146	0.62	10011	53.0	52.7
416	30627	6892	0.62	4273	38.1	33.2
417	158918	29364	0.62	18206	44.8	41.6
418	33604	13657	0.62	8468	50.9	49.9
437	73114	9315	0.62	5775	26.1	19.5
484	247414	30425	0.62	18864	20.1	13.5
510	165612	11886	0.62	7369	20.8	14.2

*For tidal marshes with W<15m: $h_R = 0.20W^{0.40}$

$^+$Cross sectional area is determined from $A_C = 0.20W^{1.4}$

References

Acker, J.G., Harding, L.W., Leptoukh, G., Zhu, T., Shen, S., 2005. Remotely-sensed chl a at the Chesapeake Bay mouth is correlated with annual freshwater flow to Chesapeake Bay. Geophysical Research Letters 32, L05601, 4 p.

Alvarez-Borrego, S., 1994. Secondary productivity in coastal lagoons, In: Kjerfve, B. (Ed.), Coastal Lagoon Processes. Elsevier Science Publishers, New York, New York, 287-309.

Ashmore, P., Parker, G., 1983. Confluence scour in coarse braided streams. Water Resources Research 19(2), 392-402.

Bachelet, G., de Montaudouin, X., Auby, I., Labourg, P-J., 2000. Seasonal changes in macrophyte and macrozoobenthos assemblages in three coastal lagoons under varying degrees of eutrophication. Journal of Marine Science 57, 1495-1506.

Battalio, B., Danmeier, D., Williams, P., 2006. Predicting closure and breaching frequencies of small tidal inlets – a quantified conceptual model. Proceedings of the 30th Conference on Coastal Engineering, San Diego, CA, 3937-3950.

Birkinshaw, S.J., Bathurst, J.C., Iroumé, A., Palacios, H., 2011. The effect of forest cover on peak flow and sediment discharge – an integrated field and modeling study in central-southern Chile. Hydrological Processes 25, 1284-1297.

Bird, E.C.F., 1994. Physical setting and morphology of coastal lagoons. In: Kjerfve, B. (Ed.), Coastal Lagoon Processes. Elsevier Science Publishers, New York, New York, 9-39.

Bruun, P., 1967. Bottom roughness: Rivers, tidal inlets, ocean. Journal of Ocean Technology 1(2), 1-18.

Bruun, P., Gerritsen, F., 1960. Stability of coastal inlets. North Holland Publishing Company, Elsevier, 123 p.

Bruun, P., Mehta, A.J., Johnsson, I.G., 1978. Stability of Tidal Inlets, Theory and Engineering. Elsevier, New York, New York, 510 p.

Buchanan, T.J., Somers, W.P., 1969. Techniques of Water-Resources Investigations of the United States Geological Survey, Book 3, Chapter A8, 65 p.

Byrne, R.J., Gammisch, R.A., Thomas, G.R., 1980. Tidal prism-inlet area relations for small tidal inlets. Proceedings of the Seventeenth Coastal Engineering Conference (American Society of Civil Engineers, New York) 3, 2517-2533.

Daviau, J-L., Adamowski, K., Patry, G.G., 2000. Regional flood frequency analysis using GIS, L-moment and geostatistical methods. Hydrological Processes 14, 2731-2753.

Davidson, N.C., Buck, A.L., 1997. An inventory of UK estuaries. Peterborough, Joint Nature Conservation Committee, 7 volumes.

de Swart, H.E., Zimmerman, J.T.F., 2009. Morphodynamics of tidal inlet systems. Annual Review of Fluid Mechanics 41, 203-229.

Dillow, J.J.A., 1996. Technique for estimating magnitude and frequency of peak flows in Maryland, U.S. Geological Society Water Resources Investigations Report 95-4154, 55 p.

Elwany, M.H.S., 2011. Characteristics, restoration, and enhancement of Southern California lagoons. Journal of Coastal Research SI59, 246-255.

Elwany, M.H.S., Flick, R.E., Aijaz, S., 1998. Opening and closure of a marginal southern California lagoon inlet. Coastal and Estuarine Research Federation 21(2), 246-254.

Escoffier, F.F., 1940. The stability of tidal inlets. Shore and Beach 8(4), 114-115.

Fenneman, N.M., 1938. Physiography of the Eastern United States. McGraw-Hill, New York, New York, 714 p.

Fitzgerald, D.M., 1988. Shoreline erosional-depositional processes associated with tidal inlets In: Aubrey, D.G., Weisher, L. (Eds.), Lecture Notes on Coastal and Estuarine Studies. Springer-Verlag, New York, New York, 29, 186-225.

Folk, R.L., Ward, W.C., 1957. Brazos River Bar: A study in the significance of grain size parameters. Journal of Sedimentary Petrology 27(1), 3-26.

French, J.R., Stoddart, D.R., 1992. Hydrodynamics of salt marsh creek systems: Implications for marsh morphological development and material exchange. Earth Surface Processes and Landforms 17, 235-252.

Gale, E., Pattiaratchi, C., Ranasinghe, R., 2007. Processes driving circulation, exchange and flushing within intermittently closing and opening lakes and lagoons. Marine and Freshwater Research 58, 709-719.

Gammisch, R.A., Hobbs, C.H., Byrne, R.T., 1988. Evolution of tidal inlet – drainage basin systems. Journal of Coastal Research 4(4), 543-550.

Gao S., Collins, M., 1994. Tidal inlet stability in response to hydrodynamic and sediment dynamic conditions. Coastal Engineering 23, 61-80.

Grasso, F., Michallet, H., Barthélemy, E., 2011. Sediment transport associated with morphological beach changes forces by irregular asymmetric, skewed waves. Journal of Geophysical Research 116, C03020, 12 p.

Gupta, V.K., 2004. Emergence of statistical scaling in floods on channel networks form complex runoff dynamics. Chaos, Solitons and Fractals 19, 357-365.

Haines, P.E., Thom, B.G., 2007. Climate change impacts on entrance processes of intermittently open/closed coastal lagoons in New South Wales, Australia. Journal of Coastal Research SI50, 242-246.

Haines, P.E., Tomlinson, R.B., Thom, B.G., 2006. Morphometric assessment of intermittently open/closed coastal lagoons in New South Wales, Australia. Estuarine, Coastal and Shelf Sciences 67, 321-332.

Harmel, R.D., King, K.W., Slade, R.M., 2003. Automated storm water sampling on small watersheds. Applied Engineering in Agriculture 19(6), 667-674.

Henderson,F.M., 1966. Open Channel Flow. Macmillan Publishing Company, Inc., New York, New York, 522 p.

Holling, C.S., 1973. Resilience and stability of ecological systems. Annual Review of Ecology and Systematics 4, 1-23.

Hughes, S.A., 2002. Equilibrium cross sectional area at tidal inlets. Journal of Coastal Research 18(1), 160-174.

Hume, T.M., Herdendorf, C.E., 1992. Factors controlling tidal inlet characteristics on low drift coasts. Journal of Coastal Research 8(2), 355-375.

Hume, T.M., Herdendorf, C.E., 1993. On the use of empirical stability relationships for characterizing estuaries. Journal of Coastal Research 9(2), 413-422.

Jarrett, J.T., 1976, Tidal prism-inlet area relationships, General Investigation of Tidal Inlets Report 3, U.S. Army Coastal Engineering Research Center and U.S. Army Engineer Waterways Experiment Station 55 p.

Jenner, B.A., 2010. Hydraulic consequences of invasive *Hydrilla* (submerged aquatic vegetation) in tidal channels: Implications for wetland maintenance. University of Maryland Undergraduate Thesis, College Park, Maryland.

Johnson, J.W., 1973. Characteristics and behavior of Pacific coast tidal inlets. Journal of Waterways, Harbors and Coastal Engineering, (American Society of Civil Engineers), 99(WW3), 325-339.

Kaushal, S.S., Groffman, P.M., Band, L.E., Shields, C.A., Morgan, R.P., Palmer, M.A., Belt, K.T., Swam, C.M., Findlay, S.E., Fisher, G.T., 2008. Interaction between urbanization and climate variability amplifies watershed nitrate export in Maryland. Environmental Science and Technology 42, 5872-5878.

Kemp, W.M., Boynton, W.R., Adolf, J.E., Boesch, D.F., Boicourt, W.C., Brush, G., Cornwell, J.C., Fisher, T.R., Gilbert, P.M., Hagy, J.D., Harding, L.W., Houde, E.D., Kimmel, D.G., Miller, W.D., Newell, R.I.E., Roman, M.R., Smith, E.M., Stevenson, J.C., 2005. Eutrophication of Chesapeake Bay: historical trends and ecological interactions. Marine Ecology Progress Series 303, 1-29.

Kefi, S., Rietkerk, M., Alados, C.L., Pueyo, Y., Papanasstasis, V.P., ElAich, A., de Ruiter, P.C., 2007. Spatial vegetation patterns and imminent desertification in Mediterranean arid ecosystems. Nature 449, 213-217.

Kemp, W.M., Boynton, W.R., Adolf, J.E., Boesch, D.F., Boicourt, W.C., Brush, G., Cornwell, J.C., Fisher, T.R., Gilbert, P.M., Hagy, J.D., Harding, L.W., Houde, E.D., Kimmel, D.G., Miller, W.D., Newell, R.I.E., Roman, M.R., Smith, E.M., Stevenson, J.C., 2005. Eutrophication of Chesapeake Bay: historical trends and ecological interactions. Marine Ecology Progress Series 303, 1-29.

Kjerfve, B., Magill, K.E., 1989. Geographic and hydrodynamic characteristics of shallow coastal lagoons. Marine Geology 88, 187-199.

Klemes, V., 1983. Conceptualization and scale hydrology. Journal of Hydrology 65, 1-23.

Knoppers, B., 1994, Aquatic primary production in coastal lagoons. In: Kjerfve, B. (Ed.) Coastal Lagoon Processes, Elsevier Science Publishers, New York, New York, 243-286.

Kraus, N. C., 1998. Inlet cross-sectional area calculated by process-based model. Proceedings from the International Conference on Coastal Engineering (American Society of Civil Engineers, New York) 3, 3265-3277.

Kraus, N., 2007. Coastal inlets of Texas, USA. Proceedings of Coastal Sediments (American Society of Civil Engineers, New Orleans, Louisiana) 1475-1488.

Langbein, W.B., 1963. The hydraulic geometry of a shallow estuary. Bulletin of the International Association of Scientific Hydrology 8(3), 84-94.

LeConte, L.J., 1905. Discussion of notes on the improvement of river and harbor outlets in the United States. Paper No. 1009 by D. A. Watts, Transactions, American Society of Civil Engineers, LV, 306-308.

Leopold, L.B., Maddock, Jr., T., 1953. The hydraulic geometry of stream channels and some physiographic implications. U.S. Geological Survey Professional Paper 252, 56 p.

Leopold, L.B., Wolman, M.G., 1957. River channel patterns: Braided, meandering and straight. U.S. Geological Survey Professional Paper 282-B, 85 p.

Leopold, Luna B., Wolman, M.G., and Miller, J.P., 1964. Fluvial Processes in Geomorphology, W.H. Freeman and Co., San Francisco, California, 522 p.

Lowrance, R., Leonard, R.A., 1988. Streamflow nutrient dynamics and Coastal Plain watersheds. Journal of Environmental Quality 17(4), 734-740.

Macedo, M.F., Duarte, P., Mendes, P., Ferreira, J.G., 2001. Annual variation of environmental variables, phytoplankton species composition and photosynthetic parameters in a coastal lagoon. Journal of Plankton Research 23(7), 719-732.

Machemehl, J.L., Herbich, J.B., Jo, C.H., 1991. Study of tidal-inlet stability. Journal of Waterway, Port, Coastal and Ocean Engineering 117(6), 588-598.

Magilligan, F.J., Nislow, K.H., 2001. Long-term changes in regional hydrologic regime following impoundment in a humid-climate watershed. Journal of the American Water Resources Association 37(6), 1551-1569.

Mandelbrot, B.B., 1983, The Fractal Geometry of Nature. W.H. Freeman, New York, New York, 516 p.

Mayor-Mora, R.E., 1977. Laboratory investigations of tidal inlets on sandy coasts. General Investigation of Tidal Inlets Report 11, U.S. Army Coast Engineering Research Center, University of California, College of Engineering, Hydraulic Engineering Laboratory, Berkeley, California, 106 p.

Meigh, J.R., Farquharson, F.A.K., Sutcliffe, J.V., 1997. A worldwide comparison of regional flood estimate methods and climate. Hydrological Sciences 42(2), 225-244.

Menabde, M., Sivapalan, M., 2001. Linking space-time variability of river runoff and rainfall fields: a dynamic approach. Advances in Water Resources 24, 1001-1014.

Myrick, R.M., Leopold, L.B., 1963. Hydraulic geometry of a small tidal estuary. US Geological Survey Professional Paper 422-B, 18 p.

Najjar, R.G., Walker, H.A., Anderson, P.J., Barron, E.J., Bord, R.J., Gibson, J.R., Kennedy, V.S., Knight, C.G., Megonigal, J.P., O'Connor, R.E., Polsky, C.D., Psuty, N.P., Richards, B.A., Sorenson, L.G., Steele, E.M., Swanson, R.S., 2000. The potential impacts of climate change on the mid-Atlantic coastal region. Climate Research 14, 219-233.

Nakano, T., 1983. A fractal study of some rias coastlines in Japan. Annual Reports from the Institute of Geosciences, University of Tsukuba, 9, 75-80.

Neff, R., Change, H., Knight, C.G., Najjar, R.G., Yarnal, B., Walker, H.A., 2000. Impact of climate variation and change on Mid-Atlantic Region hydrology and water resources. Climate Research 14, 207-218.

New South Wales (NSW) Office of the Environment and Heritage, 2010. Estuaries of NSW. <http://www.environment.nsw.gov.au/estuaries/index.htm>, accessed October 2010.

O'Brien, M. P., 1931. Estuary tidal prisms related to entrance areas. Civil Engineering 1(8), 738-739.

O'Brien, M.P., 1976. Notes on tidal inlets on sandy shores. General Investigation of Tidal Inlets Report 5, U.S. Army Coast Engineering Research Center, University of Berkeley, Berkeley, California, 26 p.

Parker, G., 1979. Hydraulic geometry of active gravel rivers. Journal of the Hydraulics Division (Proceedings of the American Society of Civil Engineers) 105 (HY9), 1185-1201.

Parker, G., Toro-Escobar, C.M., Ramey, M., Beck, S., 2003. Effect of floodwater extraction on mountain stream morphology. Journal of Hydraulic Engineering 11, 885-895.

Peel, M.C., Blöschl, G., 2011. Hydrological modeling in a changing world. Progress in Physical Geography 35(2), 249-261.

Pethick, J.S., 1980. Velocity surges and asymmetry in tidal channels. Estuarine and Coastal Marine Science 11, 331-345.

Pethick, J.S., 1981. Long-term accretion rates on tidal salt marshes. Journal of Sedimentary Petrology 51(2), 571-577.

Plotnick, R.E., Prestegaard, K.L., 1993. Fractal analysis of geologic time series. In: Lam, N.S., De Cola, L. (Eds.), Fractals in Geography. PTR Prentice Hall, Englewood Cliffs, New Jersey, pp. 193-210.

Plotnick, R.E., Prestegaard, K.L., 1995. New models require new data: Fractal and multifractal measures of gravel bedload. In: Barton, C.C., La Pointe, P.R. (Eds.), Fractals in Petroleum Geology and Earth Processes. Plenum Press, New York, New York, pp. 113-126.

Prestegaard, K.L., 1979. Stream and lagoon channels of Los Penasquitos Watershed, California, with an evaluation of possible effects of proposed urbanization. University of California Master's Thesis, Berkeley, California.

Prothero, D.R., Schwab, F., 1996. Sedimentary Geology: An introduction to sedimentary rocks and stratigraphy, 2nd ed., W.H. Freeman and Company, New York, New York, 557 p.

Rinaldo A., Rodriguez-Iturbe, I., Rigon, R., Ijjasz-Vasquez, E., Bras, R.L., 1993. Self-organized fractal river networks. Physical Review Letters 70(6), 822-825.

Rinaldo A., S. Fagherazzi, S. Lanzoni, M. Marani, and W. Dietrich. 1999*a*. Tidal networks 1. Watershed delineation and comparative network morphology. Water Resources Research 35, 3905-3917.

Rinaldo A., S. Fagherazzi, S. Lanzoni, M. Marani, and W. Dietrich. 1999*b*. Tidal networks 3. Landscape-forming discharges and studies in empirical geomorphic relationships. Water Resources Research 35, 3919-3929.

Rodriguez-Iturbe, I., Marani, M., Rigon, Riccardo, Rinaldo, A., 1994. Self-organized river basin landscapes: Fractal and multifractal characteristics. Water Resources Research 30(12), 3531-3539.

Rodriguez-Iturbe, I., Rinaldo, A., 1997. Fractal River Basins: Chance and self-organization. Cambridge University Press, New York, New York, 547 p.

Roy, P.S., Williams, RJ., Jones, A.R., Yassini, I., Gibbs, P.J., Coastes, B., West, R.J., Scanes, P.R., Hudson, J.P., Nichol, S., 2001. Structure and function of South-east Australian estuaries. Estuarine, Coastal and Shelf Sciences 53, 351-384.

Scanlon, T.M., Caylor, K.K., Levin, S.A., Rodriguez-Iturbe, I., 2007. Positive feedbacks promote power-law clustering in Kalahari vegetation. Nature 449, 209-212.

Schmith, T., Kaas, E., Li, T.-S., 1998. Northeast Atlantic winter storminess 1875-1995 re-analysed. Climate Dynamics 14, 529-536.

Seabergh, W. C.; King, D. B., and Stephens, B. E., 2001. Tidal inlet equilibrium area experiments, Inlet laboratory investigations, ERDC/CHL TR-01-02, U.S. Army Engineer Research and Development Center, Vicksburg, Mississippi.

Seldomridge, E., 2009. Importance of channel networks on nitrate retention in freshwater tidal wetlands, Patuxent River, MD. University of Maryland M.S. Thesis, College Park, Maryland.

Simon, A., Dickerson, W., Heins, A., 2004. Suspended-sediment transport rates at the 1.5-year recurrence interval for ecoregions of the United States: transport conditions at the bankfull and effective discharge? Geomorphology 58, 243-262.

Sivapalan, M., 2003. Prediction in ungauged basins: a grand challenge for theoretical hydrology. Hydrological Processes 17, 3163-3170.

Sivapalan, M., Blöschl, G., Zhang, L., Vertessy, R., 2003. Downward approach to hydrological prediction. Hydrological Processes 17, 2101-2111.

Smith, S.V., Atkinson, MJ., 1994. Mass balance of nutrient fluxes in coastal lagoons. In: Kjerfve, B. (Ed.), Coastal Lagoon Processes. Elsevier, New York, New York, pp. 133-155.

Spaulding, M.L., 1994. Modeling of circulation and dispersion in coastal lagoons. In: Kjerfve, B. (Ed.), Coastal Lagoon Processes. Elsevier, New York, New York, pp. 103-131.

Tarboton, D.G., Bras, R.L., Rodriguez-Iturbe, I., 1988. The fractal nature of river networks. Water Resources Research 25(9), 2037-2051.

Townend, I., 2005. An examination of empirical stability relationships for UK estuaries. Journal of Coastal Research 21(5), 1042-1053.

van de Kreeke, J., 1985. Stability of tidal inlets – Pass Cavallo, Texas. Estuarine, Coastal and Shelf Sciences 21, 33-43.

van de Kreeke, J., 2004. Equilibrium and cross-sectional stability of tidal inlets: application to the Frisian Inlet before and after basin reduction. Coastal Engineering 51, 337-350.

Villarini, G., Smith, J.A., 2010. Flood peak distributions for the eastern United States. Water Resources Research 46, W06504, 17 p.

Wiberg, P.L., Smith, J.D., 1987. Calculations of the critical shear stress for motion on uniform and heterogeneous sediments. Water Resources Research 23(8), 1471-1480.

Williams, G.P., 1978. Bank-full discharges of rivers. Water Resources Research 14(6), 1141-1154.

Wolman, M.G., 1995. The natural cannel of Brandywine Creek, Pennsylvania. U.S. Geological Survey Professional Paper 271, 56 p.

Wolman, M.G., Miller, J.P., 1960. Magnitude and frequency of forces in geomorphic processes. The Journal of Geology 68(1), 54-74.

Yanez-Arancibia, A., Dominguez, A.L.L., Pauly, D., 1994. Coastal lagoons as fish habitats. In: Kjerfve, B. (Ed.) Coastal Lagoon Processes. Elsevier Science Publishers, New York, 363-376.